INTERFACE STABILITY DURING ISOTHERMAL TERNARY PHASE TRANSFORMATIONS

INTERFACE STABILITY DURING ISOTHERMAL TERNARY PHASE TRANSFORMATIONS

By

DENTON EDWARD COATES, B.A.Sc.

A Thesis

Submitted to the Faculty of Graduate Studies

in Partial Fulfilment of the Requirements

for the Degree

Doctor of Philosophy

McMaster University

October, 1970

DOCTOR OF PHILOSOPHY (1970) McMASTER UNIVERSITY
(Metallurgy and Materials Science) Hamilton, Ontario.

TITLE: Interface Stability During Isothermal Ternary Phase Transformations

AUTHOR: Denton Edward Coates, B.A.Sc. (University of British Columbia)

SUPERVISOR: Professor J. S. Kirkaldy

NUMBER OF PAGES: xv, 201

SCOPE AND CONTENTS:

This dissertation is concerned with establishing the conditions under which planar phase interfaces are morphologically unstable during phase transformations in isothermal ternary systems. First, linear perturbation methods are employed in a detailed treatment of precipitate-matrix interface stability for dilute ternary systems. Following this, the stability of the planar interface in a two-phase ternary diffusion couple is examined with the aid of perturbation theory. An experimental investigation into the stability of α-β phase interfaces in the Cu-Zn-Ni system at 775°C is described. The results of this experimental study are shown to be in good agreement with the earlier theoretical predictions.

TO THE MEMORY OF MY MOTHER

ACKNOWLEDGEMENTS

I would like to express my appreciation to Professor J. S. Kirkaldy for his encouragement and guidance throughout the course of this work. I would also like to thank the many members of the Department of Metallurgy and Materials Science who contributed helpful comments and advice.

Scholarship support from the National Research Council of Canada and the Steel Company of Canada is gratefully acknowledged. Further financial support, in the form of research grants to Professor Kirkaldy, was received from the National Research Council of Canada and the American Iron and Steel Institute.

TABLE OF CONTENTS

LIST OF TABLES

LIST OF ILLUSTRATIONS

LIST OF IMPORTANT SYMBOLS[†]

		Page
J_i	flux of component i	3
μ_i	chemical potential of component i	4
C_i	concentration of component i	4
D_{ik}	elements of the chemical diffusion coefficient matrix	4
u_j	eigenvalues of the matrix $[D_{ik}]$	6
ξ	interface position in a system involving two phases	9
b	rate constant equal to $\xi/\sqrt{t}$	12
C_{im}	concentration of component i in the bulk of phase m which is a terminal phase in an infinite diffusion couple	13
C_i^{mn}	concentration of component i in phase m at a planar m-n interface	13
ξ^{mn}	position of the interface separating phases m and n	13
J_i^{mn}	interface flux of component i in phase m when adjacent to phase n	16
$\vec{V}$	interface velocity	24
V	velocity of a planar interface	46
$\phi(x,t)$	function describing shape of a perturbed interface	47

[†]This list contains only those symbols which are used repeatedly in various parts of the text.

		Page
ω	spatial frequency of a sinusoidal perturbation $\delta \sin \omega x$	48
$\delta(\omega,t)$	amplitude of a sinusoidal perturbation $\delta \sin \omega x$	48
$f(\omega)$	dispersion relation governing the stability of a planar interface	48
$v(x)$	velocity of a perturbed planar interface	52
G_i^{mn}	interface concentration gradient of component i in phase m at a planar m-n interface	58
$\tilde{C}_i$	disturbance in the diffusion field of component i resulting from a perturbation	58
$C_{i\phi}^m$	concentration of component i in phase m at a perturbed planar interface	59
k_i	solute partition coefficient of component i	59
m^I, m^{II}	slopes, including sign, of tangents to the phase boundary lines I/I+II and II/I+II, respectively, on the ternary phase diagram	76
m	slope of tie-line	77
ψ^m	parameter relating to the interfacial gradient of supersaturation in phase m	77
b^I, b^{II}	intercepts in equation of tangents to the phase boundary lines I/I+II and II/I+II, respectively	84
$m^{II\ I}$, $b^{II\ I}$	slope and intercept, respectively, in equation of tangent to interface concentration of 2 in phase II versus 2 in phase I	84

CHAPTER 1

INTRODUCTION

A complete phenomenological analysis of phase transition must yield, as functions of time, the distribution of each of the entities involved and the position of every element of the interphase boundary. It transpires that one can often find a mathematical solution which involves an interface whose shape is preserved as the transformation proceeds (ie., only the scale of the interface shape changes with time as, for example, in the case of spherical precipitate growth). Unfortunately, under certain circumstances such mathematically predicted shapes are not physically stable and, therefore, they are not sustained during actual phase transition. Clearly it is important to establish the range of conditions under which a certain interface morphology is stable. This dissertation is concerned with the stability of the shape of moving phase interfaces in isothermal ternary systems. That is to say, a ternary system in which a phase, I, is undergoing transformation to a second phase, II, is considered and one seeks to establish the conditions under which certain shapes for the moving interphase boundary, I-II, are thermodynamically and kinetically stable.

The dissertation can be conveniently divided into three parts. In the first part, the mathematical theory of multicomponent diffusion (chapter 2) and important qualitative (chapter 3) and quantitative (chapter 4) aspects of morphological stability theory are reviewed. The second part of the thesis describes theoretical investigations which were undertaken by the author. In chapter 5, the problem of precipitate-matrix interface stability in dilute ternary systems is examined using linear perturbation theory. A generalized analysis of phase interface stability in ternary systems of arbitrary constitution is given in Chapter 6. The final part of the dissertation describes an experimental study of α-β phase interface stability in the Cu-Zn-Ni system at 775°C. The results of this study (chapter 7) are compared (chapter 8) with the theoretical predictions of chapter 6 and are found to be in excellent agreement.

CHAPTER 2

THE MATHEMATICS OF TERNARY DIFFUSION

2.1 INTRODUCTION

To study the problem of interface stability in isothermal ternary phase transformations, it is necessary to first examine certain elements of multicomponent diffusion theory. The format for the present chapter is: a) to give the general phenomenological equations of multicomponent diffusion, b) to indicate how the corresponding ternary diffusion equations are solved, c) to discuss a few pertinent examples and d) to show how such solutions can be used to determine the diffusion path on the corresponding ternary phase diagram.

2.2 THE PHENOMENOLOGICAL EQUATIONS

The phenomenological basis of multicomponent diffusion was outlined completely by Onsager[1] in 1945-46. This work followed directly from his earlier and much celebrated papers[2,3] on "Reciprocal Relations in Irreversible Processes".

In a volume-fixed reference frame, the molar flux of component i in an n-component system is given by[1,4,5,6,7]

$$J_i = \sum_{k=1}^{n-1} L_{ik} X_k \qquad (i = 1,\ldots,n-1) \qquad (2\text{-}1)$$

where the forces X_k are expressed in terms of the chemical potentials μ_k as

$$X_k = - \nabla (\mu_k - \frac{\bar{V}_k}{\bar{V}_n} \mu_n) \quad . \tag{2-2}$$

The $\bar{V}_k$ are partial molar volumes (assumed constant). The volume-fixed reference frame is defined by the condition

$$\sum_{i=1}^{n} \bar{V}_i J_i = 0 \tag{2-3}$$

and therefore the flux of component n can be regarded as a dependent variable. As a consequence of Onsager's reciprocity theorem, the matrix $[L_{ik}]$ is symmetric, viz.,

$$L_{ik} = L_{ki} \quad . \tag{2-4}$$

Furthermore, the Second Law of Thermodynamics and thermodynamic stability require that the matrices $[L_{ik}]$ and $[\mu_{ik}]$, respectively, be positive definite. The elements of the latter matrix are given by

$$\mu_{ik} = \frac{\partial \mu_i}{\partial n_k} \tag{2-5}$$

where the n_k are mole numbers.

Equation (2-1) can be transformed to the following expression which involves molar concentrations C_k:[1]

$$J_i = - \sum_{k=1}^{n-1} D_{ik} \nabla C_k \tag{2-6}$$

with

$$D_{ik} = \sum_{j=1}^{n-1} L_{ij} \frac{\partial}{\partial C_k} \left(\mu_j - \frac{\bar{V}_j}{\bar{V}_n} \mu_n\right). \qquad (2\text{-}7)$$

Equation (2-6) is recognized as a generalization of Fick's first law. It is invariably assumed that the molar volume of the system is independent of composition. As a result, the concentration of one of the components, usually taken as the n^{th}, is dependent. When applied to Eq. (2-7), the requirements that $[L_{ij}]$ and $[\mu_{ij}]$ be positive definite ensure that the diffusion coefficient matrix $[D_{ik}]$ has positive (real) eigenvalues[8]. Notice that the elements of this matrix are in general functions of concentration.

On combining Eq. (2-6) with the continuity equation

$$\frac{\partial C_i}{\partial t} + \nabla \cdot J_i = 0 \qquad (2\text{-}8)$$

one obtains the set of n-1 partial differential equations

$$\frac{\partial C_i}{\partial t} = \nabla \cdot \sum_{k=1}^{n-1} D_{ik} \nabla C_k \qquad (2\text{-}9)$$

2.3 SOLUTIONS TO THE TERNARY DIFFUSION EQUATIONS

For a ternary system in which the relative changes in concentration are small, the diffusion coefficients may be approximated by constants and Eq. (2-9) reduces to

$$\frac{\partial C_1}{\partial t} = D_{11} \nabla^2 C_1 + D_{12} \nabla^2 C_2 \qquad (2\text{-}10)$$

$$\frac{\partial C_2}{\partial t} = D_{21} \nabla^2 C_1 + D_{22} \nabla^2 C_2 \qquad (2\text{-}11)$$

If the boundary conditions on the two independent components are formally the same, one seeks solutions to this set of equations as linear superpositions of the form[1,8,9]

$$C_i = a_{io} + \sum_{k=1}^{2} a_{ik} C^k \qquad (2\text{-}12)$$

where the C^k are solutions of the binary type diffusion equations

$$\frac{\partial C^k}{\partial t} = u_k \nabla^2 C^k \qquad (2\text{-}13)$$

Substitution of Eq. (2-12) into (2-10) and (2-11) yields the characteristic equations

$$u_k a_{ik} = \sum_{j=1}^{2} D_{ij} a_{jk} \quad (i,k=1,2) \qquad (2\text{-}14)$$

which in matrix notation become

$$[D_{ij} - u_k \delta_{ij}][a_k] = 0 \qquad (2\text{-}15)$$

where $[a_k]$ represents the column vectors of $[a_{ik}]$. This is recognized as the standard eigenvalue problem. The eigenvalues u_k are the roots of the secular determinant equation

$$|D_{ij} - u \delta_{ij}| = 0 \ . \qquad (2\text{-}16)$$

For the ternary system, this equation yields the eigenvalues:

$$u_{1,2} = \frac{1}{2}\{(D_{11}+D_{22}) \pm [(D_{11}+D_{22})^2 - 4(D_{11}D_{22}-D_{12}D_{21})]^{\frac{1}{2}}\} \qquad (2\text{-}17)$$

To each eigenvalue u_k there corresponds an eigenfunction C^k which is obtained from Eq. (2-13) and an eigenvector $[a_k]$ which is determined by Eq. (2-14) to within a multiplicative constant. The latter and the constants a_{io} are determined by the boundary conditions.

Numerous solutions to the binary diffusion equation

$$\frac{\partial C}{\partial t} = D\nabla^2 C \qquad (2\text{-}18)$$

can be found in the literature, for example in the monographs of Crank[10], Jost[11] and Carslaw and Jaeger[12]. It has just been demonstrated that such solutions can be utilized in the construction of solutions to the multicomponent diffusion equations, provided the boundary conditions on each component are formally the same.

2.3.1 Unidirectional Diffusion in One Phase

Unidirectional transport in infinite and semi-infinite systems is of considerable significance in this dissertation. Thus a solution to Eq. (2-18), subject to boundary conditions corresponding to a single phase infinite diffusion couple, is of particular interest. Such conditions correspond to a linear step-function at the origin, ie.,

$$\left.\begin{aligned} C(Z>0,0) &= C(\infty,t) = C_0 \\ C(Z<0,0) &= C(-\infty,t) = C_1 \end{aligned}\right\} . \qquad (2\text{-}19)$$

The desired solution is well-known and has the form

$$C = \frac{C_1 + C_0}{2} - \frac{C_1 - C_0}{2} \operatorname{erf}\left(\frac{Z}{2\sqrt{Dt}}\right) \qquad (2\text{-}20)$$

Notice that this equation is parametric in $\lambda = Z/\sqrt{t}$.

Turn now to the problem of determining similar solutions to the ternary diffusion equations (2-10) and (2-11). Consider first a single phase infinite diffusion couple which, as already noted, has boundary conditions corresponding to a step function at the origin,

$$\left.\begin{aligned} C_i(Z>0,0) &= C_i(\infty,t) = C_{i0} \\ C_i(Z<0,0) &= C_i(-\infty,t) = C_{i1} \end{aligned}\right\}. \qquad (2\text{-}21)$$

In view of Eqs. (2-20), (2-18) and (2-13), it is obvious that the eigenfunctions C^k in Eq. (2-12) are of the form

$$C^k \propto \operatorname{erf}\left(\frac{Z}{2\sqrt{u_k t}}\right) .$$

Thus the solution to Eqs. (2-10) and (2-11), subject to (2-21), is easily shown to be[13,14]

$$C_i = a_{i0} + a_{i1} \operatorname{erf}\left(\frac{Z}{2\sqrt{u_1 t}}\right) + a_{i2} \operatorname{erf}\left(\frac{Z}{2\sqrt{u_2 t}}\right) \qquad (2\text{-}22)$$

where the eigenvalues u_1 and u_2 are given in Eq. (2-17) and

$$
\left.
\begin{aligned}
a_{10} &= \tfrac{1}{2}(C_{10}+C_{11}) \\
a_{11} &= \frac{1}{2D^*}\{D_{12}(C_{20}-C_{21})-[(D_{22}-D_{11}) - D^*]\ \frac{(C_{10} - C_{11})}{2}\} \\
a_{12} &= \tfrac{1}{2}(C_{10}-C_{11}-2a_{11}) \\
a_{20} &= \tfrac{1}{2}(C_{20}+C_{21}) \\
a_{21} &= \frac{1}{2D^*}\{D_{21}(C_{10}-C_{11}) - [(D_{11}-D_{22})-D^*]\ \frac{(C_{20}-C_{21})}{2}\} \\
a_{22} &= \tfrac{1}{2}(C_{20}-C_{21}-2a_{21}) \\
D^* &= \sqrt{(D_{11}-D_{22})^2 + 4D_{12}D_{21}}
\end{aligned}
\right\} \qquad (2\text{-}23)
$$

Notice that just as in the binary case Eq. (2-20), Eq. (2-22) is parametric in $\lambda = Z/\sqrt{t}$.

2.3.2 Precipitate Growth

Consider next the unidirectional growth of a homogeneous precipitate in an infinite medium, the matrix. Let C_{i2}, C_{i1} and C_{i0} be, respectively, the concentrations in the precipitate, in the matrix at the precipitate-matrix interface and in the bulk matrix. It is assumed that local equilibrium maintains at the interface and therefore C_{i2} and C_{i1} have values which do not vary with time. The boundary conditions are (see Fig. 2-1)

$$
\left.
\begin{aligned}
C_i(Z<\xi, t>0) &= C_{i2} \\
C_i(\xi_+,\ t>0) &= C_{i1} \\
C_i(Z>0,0) = C_i(\infty,t) &= C_{i0}
\end{aligned}
\right\} \qquad (2\text{-}24)
$$

where ξ is the position of the precipitate-matrix interface.

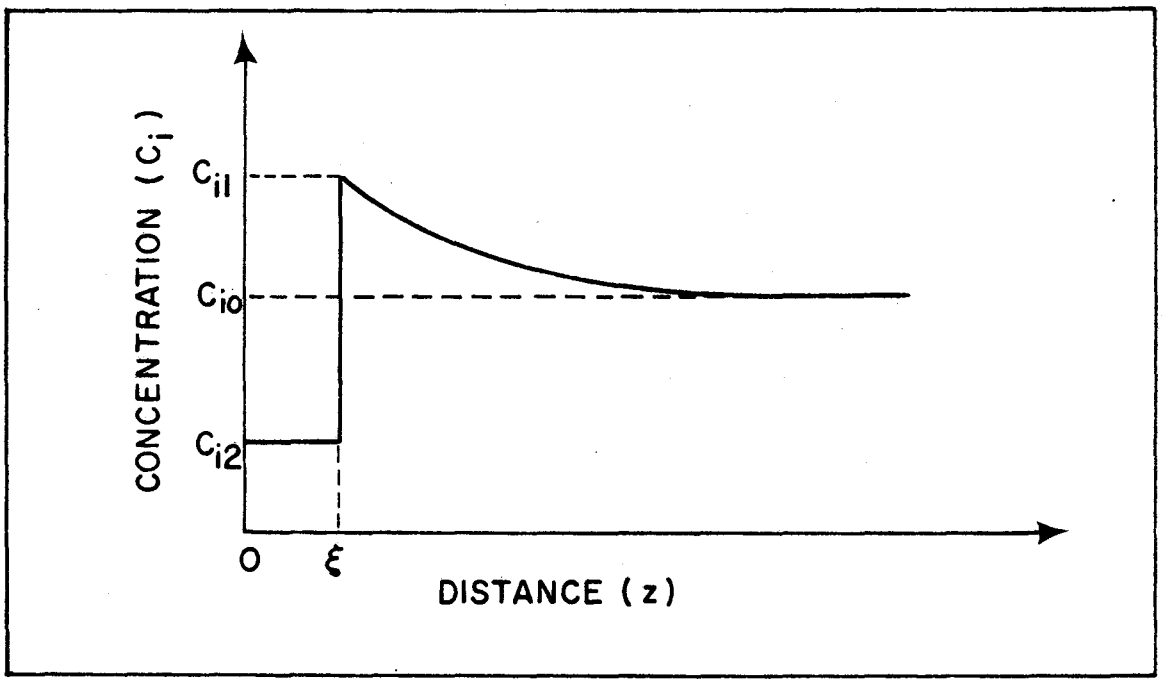

Fig. 2-1 Solute distribution during precipitate growth

The solution to the corresponding binary problem[15,16] involves a normalized error function complement distribution of solute. Thus the eigenfunctions C^k in Eq. (2-12) are of the form $\text{erfc}(Z/2\sqrt{u_k t})/\text{erfc}(\xi/2\sqrt{u_k t})$ and the solution to Eqs. (2-10) and (2-11), subject to (2-24), can be expressed as[17]

$$C_i = a_{i0} + \frac{a_{i1}}{I_1}\,\text{erfc}\left(\frac{Z}{2\sqrt{u_1 t}}\right) + \frac{a_{i2}}{I_2}\,\text{erfc}\left(\frac{Z}{2\sqrt{u_2 t}}\right) \qquad (2\text{-}25)$$

where the normalization integrals are

$$I_k = \text{erfc}\left(\frac{\xi}{2\sqrt{u_k t}}\right) \qquad (2\text{-}26)$$

and the eigenvalues u_1 and u_2 are given by Eq. (2-17). Application of Eqs. (2-14) and (2-24) yields

$$\left.\begin{aligned}
a_{10} &= C_{10} \\
a_{11} &= \{D_{12}(C_{21}-C_{20}) + [(D_{11}-D_{22})+D^*](C_{11}-C_{10})/2\}/D^* \\
a_{12} &= C_{11}-C_{10}-a_{11} \\
a_{20} &= C_{20} \\
a_{21} &= \{D_{21}(C_{11}-C_{10})-[(D_{11}-D_{22})-D^*](C_{21}-C_{20})/2\}/D^* \\
a_{22} &= C_{21}-C_{20}-a_{21} \\
D^* &= \sqrt{(D_{11}-D_{22})^2 + 4D_{12}D_{21}}
\end{aligned}\right\} \qquad (2\text{-}27)$$

There are two matters which must be dealt with in order to complete this solution. It follows from the Gibbs' phase rule that in an isothermal isobaric ternary system which involves two coexisting phases, there is one thermodynamic degree of

freedom (ie., there are four unknowns C_{i1}, C_{i2} (i=1,2) and only three equations $\mu_{j1}(C_{11},C_{21})=\mu_{j2}(C_{12},C_{22})$ (j = 1,2,3)). For the present circumstances, this means that one must determine which of the tie-lines on the given ternary phase diagram specifies the interface concentrations C_{i1} and C_{i2}. Thus one of the four interface concentrations is independent and its value must be fixed by a kinetic condition†. Furthermore, the position of the precipitate-matrix interface, ξ, is as yet unspecified. In summary, the independent interface concentration and the interface position are not known *ab initio* and they must be determined as part of the solution to the problem. The extra boundary conditions which provide this added information are the two independent mass conservation conditions at the interface, viz.,

$$-J_i(\xi) = (C_{i2}-C_{i1})\frac{d\xi}{dt} = (C_{i2}-C_{i1})\frac{b}{2\sqrt{t}} \qquad (2\text{-}28)$$

where it is assumed

$$\xi = b\sqrt{t} \qquad (2\text{-}29)$$

and b is a constant. This functional form for $\xi(t)$ is chosen because the concentration distributions, Eq. (2-25), are parametric in $Z/\sqrt{t}$. It therefore follows that the motion

---

†If one arbitrarily selects C_{11} as the independent concentration, then C_{12}, C_{21} and C_{22} are dependent variables and are related to C_{11} by known thermodynamic relations (eg., they are defined by the tie-line on the isothermal phase diagram that passes through C_{11}).

of points of constant composition, for example the precipitate-matrix interface, goes as $t^{\frac{1}{2}}$. Substitution of Eqs. (2-6) and (2-25) into (2-28) and simultaneous solution of the latter yields the values of b and C_{11} (if it is chosen as the independent concentration). The solution is now complete.

2.3.3 Multiphase Systems

As a final example, consider an infinite diffusion couple within a linear N-phase system[18]. The appropriate boundary conditions are

$$\left.\begin{aligned} C_i(Z<0,0) &= C_i(-\infty,t) = C_{iN} \\ C_i(Z>0,0) &= C_i(\infty,t) = C_{i1} \\ C_i(\xi_-^{mn},t>0) &= C_i^{mn} \\ C_i(\xi_+^{mn},t>0) &= C_i^{nm} \end{aligned}\right\} \qquad (2\text{-}30)$$

In Fig. 2-2, is shown a schematic penetration curve for one of the two independent components, after annealing for time t. The system of notation is such that C_i^{mn} is the interface concentration of component i in phase m when adjacent to phase n and ξ^{mn} is the position of the interface separating phases m and n (clearly here n=m-1). Each continuous region of the penetration curve is a solution of Eqs. (2-10) and (2-11). The eigenfunctions C^k in Eq. (2-12) are of the form

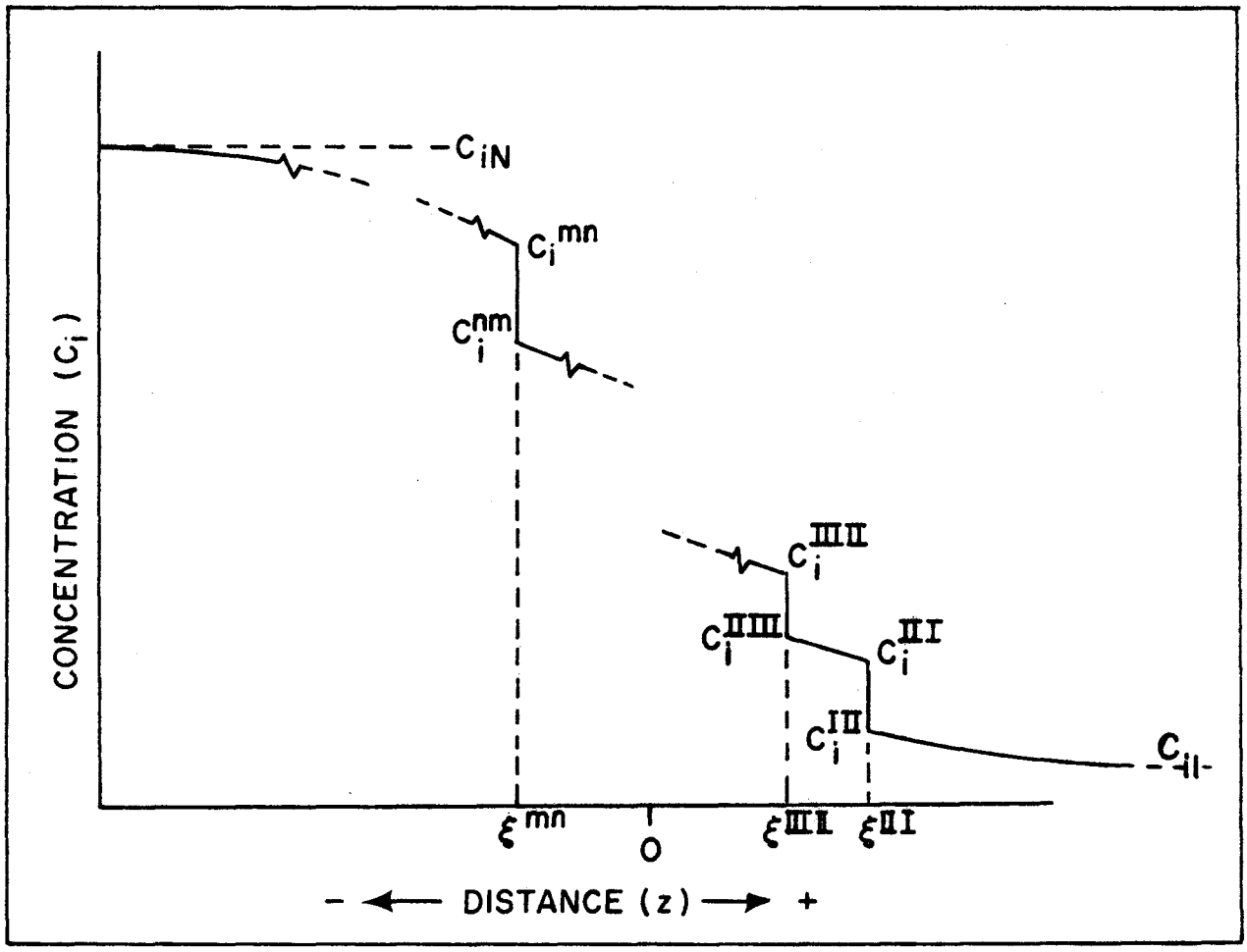

Fig. 2-2 Solute distribution in an N-phase diffusion couple

$$[\mathrm{erfc}(\frac{z}{2\sqrt{u_k t}}) - \mathrm{erfc}(\frac{\xi^{mn}}{2\sqrt{u_k t}})]/[\mathrm{erfc}(\frac{\xi^{m+1,n+1}}{2\sqrt{u_k t}}) - \mathrm{erfc}(\frac{\xi^{mn}}{2\sqrt{u_k t}})]$$

and the required solutions (in the m^{th} phase) subject to Eq. (2-30), can be expressed as[18]

$$C_i^m = a_{i0}^m + \frac{a_{i1}^m}{I_1^m}[\mathrm{erfc}(\frac{z}{2\sqrt{u_1^m t}}) - \mathrm{erfc}(\frac{\xi^{mn}}{2\sqrt{u_1^m t}})] + \frac{a_{i2}^m}{I_2^m}[\mathrm{erfc}(\frac{z}{2\sqrt{u_2^m t}}) - \mathrm{erfc}(\frac{\xi^{mn}}{2\sqrt{u_2^m t}})] \qquad (2\text{-}31)$$

where the normalization integrals are

$$I_k^m = \mathrm{erfc}(\frac{\xi^{m+1,n+1}}{2\sqrt{u_k^m t}}) - \mathrm{erfc}(\frac{\xi^{mn}}{2\sqrt{u_k^m t}}) \qquad (2\text{-}32)$$

and, as usual, u_1^m and u_2^m are defined in Eq. (2-17)†. Application of the boundary conditions (2-30) and the characteristic equations (2-14) allows the a_{i0}^m, a_{i1}^m and a_{i2}^m to be expressed in terms of the diffusion coefficients, terminal concentrations (C_{i1} and C_{iN}) and interface concentrations (C_i^{mn}).

For local equilibrium at all phase interfaces, the C_i^{mn} are constant and therefore, following arguments similar to those used for the previous example, one writes

$$\xi^{mn} = b^{mn} \sqrt{t} \qquad (2\text{-}33)$$

---

†For the terminal phases (m=1,N), Eqs. (2-31) and (2-32) are replaced by less complex equations of a form similar to Eqs. (2-25) and (2-26).

where the b^{mn} are constants. There are N-1 constants b^{mn} plus $2\times2(N-1)$ interface concentrations† C_i^{mn} yet to be specified, a total of 5(N-1) unknowns. These are uniquely determined by 2(N-1) interfacial mass conservation conditions of the form

$$J_i^{mn} - J_i^{nm} = (C_i^{mn}-C_i^{nm})\frac{d\xi^{mn}}{dt} = (C_i^{mn} - C_i^{nm})\frac{b^{mn}}{2\sqrt{t}} \quad (n=m-1) \qquad (2\text{-}34)$$

and 3(N-1) local equilibrium relations of the form

$$\mu_j^{mn}(C_1^{mn},C_2^{mn}) = \mu_j^{nm}(C_1^{nm},C_2^{nm}) \qquad (^{n=m-1}_{j=1,2,3}) \qquad (2\text{-}35)$$

where μ_j is the chemical potential of component j. As pointed out earlier, the isothermal phase diagram is equivalent to the latter set of equations.

2.4 THE DIFFUSION PATH ON A TERNARY ISOTHERM

Consider the isothermal ternary system shown in Fig. 2-3. If a three-phase infinite diffusion couple of terminal compositions defined by points P and U is annealed for a time t, concentration profiles for the independent components 1 and 2 might be as shown in Fig. 2-4. It is assumed that the interfaces maintain their initial planar shapes. In

†Keep in mind that it has been assumed that the alloy has constant molar volume and therefore the concentration of the third component is dependent and need never enter the calculations.

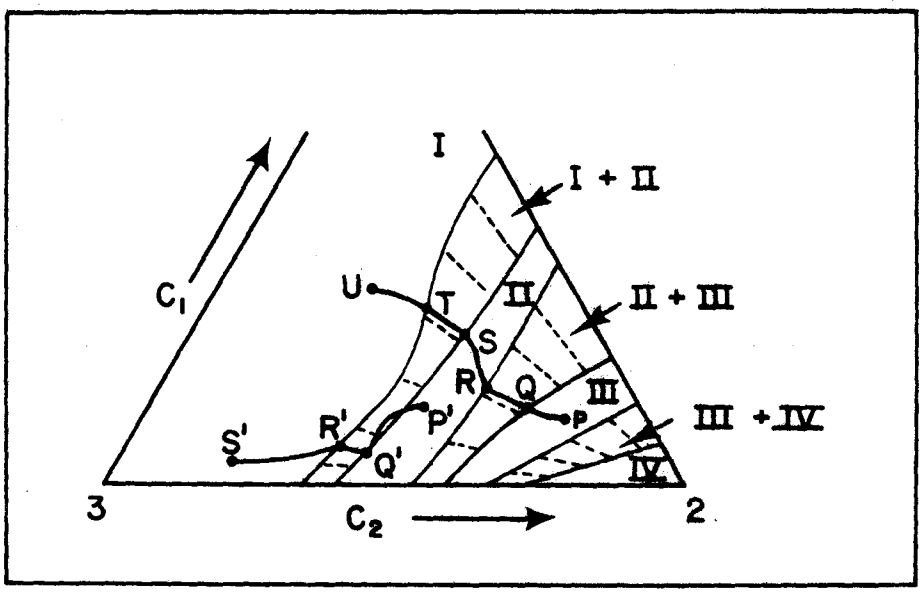

Fig. 2-3 Diffusion paths superimposed on an isothermal ternary phase diagram (cf., Cu-Zn-Ni System Fig. 7-2)

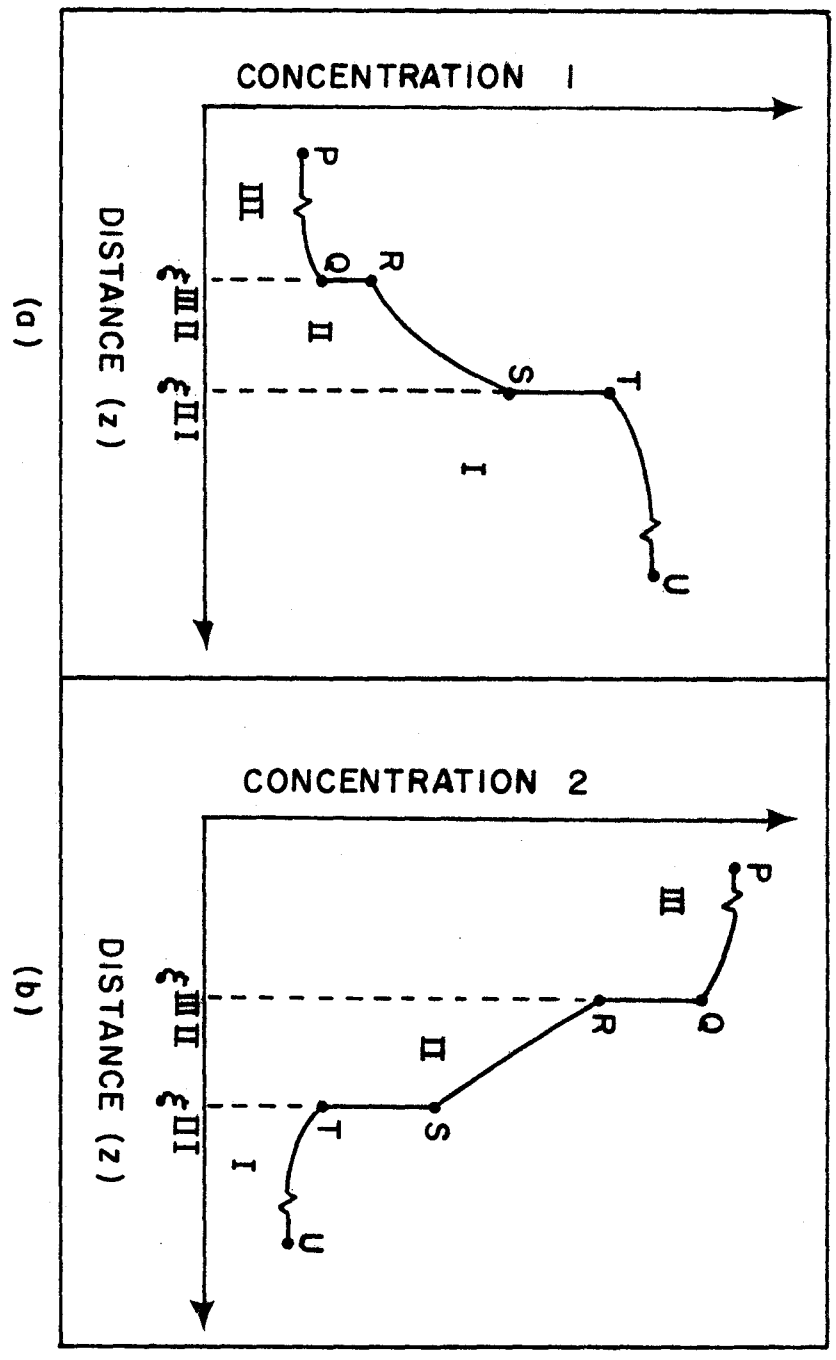

Fig. 2-4 Concentration distributions in a three-phase infinite diffusion couple. The corresponding diffusion path is the line PU in Fig.2-3

the previous section it was demonstrated that, provided local equilibrium prevails at the interfaces, the solutions to the diffusion equations can be expressed as a function of a single independent parameter $\lambda = Z/\sqrt{t}$. Clearly, for each phase one can eliminate λ between the solutions for the two concentration distributions to give relations of the form $C_1^I = C_1^I(C_2^I)$, $C_1^{II} = C_1^{II}(C_2^{II})$ and $C_1^{III} = C_1^{III}(C_2^{III})$. These expressions are distance and time independent and therefore can be plotted on the ternary phase diagram as shown in Fig. 2-3 (cf., Fig. 2-4). In conjunction with the appropriate (unique) tie-lines, they define the diffusion path (solid line joining points P and U) for the given diffusion couple.

Kirkaldy and Brown[19] have developed a number of useful theorems pertaining to the construction of diffusion paths on ternary isotherms. They point out that if the calculated path does not enter a two-phase field, other than to cross such a region coincident with a tie-line (as with the path segments QR and ST in Fig. 2-3), then this path will coincide with the actual composition path. If, on the other hand, the calculated path dips into a two-phase field and thereby cuts tie-lines (as with the path segment P'Q' of the 2-phase couple P'S' in Fig. 2-3), then the calculated path should be regarded as being "virtual" since, in view of the supersaturated material adjacent to the interface, such a situation is unstable. The actual system may involve non-planar interfaces or internal precipitates or both.

CHAPTER 3

MORPHOLOGICAL INSTABILITY

3.1 INTRODUCTION

In this chapter, important examples of morphological instability of moving interphase boundaries are described qualitatively. Following a general description of the problem of morphological instability, situations which involve transport of only one entity (heat or solute) are considered. Then examples are considered wherein two entities are transported; ie., a solute and heat and finally two solutes.

3.2 THE GENERALIZED PROBLEM

Consider a system (Fig. 3-1) in which a phase II is growing at the expense of a different phase I; ie., a phase transformation I → II is in progress. The two phases are assumed to be separated by a continuous surface, the interface. For the phase transformation to proceed, transport of heat or one or more solutes or both must take place[†]. The distributions of the various entities must satisfy a system of 'transport' or 'field' (differential) equations.

[†]Phase transformations which occur by means other than the long range transport of heat or solute are not considered.

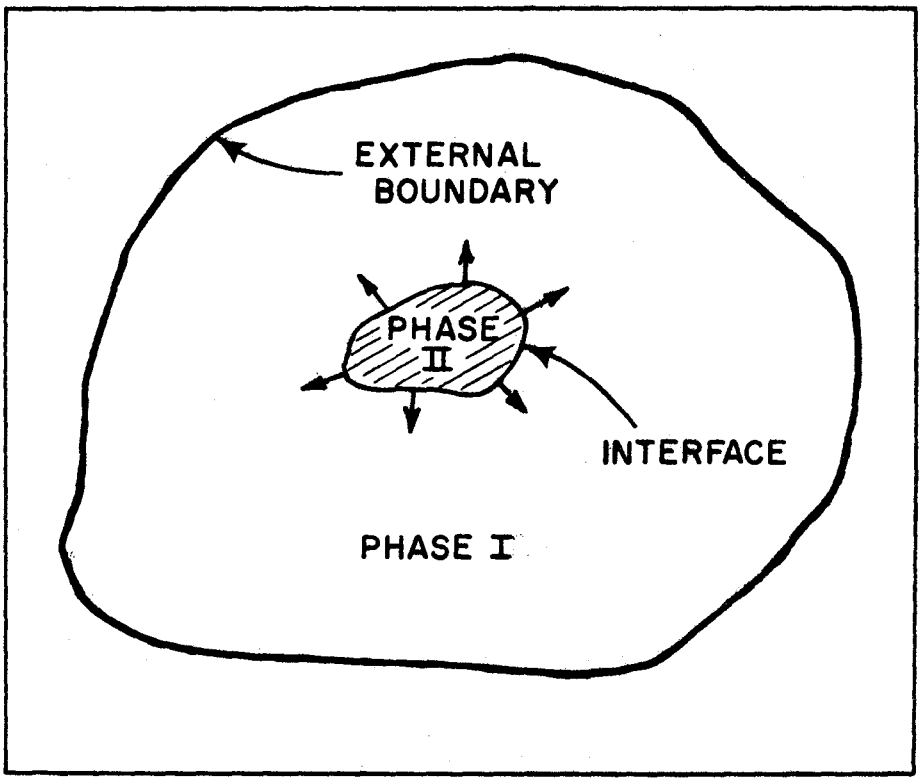

Fig. 3-1 Generalized phase transformation, I → II (after Sekerka[20]).

For example, for mass transport of one solute and for heat flow, the field equations are, respectively, Eq. (2-18) and

$$\frac{\partial T}{\partial t} = D_{th} \nabla^2 T \qquad \text{(the heat equation)} \qquad (3\text{-}1)$$

where $D_{th} = k/c_p$ is the thermal diffusivity, k is the thermal conductivity and c_p is the specific heat per unit volume. Furthermore, certain boundary conditions must be satisfied at the interface and at the external boundary. Because two phases are in coexistence at the interface, there must be a boundary condition pertaining to the state of local equilibrium at the interface. In addition, the flow of mass and heat across the interface must be conserved.

It is assumed that some exact theoretical solution to this problem exists when the interface is 'smooth' (eg., a sphere, a plane or a cylinder depending on conditions at and the geometry of the external boundary). Such a solution must give the distributions of all species and the position of every element of the interface as functions of time.

At this juncture it is convenient to digress and comment upon the determination of such solutions. Problems dealing with phase change belong to a peculiar class of boundary value problems which are often referred to as free

boundary problems[21,22,23,24]†. The usual boundary value problem involves determination of a function, U(x,y) say, in a specified domain of the xy plane (ie., within a region of the xy plane which is enclosed by a known stationary boundary). The situation at the boundary is prescribed by various possible types of boundary conditions (Dirichlet, Neumann, Cauchy etc.), depending on the kind of field equation (elliptic, hyperbolic or parabolic) and the given physical circumstances. A free boundary problem is one whose solution is defined over a domain that is not given in advance. That is, the location of the domain boundary must be established simultaneously with the solution of the differential equations. As a result, such problems always involve an extra boundary condition at the free boundary.

Clearly the change of phase problem just described is a free boundary problem since one must determine solutions to the field equations simultaneously with the shape and position of the interface. The extra boundary condition is an interfacial mass or heat conservation condition and it must be emphasized that such conditions are, in general, nonlinear and nonhomogeneous. The problem is further compli-

---

†Most monographs on boundary value problems make only cursory mention of free boundary problems. An exception is the book by Garabedian[21] which contains numerous references to the literature on this subject.

cated by the fact that the two phases have different thermal and diffusive properties.

It is worthwhile examining the conservation boundary condition in further detail in order to understand how it influences the interface morphology. For conservative mass flow at the interface, the following condition must be satisfied:

$$\vec{n}\cdot(C^{II\ I}-C^{I\ II})\vec{V} = \vec{n}\cdot\vec{J}^{II\ I} - \vec{n}\cdot\vec{J}^{I\ II}$$

or

$$\vec{n}\cdot[(C^{II\ I}-C^{I\ II})\vec{V} + D^{II}\vec{\nabla}_{int}C^{II} - D^{I}\vec{\nabla}_{int}C^{I}] = 0 \quad (3\text{-}2)$$

where $\vec{n}$ is a unit vector normal to the interface (directed towards phase I) and $\vec{\nabla}_{int}$ signifies the gradient is evaluated at the interface[†]. Consider a generalized set of orthogonal curvilinear coordinates (ξ_1, ξ_2, ξ_3), with the corresponding unit vectors $(\vec{a}_1, \vec{a}_2, \vec{a}_3)$. Let

$$\vec{n} = n_1\vec{a}_1 + n_2\vec{a}_2 + n_3\vec{a}_3 \quad (3\text{-}3)$$

$$\vec{V} = V_1\vec{a}_1 + V_2\vec{a}_2 + V_3\vec{a}_3 \quad (3\text{-}4)$$

and

$$\vec{\nabla}_{int} = \nabla_1\vec{a}_1 + \nabla_2\vec{a}_2 + \nabla_3\vec{a}_3 \quad (3\text{-}5)$$

[†]The ensuing arguments apply equally well to the corresponding heat flow conservation condition

$$\vec{n}\cdot(\Delta H^{I\to II}\vec{V} + k^{I}\vec{\nabla}_{int}T^{I} - k^{II}\vec{\nabla}_{int}T^{II}) = 0$$

where $\Delta H^{I\to II}$ is the enthalpy change per unit volume. If I and II are liquid and solid respectively, $\Delta H^{I\to II} = L$ where L is the latent heat of fusion per unit volume.

where the n_i (i = 1,2,3) are direction cosines† Substitution of Eqs. (3-3), (3-4) and (3-5) into (3-2) yields

$$n_1[(C^{II\ I}-C^{I\ II})V_1 + D^{II}\nabla_1 C^{II} - D^{I}\nabla_1 C^{I}]$$

$$+ n_2[(C^{II\ I}-C^{I\ II})V_2 + D^{II}\nabla_2 C^{II} - D^{I}\nabla_2 C^{I}]$$

$$+ n_3[(C^{II\ I}-C^{I\ II})V_3 + D^{II}\nabla_3 C^{II} - D^{I}\nabla_3 C^{I}]$$

$$= 0. \qquad (3\text{-}6)$$

Obviously for an arbitrary surface, this is a very complex boundary condition. It is now clear why it is much easier to obtain mathematical solutions which involve interface shapes of high symmetry (the 'smooth' interfaces mentioned earlier). If the normal to the interface is everywhere parallel to one of the coordinate directions, $\vec{n}\cdot\vec{a}_1 = 1$ say, then $n_1 = 1$, $n_2 = n_3 = 0$, and the above boundary condition is much simplified. As a result, mathematical solutions have been determined for phase transitions involving a parent phase of infinite extent and the following interface shapes:

a) Planar front[25,26] - If one uses cartesian coordinates (x,y,z), the interface is simply x = constant and therefore $n_1 = 1$, $n_2 = n_3 = 0$.

b) Circular cylinder[27] - If circular cylindrical coordinates (r,θ,z), are used, the interface is given by r = constant and therefore $n_1 = 1$, $n_2 = n_3 = 0$.

†The ∇_i in general include a scale factor as well as the appropriate partial derivative.

c) Sphere[16] - Using spherical polar coordinates (r,θ,ϕ), the interface is r = constant and hence $n_1 = 1$, $n_2 = n_3 = 0$.

d)† Ellipsoid[28,29] - If one uses prolate spheroidal coordinates[30] (u,v,ϕ), the interface is given by u = constant and therefore $n_1 = 1$, $n_2 = n_3 = 0$.

e) Paraboloid of revolution[31,32] - Using parabolic coordinates[30] (ξ,η,ϕ), the interface is given by ξ = constant and thus $n_1 = 1$, $n_2 = n_3 = 0$.

For present purposes, it is assumed that an exact theoretical solution to a given change of phase problem exists when the interface shape is highly symmetric (in the sense just described). However, it may transpire that this solution, and hence the 'smooth' interface shape, is not a physically stable one. If the idealized system is subjected to perturbations, such as exist in all real systems, the resultant changes in the interface shape will either grow or decay in time. Accordingly, the 'smooth' interface morphology is unstable or stable, respectively, depending upon which of these responses occurs. It is emphasized that an unstable interface is a manifestation of a physically unstable distribution of the various entities. If the interface corresponding to the idealized solution is not stable, it will undergo morphological breakdown and will evolve to a new stationary shape, if such exists. The latter often involve a periodic variation

†It should be recalled that the influence of capillarity is being ignored in the present discussion.

in the interface shape. This dissertation is not concerned with predicting the ultimate morphology to which an unstable interface evolves. Rather it is concerned with establishing precisely the marginal (incipient) state of instability in terms of the growth conditions and system parameters.

3.3 MORPHOLOGICAL BREAKDOWN INVOLVING TRANSPORT OF ONE ENTITY

Hitherto the point-of-view has been quite general and, to some extent, abstract. In the remaining sections of this chapter, an attempt is made to understand the physical circumstances which result in morphologically unstable phase interfaces. Accordingly, specific examples of morphological breakdown are briefly considered with a view to establishing the driving force which is responsible for the instability. These examples are conveniently grouped according to the nature and number of entities being transported.

3.3.1 Heat Transport Only

Consider the growth of a solid in an initially uniformly supercooled pure liquid. One wants to establish whether an initially 'smooth' solid-liquid interface is physically stable when in contact with a supercooled melt. For simplicity consider the advance of a planar interface, for which the corresponding temperature distribution is given in Fig. 3-2a. Notice that the velocity of the interface is controlled by the rate at which the latent heat which is

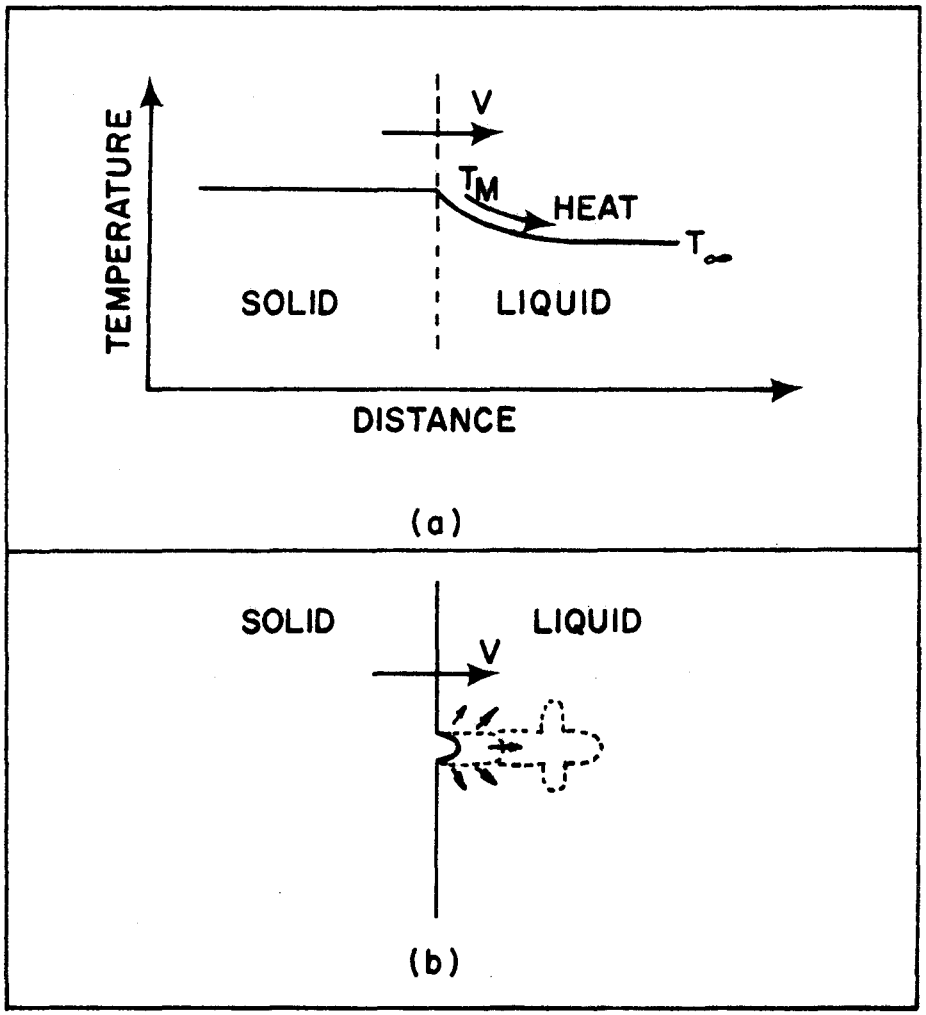

Fig. 3-2 (a) Temperature distribution during growth of a solid in a pure liquid.

(b) Growth of a perturbation in the shape of the solid-liquid interface.

released at the interface can escape into the bulk liquid. Now assume the interface is perturbed as shown in Fig. 3-2b. The latent heat emitted along the perturbation can escape very rapidly into the bulk liquid because of the divergence of the corresponding heat flow. As a result, the perturbation advances into the liquid at a faster rate than the remainder of the interface[†]. This shape instability ultimately develops into a long spike reaching into the liquid and is recognized as a primary dendrite arm. Because the approximately cylindrical trunk of the dendrite is undergoing radial growth while in contact with a supercooled liquid, it is unstable for the same reasons as the original planar solid-liquid interface. For this reason, the familiar dendrite branching phenomenon takes place and a structure similar to that in Fig. 3-3 results. In the present instance, the driving force for morphological breakdown is referred to as 'thermal' supersaturation because it is produced by quenching from a temperature above the melting point to one below it.

3.3.2 Solute Transport in an Isothermal Binary System

It is assumed that a precipitate phase (II) is growing into an initially uniformly supersaturated phase (I). Consider

---

[†]For the present qualitative discussion, the influences of surface energy (ie., capillarity) on the stability problem are not considered.

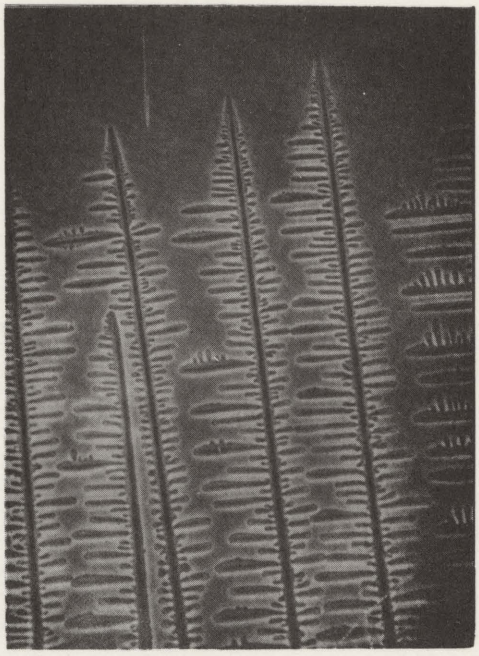

Fig. 3-3 Dendritic growth of carbon tetrabromide from the melt (from Jackson [33]) 150X.

the advance of a planar II-I interface, for which the corresponding solute distribution is shown in Fig. 3-4. Clearly the velocity of the interface is controlled by the rate at which solute is fed into the bulk matrix. Thus a perturbation advances forward at a much faster rate than the remainder of the interface because it can push solute into a greater volume of the matrix†. This phenomenon is often referred to as the point effect of diffusion. In solids the perturbation often develops into the Widmanstätten plate structure as shown in Fig. 3-5[34]. Because of strong crystallographic effects, no side branching occurs. As in the previous solidification example, the driving force for morphological breakdown is 'thermal' supersaturation (ie., supersaturation produced by quenching from a higher temperature into the I+II or II phase field). Furthermore, it is important to notice that the supersaturation increases (from zero at the interface, assuming local equilibrium) with distance ahead of the advancing solid-liquid and precipitate-matrix interfaces. It is this gradient of supersaturation which is responsible for magnification of a microscopic perturbation to a macroscopic alteration in the interface morphology.

---

†Similar conclusions apply to the case in which $(C^{I\ II}-C^{II\ I})<0$ and $(C^{I\ II}-C_{\infty})<0$ in Fig. 3-4.

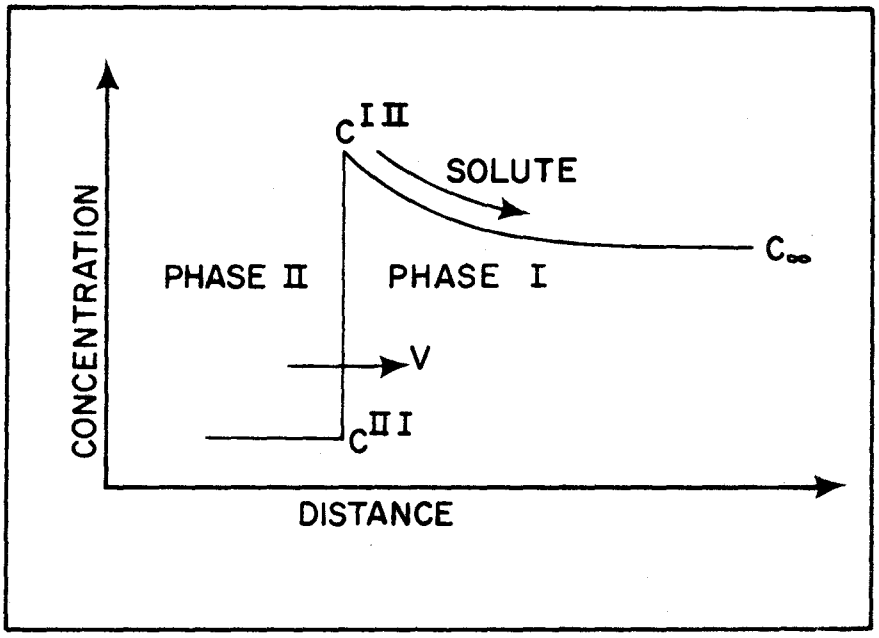

Fig. 3-4 Solute distribution during precipitate growth.

Fig. 3-5 Widmanstätten ferrite formation in Fe-0.235% C (from Townsend and Kirkaldy[34]) 685 X.

3.4 MORPHOLOGICAL BREAKDOWN INVOLVING TRANSPORT OF TWO ENTITIES

Certain phenomena involving transport of two entities are not generically different from the two cases already considered. Examples are dendrite growth in a binary system, which involves a thermal and a diffusion field, and Widmanstätten growth in a ternary system, which involves two diffusion fields. The driving force for morphological breakdown is again 'thermal' supersaturation, although it now acts simultaneously on the distributions of two entities. In the next sections attention is focussed on situations in which the driving force for morphological breakdown is not 'thermal' supersaturation.

3.4.1 Solute and Thermal Transport in a Binary System

Consider the steady state unidirectional solidification of a molten binary alloy of composition C_o. In the steady state, the composition of the solid being formed is the same as that of the bulk melt[35] and the solute distribution is as shown in Fig. 3-6b. On combining this with Fig. 3-6a, one can determine the variation of the equilibrium liquidus temperature ahead of the interface, Fig. 3-6c. Also shown is the actual temperature distribution in the liquid metal which is imposed by the growth conditions. If at a certain distance ahead of the interface the actual melt temperature

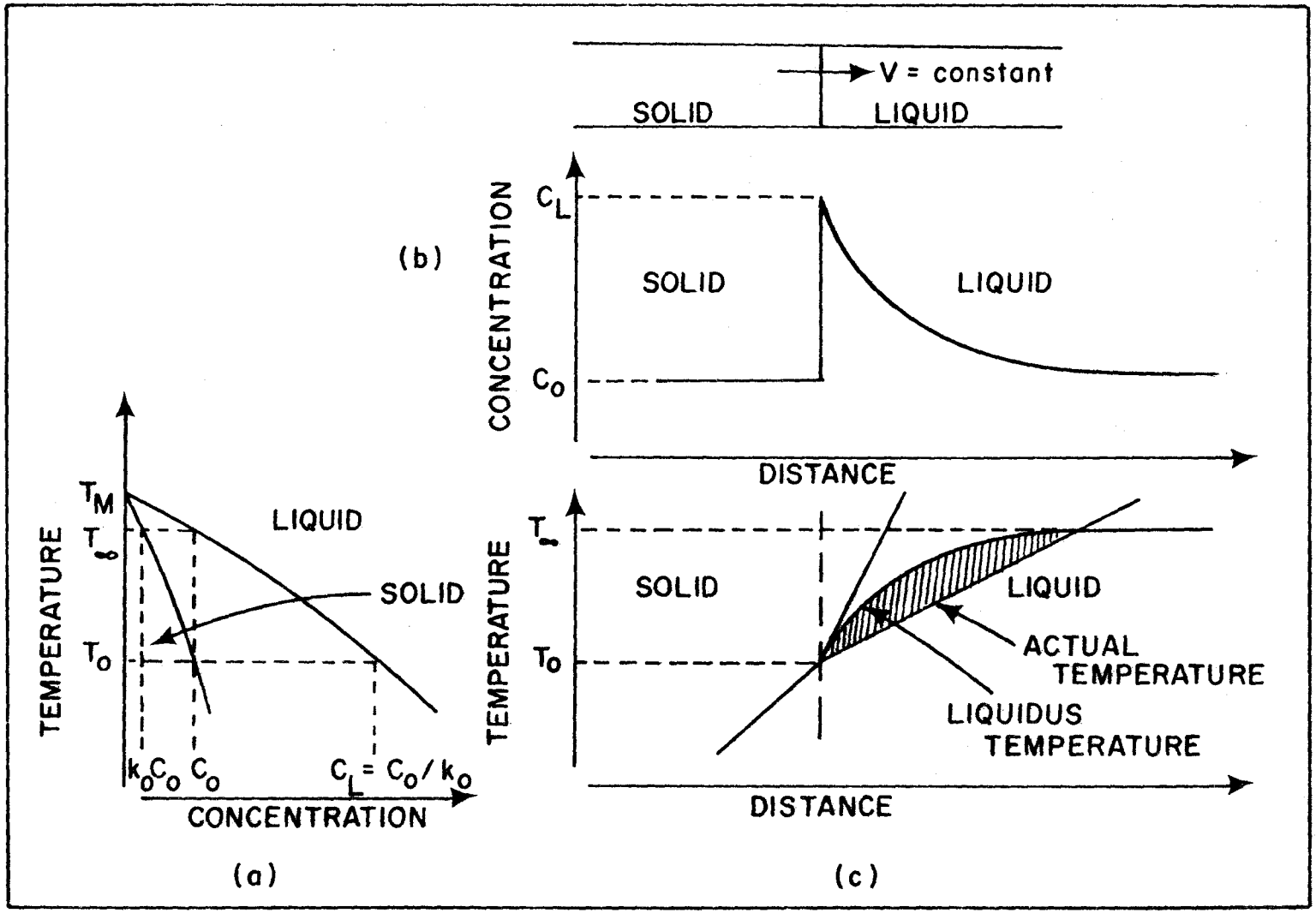

Fig. 3-6 (a) Phase diagram, (b) solute distribution and (c) temperature distribution corresponding to steady state unidirectional solidification of a molten binary alloy.

is lower than the equilibrium liquidus temperature, then the liquid at that point is said to be constitutionally supercooled. The possibility of developing supercooling in the above manner and its relationship to morphological breakdown was first recognized by Rutter and Chalmers[36].

The question arises as to whether or not a planar solid-liquid interface is stable when in contact with a constitutionally supercooled liquid region. Clearly the velocity of a solid-liquid interface increases as the degree of supercooling in the liquid volume element immediately adjacent to the interface is increased. Thus a perturbation in the shape of the interface corresponding to Fig. 3-6 will grow because in doing so it moves into regions of increased supercooling. Unlike the situations discussed in Sec. 3.3, the region of supercooling does not extend to infinity. As a result, the protrusion develops to a certain size and then ceases to grow. The result is the well known cellular structure first noted by Buerger[37] and shown in Fig. 3-7. One can see that the marginal state of instability is defined by tangency of the actual and equilibrium liquidus temperature distributions (as shown in Fig. 3-6c). This observation leads to the following stability criterion[35]

$$m_L G_C - G_T > 0 \qquad \text{(unstable)} \qquad (3\text{-}7)$$

where m_L is the slope (including sign) of the liquidus line

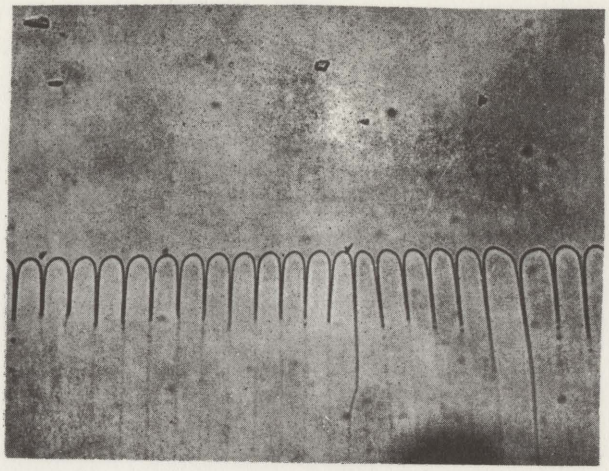

Fig. 3-7 Cellular growth of carbon tetrabromide containing a small amount of impurity (after Jackson[33]) 150 X.

and G_c and G_T are the interfacial concentration gradient and thermal gradient, respectively.

3.4.2 Solute Transport in an Isothermal Ternary System

Kirkaldy and Fedak[38] have noted that just as a conjoint diffusion field and thermal field under the proper circumstances can produce a constitutionally supercooled region, so it is possible to produce regions of (constitutional) supersaturation with two independent conjoint diffusion fields (ie., in an isothermal ternary system). Such a situation corresponds to the virtual diffusion path for a planar interface (see section 2.4) entering a two-phase field as indicated by the line P'Q' in Fig. 2-3†. Under these circumstances a planar interface would be in contact with a zone of supersaturated material and, therefore, one would expect a shape perturbation to grow (for reasons already discussed at length). This phenomenon will be analyzed in considerable detail in later chapters.

3.5 CONCLUDING REMARKS

It is clear that one could consider morphological breakdown in situations involving the transport of three or

---

†It is obvious that, depending on the terminal compositions and the nature of the system, the virtual diffusion path can dip into the two-phase field on neither, either or both sides of the interface.

more entities. However, it is unlikely that any principles are involved in the behaviour of these more complex systems, beyond those which appear in the examples in Secs. 3.3 and 3.4.

Thus far, attention has only been focussed on the question as to whether or not a driving force for morphological breakdown exists. This thermodynamic approach proves to be inadequate for developing a quantitative stability criterion because morphological breakdown is an irreversible process taking place in an open system. One must therefore consider the dynamics of the whole system during breakdown. It will transpire that, under certain circumstances, breakdown is not kinetically feasible even in the presence of a thermodynamic driving force. Alternatively, a system may be kinetically unstable in the absence of a thermodynamic driving force. A good example of the latter is the problem of oxide-alloy interface stability during oxidation of binary alloys[39,40].

At this point it should be noted that there are a number of intrinsic considerations in morphological breakdown which have yet to be considered in this chapter. One of these is the stabilizing influence of capillarity; formation of a perturbation results in an increase in total surface energy and therefore concomitant changes in the interfacial concentration or temperature (the Gibbs-Thompson effect) result in gradients which tend to annihilate the perturbation. Similarly, interface attachment kinetics, interface diffusion,

strain energy (in solids) and convective mixing (in liquids), all of which influence the dynamics of interface breakdown, have not been examined.

Perturbation theory provides a means of studying the dynamics of morphological breakdown and of accounting for the complications discussed in this section. It is the subject of the following chapter.

CHAPTER 4

LINEAR PERTURBATION THEORY

4.1 GENERAL INTRODUCTION†

The nature of stability problems is summarized by Sekerka when he says that "for a physical system to follow the course predicted by an idealized theoretical law, that course must not only be a correct one but must be preferred - or stable - with respect to all other possible courses accessible via the perturbations at hand"[20]. Perturbation theory is concerned with testing the stability of such a system by calculating the reaction of the system to small disturbances. Specifically, one asks: if the system is perturbed, will the perturbation decay, or will it grow in amplitude in such a way that the system progressively departs from a particular course predicted by the idealized physical law. Clearly, a system must be regarded as unstable even if there is only one special mode of disturbance with respect to which it is unstable. Alternatively, a system cannot be regarded as stable unless it is stable with respect to every possible mode of disturbance.

---

†This section is drawn largely from the first chapter of Chandrasekhar's treatise on hydrodynamic and hydromagnetic stability[41].

Mathematically, linear perturbation theory usually proceeds along the following lines. By supposing that the various physical variables (eg., temperature or composition) describing the idealized situation suffer infinitesimal increments, one first obtains the differential equations and boundary conditions governing these increments. The assumption of infinitesimal increments allows one to neglect all higher order and nonlinear terms,thus leaving only terms which are linear in the increments. Linear perturbation theory is based on such linearized equations, in contrast to nonlinear perturbation theory which attempts to allow for perturbations of finite amplitude.

As was explained earlier, it is necessary that the reaction of the system to all possible disturbances be examined. This is accomplished by expressing an arbitrary perturbation as a superposition of a complete set of normal modes[†]. Then one examines the stability of the system with respect to each of these normal modes. The latter is valid because the perturbation equations are linear and therefore the reaction of the system can be determined from the reaction of the system to each of the normal modes. In particular, the

---

[†]The arbitrary perturbation is expanded in an infinite series of orthogonal functions. Depending on geometrical symmetry considerations, the set of orthogonal functions might be sines and cosines, Bessel functions, spherical harmonics, etc.

stability of the system will depend on its stability to all normal modes; instability will follow from instability to even one normal mode.

Following Chandrasekhar[41], let the various modes appropriate to a particular problem be distinguished by the symbol $\underline{k}$. If $A(\vec{r},t)$ is the amplitude of an arbitrary perturbation, then one can symbolically expand it in the manner

$$A(\vec{r},t) = \int A_{\underline{k}}(\vec{r},t)\, d\underline{k} \qquad (4\text{-}1)$$

or in the alternative manner

$$A(\vec{r},t) = \sum_{\underline{k}} A_{\underline{k}}(\vec{r},t) \qquad (4\text{-}2)$$

where $A_{\underline{k}}(\vec{r},t)$ is the amplitude of the $\underline{k}^{th}$ normal mode. The (linear) differential equations governing the arbitrary perturbation can be specialized for application to the normal modes. One can then eliminate the dependence on time by seeking solutions of the form

$$A_{\underline{k}}(\vec{r},t) = A_{\underline{k}}(\vec{r})\, e^{p_{\underline{k}}t} \qquad (4\text{-}3)$$

where $p_{\underline{k}}$ is a constant whose value depends on the particular mode (as distinguished by $\underline{k}$). In general $p_{\underline{k}}$ is a complex number. However, for present purposes, it is sufficient to assume it is real. With the dependence on time separated in this manner, the perturbation equations will involve $p_{\underline{k}}$ as a parameter. The requirement that the equations allow non-trivial solutions satisfying the various boundary con-

ditions leads directly to an eigenvalue problem for $p_{\underline{k}}$. The overall stability problem is thus reduced to determining $p_{\underline{k}}$ for the various modes. The condition for stability is that $p_{\underline{k}}$ be negative for all $\underline{k}$ (cf., Eq. (4-3).

4.2 PHASE INTERFACE STABILITY

Although perturbation methods are useful in many areas of applied mathematics (see for example Cole[42]),fluid dynamical problems, for obvious reasons, have attracted the most attention[41,43,44]. The analysis of phase interface stability via linear perturbation theory is a relatively recent development.

To this writer's knowledge, the first application of perturbation methods to a problem of phase interface stability was due to Wagner[45] who in 1954 considered the decay of a perturbation in the planar surface of an electrode undergoing electropolishing. Shortly after completing this study, Wagner undertook to analyze a much more complex stability problem. He used linear perturbation methods to examine the stability of a planar oxide-alloy interface during the oxidation of binary alloys[40]. The methods employed by Wagner were sufficiently refined that they could have been readily applied to other phase interface stability problems, such as were discussed in the previous chapter. However, his work for a time passed unnoticed. Thus, seven years later and

independently of Wagner, Mullins and Sekerka used perturbation methods in their celebrated papers on the morphological stability of a spherical particle growing by diffusion or heat flow[46] and on the stability of a planar interface during solidification of a dilute binary alloy[47]. Also independently of both Wagner and Mullins and Sekerka, Voronkov[48] used perturbation methods to treat the latter problem.

The work of Mullins and Sekerka awakened considerable interest in various aspects of phase interface stability and a flood of theoretical articles followed. A recent review paper by Sekerka[20] can be used as an entry into this literature.

In applying perturbation methods to problems relating to phase interface stability, one proceeds essentially as outlined in the previous section. However, whereas the perturbation is generally applied to the solutions of the field equations, in treating interface stability it is convenient (although not necessary) to apply the perturbation to the interface itself. If the interface perturbation is expanded as an infinite series of orthogonal functions and if the corresponding perturbation in the thermal or diffusion field is expanded in terms of the same functions, then since the perturbation field equations and boundary conditions have been linearized, there is a one to one correspondence between the coefficients in the two expansions. Hence, although it is

conceptually convenient to focus attention on the interface perturbation, rather than the field perturbation, the examination of either will lead to the same stability criterion.

The fact that consideration of very small perturbations results in the linearization of all perturbation equations has been discussed in the previous section. Nevertheless, with respect to phase interface stability it should be pointed out that the field equations (eg., Eqs. (2-18) and (3-1)) are linear anyway and therefore they are comparatively easy to handle. However, as discussed in Sec. 3.2, the mass and heat conservation conditions are in general nonlinear. For this reason, linearization is necessary.

4.3 PLANAR INTERFACE STABILITY†

In this dissertation, the stability of planar interfaces is of principle concern. Therefore, the interface stability problem is now more carefully examined for such a geometry.

At time t=0, assume that a planar II-I phase interface is in unidirectional motion at velocity V as shown in Fig. 4-1. The x-z* reference frame moves with the interface. A perturbation is introduced into the shape of the interface such that

$$z^* = \phi(x,t) \qquad (4\text{-}4)$$

†Some parts of this section follow Sekerka's review article[20].

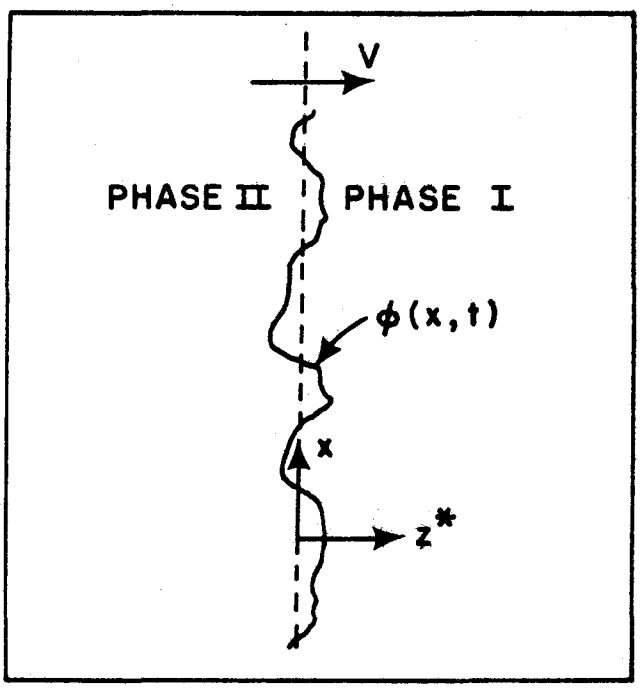

Fig. 4-1 An originally planar interface into which a perturbation, $\phi(x,t)$, is introduced. The x-z* coordinate frame is attached to the original interface.

for $t>0$. As has been already discussed at length, restriction to perturbations of very small amplitude results in linearization of the problem. Thus it is convenient to deal with the Fourier transform of $\phi(x,t)$

$$\bar{\phi}(\omega,t) = \int_{-\infty}^{\infty} e^{-i\omega x}\, \phi(x,t)\,dx \qquad (4\text{-}5)$$

whose inverse is

$$\phi(x,t) = \frac{1}{2\pi} \int_{-\infty}^{\infty} e^{i\omega x}\, \bar{\phi}(\omega,t)\,d\omega \qquad (4\text{-}6)$$

where $\omega = 2\pi/\lambda$ is the spatial frequency and λ is the corresponding wave length. Clearly Eq. (4-6) corresponds to Eq. (4-1) of Sec. 4.1. In carrying out calculations, it is sufficient to deal with a sinusoidal perturbation, $\phi(x,t) = \delta(\omega,t)\sin \omega x$, of amplitude $\delta(\omega,t) \equiv \bar{\phi}(\omega,t)$ and arbitrary spatial frequency ω. As suggested by Eq. (4-3), one seeks solutions of the form

$$\delta(\omega,t) \equiv \bar{\phi}(\omega,t) = \bar{\phi}_o(\omega)e^{f(\omega)t} \qquad (4\text{-}7)$$

where $\bar{\phi}_o(\omega)$ is the Fourier transform of the initial perturbed shape of the interface (or alternatively, the initial amplitude of the sinusoidal perturbation). In view of Eq. (4-7), it is clear that the stability of the interface depends on the sign of $f(\omega)$. The determination of this function is, of course,

the central problem. Substitution of Eq. (4-7) into (4-6) yields

$$\phi(x,t) = \frac{1}{2\pi} \int_{-\infty}^{\infty} e^{i\omega x} \bar{\phi}_o(\omega) e^{f(\omega)t} d\omega \qquad (4\text{-}8)$$

Whereas analysis of $f(\omega)$ yields an interface stability criterion, Eq. (4-8) gives the time evolution of the interface shape.

Typical sketches of $f(\omega)$ versus ω are shown in Fig. 4-2. For stability to obtain, $f(\omega)$ must be negative for all ω (case (b)). The shape of the curve for unstable situations (case (a)) indicates that normal modes close to the limits $\omega \to 0$ and $\omega \to \infty$ all decay out. For ω very small, the wavelength of the corresponding mode is very large. Hence there is insufficient time for the lateral transport which is required to sustain such harmonics and they decay out. For ω very large, the corresponding normal mode has a very short wavelength. The surface area increase , and hence total surface energy increase , with respect to a planar interface is so great that these modes also decay out. The fastest growing mode, ω_{max} in Fig. 4-2, reflects a balance between the kinetic or thermodynamic driving force for instability and the two stabilizing influences just discussed.

At this juncture it is convenient to introduce certain technical matters. As was just mentioned, the problem of

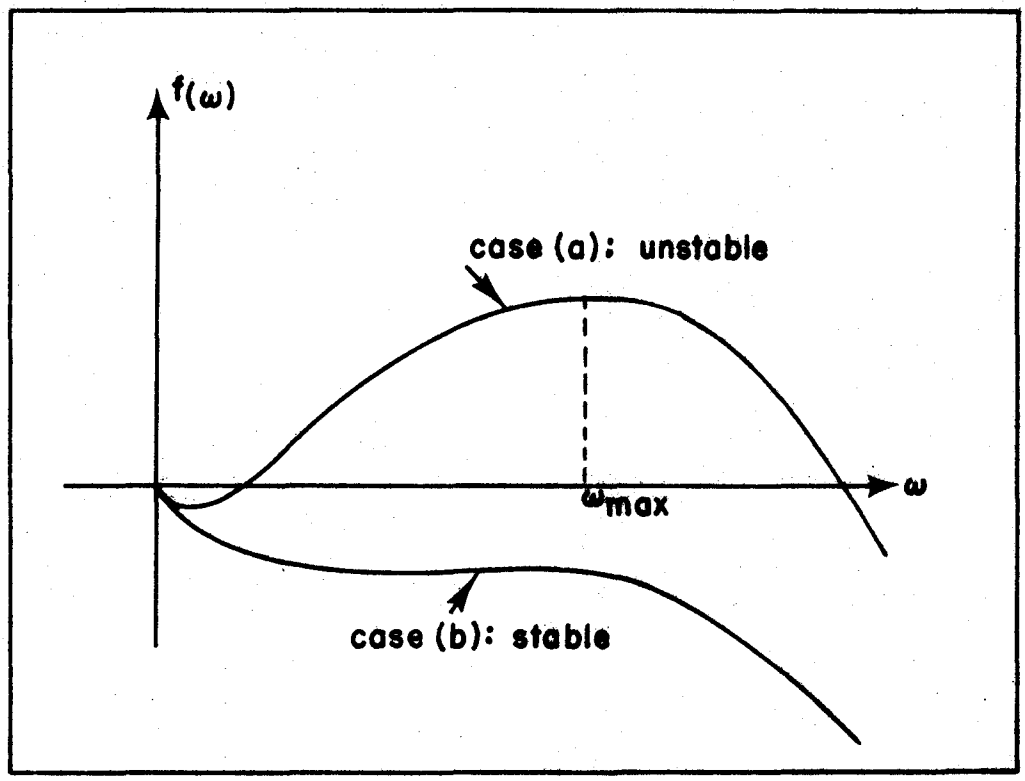

Fig. 4-2 Two possibilities for the function f(ω).

calculating $f(\omega)$ is approached by considering a sinusoidal disturbance $z^* = \delta(\omega,t)\sin\omega x$ and seeking to calculate $\delta(\omega,t)$. One commences by applying the boundary conditions of the problem to this shape. The next step is to solve the field equations subject to these conditions. For illustrative purposes consider Eq. (2-18), which for a stationary x-z reference frame is

$$\left(\frac{\partial^2}{\partial x^2} + \frac{\partial^2}{\partial z^2}\right)\tilde{C} = \frac{1}{D}\frac{\partial \tilde{C}}{\partial t} \qquad (4\text{-}9)$$

where $\tilde{C}$ refers to that part of the diffusion field corresponding to the perturbation. Noting that the relationship between the x-z frame and the moving x-z* frame of Fig. 4-1 is simply

$$z^* = z - Vt, \qquad (4\text{-}10)$$

Eq. (4-9) can be transformed to

$$\left(\frac{\partial^2}{\partial x^2} + \frac{\partial^2}{\partial z^{*2}} + \frac{V}{D}\frac{\partial}{\partial z^*}\right)\tilde{C} = \frac{1}{D}\frac{\partial \tilde{C}}{\partial t}\,. \qquad (4\text{-}11)$$

If $D^{-1}\,\partial\tilde{C}/\partial t$ in Eq. (4-11) is neglected, one obtains a quasi-steady state transport equation. It has been demonstrated by Sekerka[49,50] and Delves[51,52] that one can safely use solutions of the steady state equation, rather than the complete field equation (4-11), in order to calculate a stability

criterion†. If both $D^{-1}\,\partial\tilde{C}/\partial t$ and $VD^{-1}\,\partial\tilde{C}/\partial z^*$ are neglected in Eq. (4-11), one is left with Laplace's equation. Clearly solutions of Laplace's equation are equivalent in both the moving x-z* and stationary x-z reference frames if the frames are coincident at the given instant of time. This is the case at time t=0 when the perturbation is introduced (Eq.(4-10)) and therefore ignoring $VD^{-1}\,\partial\tilde{C}/\partial z^*$ and $D^{-1}\,\partial\tilde{C}/\partial t$ in Eq. (4-11) is equivalent to ignoring $D^{-1}\,\partial\tilde{C}/\partial t$ in Eq. (4-9). Solutions of Laplace's equation can be used to obtain a stability criterion if the average velocity of the interface is slow enough that the diffusion field in the vicinity of the perturbed interface is essentially the same as for a stationary interface subject to the same boundary conditions. Sekerka[50] examined interface stability for an isothermal binary phase transformation and found that the stability criteria based on the time-dependent field equation, the steady state equation and the Laplace equation were in exact agreement.

Once the field equations have been solved, one is in a position to calculate $\delta(\omega,t)$ (and hence $f(\omega)$). The velocity of the perturbed interface is given by

$$v(x) = \frac{dz}{dt} = V + \frac{d\delta(\omega,t)}{dt} \sin\omega x \qquad (4\text{-}12)$$

and therefore because substitution of the solutions to the

---

†This is not the case however, if one is concerned with the time evolution of perturbations[50].

field equations into the appropriate conservation boundary conditions yields $v(x)$, $\frac{d\delta}{dt}(\omega,t)$ can be calculated directly. It transpires that $d\delta/dt$ is directly proportional to δ and on integration leads to an equation of the form of Eq. (4-7). This yields $f(\omega)$ and hence the desired stability criterion.

CHAPTER 5

PRECIPITATE-MATRIX INTERFACE STABILITY IN DILUTE TERNARY SYSTEMS

5.1 INTRODUCTION

In Sec. 3.3.2, the physical structure of the problem of precipitate-matrix interface stability was discussed for binary systems. Numerous perturbation analyses of this problem have been made so as to assess the influence of capillarity[46], strain energy[53], interface reaction kinetics[53,54,55] and surface diffusion[53,56] upon the morphological stability of such systems. However, very little attention has been directed towards the study of this problem in ternary systems. Using qualitative arguments, Shewmon[53] has suggested that, provided local equilibrium prevails at the interface, the concentration gradient of a second solute will tend to give instability in the same manner that a single solute's does. Unfortunately, studies of diffusing ternary systems often mask subtleties and lead to naive conclusions when they proceed by rigorously analyzing a binary system and then qualitatively considering the effect of adding a second solute rather than by formulating the ternary problem at the outset and making a rigorous analysis.

In the present chapter, perturbation methods are utilized to investigate the stability of the interface between a growing precipitate and an initially uniformly supersaturated matrix. In particular, consider ternary systems for which the dilute corner of the corresponding phase diagram isotherm has a form as shown in Fig. 5-1. The phases I and II are dilute solutions of components 1 and 2 in component 3. It is considered that a quench from phase I into the (I+II) phase field has been made thus precipitating phase II from a supersaturated matrix.

The principal physical assumption is that local equilibrium is maintained at the precipitate-matrix interface. Hence the analysis is not applicable to the initial period of growth for which the interface reaction controls the transformation rate. The solute diffusion fields are permitted to interact in each phase and it is assumed that the corresponding diffusion coefficients are all concentration independent. To simplify the mathematics, a linear geometry is used; ie., the stability of a planar interface in unidirectional motion is considered. Prior to breakdown of this interface, the precipitate is assumed to be of homogeneous composition. However, once the planar interface is perturbed, diffusion in both the matrix and precipitate is considered.

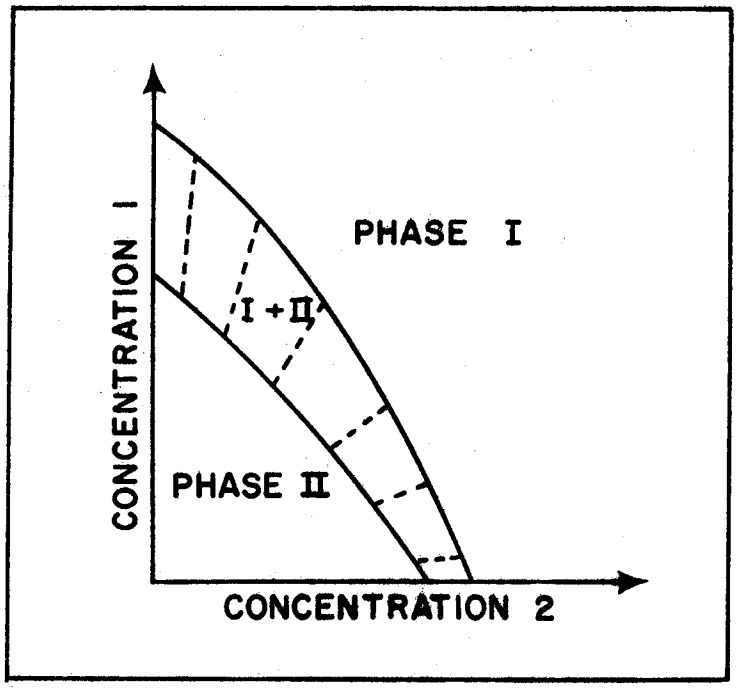

Fig. 5-1 Phase diagram corresponding to a system in which phases I and II are dilute solutions of components 1 and 2 in component 3.

5.2 PERTURBATION ANALYSIS

Consider a planar precipitate-matrix interface, in unidirectional motion, at time t. The position of the interface and concentration distributions in the matrix can be determined from Eqs. (2-25) to (2-29). It is assumed that the interface is coincident with the x-axis of a stationary coordinate system whose z-axis is directed towards the matrix I. In Sec. 4.1 it was pointed out that it is convenient to express an arbitrary perturbation as a superposition of a complete set of normal modes and then to examine the stability of the system with respect to each of these normal modes. Thus in the present situation one follows the methodology outlined in Sec. 4.3. An interfacial perturbation of arbitrary shape is analyzed into sinusoidal Fourier components and the stability of the interface with respect to a sinusoidal perturbation of arbitrary wave length is examined. Accordingly a sinusoidal perturbation of infinitesimal amplitude δ is introduced into the shape of the interface such that the equation of the latter becomes

$$z = \delta(\omega,t)\sin\omega x = \phi(x,t) \qquad (5\text{-}1)$$

where $\omega = \frac{2\pi}{\lambda}$ is the spatial frequency of the perturbation and λ is the wavelength. The object now is to establish whether the perturbation grows or decays and hence whether or not the originally planar interface is stable. To this

end, the concentration distributions of the two independent components (1 and 2) in each phase must be found for the vicinity of the perturbed interface. For regions adjacent to the interface, one can write expressions for these concentration distributions as follows:

$$C_i^m = C_i^{mn} + G_i^{mn} z + \tilde{C}_i^m \qquad (5\text{-}2)$$

where C_i^{mn} ($i = 1,2$; $m \neq n = I,II$) is the concentration of component i in phase m at a planar m-n interface, G_i^{mn} ($i = 1,2$; $m \neq n = I,II$) is the corresponding interfacial concentration gradient, and $\tilde{C}_i^m$ ($i = 1,2$; $m = I,II$) is the disturbance in the diffusion field of i which results from the perturbation. It is to be noted that: (a) the $\tilde{C}_i^m$ must go to zero as $z \to \pm\infty$, (b) $G_1^{II\ I} = G_2^{II\ I} = 0$ because the precipitate is of uniform composition before introduction of the perturbation and (c) the C_i^{mn} and $G_i^{I\ II}$ are obtained from Eqs. (2-25) to (2-29) which determine the solutions corresponding to a planar interface. The $\tilde{C}_i^m$ are solutions of Fick's second law, Eqs. (2-10) and (2-11). It is assumed the average interface advances at a slow enough rate and the perturbation grows or decays slowly enough that one can ignore the time derivatives in Eqs. (2-10) and (2-11). Under such conditions, it follows that the four $\tilde{C}_i^m$ must be solutions of Laplace's equation

$$\nabla^2 \tilde{C}_i^m = 0 \quad . \qquad (5\text{-}3)$$

It was noted earlier that Sekerka[50] demonstrated that Laplacian and complete time-dependent solutions lead to the same stability criterion for precipitate-matrix interfaces in binary systems. This suggests that use of Laplacian solutions will lead to a good approximation in the present more complicated situation.

The following boundary conditions are assumed:

i) Local equilibrium must be maintained at every position along the perturbed interface $z = \phi(\kappa,t)$. To express this boundary condition in mathematical form, it is first assumed that

$$\frac{C_{i\phi}^{II}}{C_{i\phi}^{I}} = k_i \qquad (5\text{-}4)$$

where the $C_{i\phi}^{m}$ ($i = 1,2$; $m = I,II$) are the interface concentrations at a point on the perturbed interface and the solute partition coefficients k_1 and k_2 (assumed constant) are given by the corresponding concentration ratios for a planar interface†. Assumption (5-4) is supported by a recent analysis of terminal phase equilibria in ternary systems[57] which indicates that two-phase fields in the dilute corner of ternary

---

†That is to say $k_i \equiv C_i^{II\ I}/C_i^{I\ II}$. Clearly k_1 and k_2 are specified by the unique tie-line on the appropriate ternary isotherm (as determined by the solutions for a planar interface, Eqs. (2-25) to (2-29)).

isotherms are characterized by constant solute partition coefficients. The next step is to account for the effect of curvature (capillarity) on the interface concentrations. In Appendix I, the following Gibbs-Thomson type equation for a dilute ternary system, having a constitution as shown in Fig. 5-1, is derived:

$$(C^{I}_{1\phi} - C^{I\ II}_{1})(k_1 - 1) + (C^{I}_{2\phi} - C^{I\ II}_{2})(k_2 - 1) = \psi\delta\omega^2 \sin\omega x \quad (5\text{-}5)$$

where $\psi = \sigma/RT$, σ is the interfacial free energy, R is the gas constant and T is the absolute temperature. Together, Eqs. (5-4) and (5-5) constitute the local equilibrium boundary condition.

ii) The following mass balance boundary conditions apply to every position along the perturbed interface:

$$v(x) = [D^{I}_{11}(\frac{\partial C^{I}_{1}}{\partial z})_{\phi} + D^{I}_{12}(\frac{\partial C^{I}_{2}}{\partial z})_{\phi} - D^{II}_{11}(\frac{\partial C^{II}_{1}}{\partial z})_{\phi} - D^{II}_{12}(\frac{\partial C^{II}_{2}}{\partial z})_{\phi}]/C^{I}_{1\phi}(k_1 - 1) \quad (5\text{-}6)$$

$$= [D^{I}_{21}(\frac{\partial C^{I}_{1}}{\partial z})_{\phi} + D^{I}_{22}(\frac{\partial C^{I}_{2}}{\partial z})_{\phi} - D^{II}_{21}(\frac{\partial C^{II}_{1}}{\partial z})_{\phi} - D^{II}_{22}(\frac{\partial C^{II}_{2}}{\partial z})_{\phi}]/C^{I}_{2\phi}(k_2 - 1) \quad (5\text{-}7)$$

where v(x) is the local velocity of the perturbed interface. It should be noted that for a planar interface v(x) = V and Eqs. (5-6) and (5-7) reduce to

$$V = \frac{D^{I}_{11}\ G^{I\ II}_{1} + D^{I}_{12}\ G^{I\ II}_{2}}{C^{I\ II}_{1}\ (k_1 - 1)} = \frac{D^{I}_{21}\ G^{I\ II}_{1} + D^{I}_{22}\ G^{I\ II}_{2}}{C^{I\ II}_{2}\ (k_2 - 1)} \quad (5\text{-}8)$$

noting that there are no concentration gradients in the precipitate adjacent to a planar interface.

Solutions of Eq. (5-3) which vanish at distances far removed from the perturbed interface and which, when introduced into Eq. (5-2), yield expressions which to the first order in δ satisfy Eqs. (5-4) and (5-5) are determined. These expressions for the concentration distributions in the vicinity of the perturbed interface are

$$C_1^{II} = C_1^{II\ I} + k_1\left[\frac{\psi\omega^2}{k_1-1} - \left(\frac{k_2-1}{k_1-1}\right) A\right]\delta \sin\omega x\ e^{\omega z} \qquad (5\text{-}9)$$

$$C_2^{II} = C_2^{II\ I} + k_2\ A\ \delta \sin\omega x\ e^{\omega z} \qquad (5\text{-}10)$$

$$C_1^{I} = C_1^{I\ II} + G_1^{I\ II}\ z + \left[\frac{\psi\omega^2}{k_1-1} - \left(\frac{k_2-1}{k_1-1}\right)A - G_1^{I\ II}\right]\delta \sin\omega x\ e^{-\omega z} \qquad (5\text{-}11)$$

$$C_2^{I} = C_2^{I\ II} + G_2^{I\ II}\ z + (A - G_2^{I\ II})\delta \sin\omega x\ e^{-\omega z} \qquad (5\text{-}12)$$

The constant A is obtained by substituting Eqs. (5-9) - (5-12) into the mass balances (5-6) and (5-7) and equating the latter to give

$$A = \psi\omega^2[V(k_1-1)(k_2-1)C_2^{I\ II} + \omega C_2^{I\ II}(k_2-1)\bar{D}_{11} - \omega C_1^{I\ II}(k_1-1)\bar{D}_{21}]/$$
$$\left[\begin{array}{l} V[C_1^{I\ II}(k_1-1)^2(k_2-1) + C_2^{I\ II}(k_1-1)(k_2-1)^2]+ \\ \omega\{(k_2-1)[C_2^{I\ II}(k_2-1)\bar{D}_{11} - C_1^{I\ II}(k_1-1)\bar{D}_{21}] - (k_1-1) \\ [C_2^{I\ II}(k_2-1)\bar{D}_{12} - C_1^{I\ II}(k_1-1)\bar{D}_{22}]\} \end{array}\right] \qquad (5\text{-}13)$$

where

$$\bar{D}_{ij} = D_{ij}^{I} + k_j\ D_{ij}^{II} \qquad (i = 1,2;\ j = 1,2) \qquad (5\text{-}14)$$

The derivative of the amplitude of the perturbation is given by Eq. (4-12). The right hand side of Eq. (4-12) can be equated to either of Eqs (5-6) or (5-7); Eq. (5-7) is arbitrarily chosen. Accordingly, Eqs. (5-9) - (5-13) are substituted into (5-7) and everything is expanded to the first order in δ. Then the coefficient of sin ωx is equated to $\frac{d\delta}{dt}$ in Eq. (4-12) to give the following result after rearranging with Eq. (5-8):

$$\frac{d\delta/dt}{\delta} = \omega V - \frac{\psi\omega^2}{(k_1-1)(k_2-1)} \times$$

$$\left\{ \frac{V^2(k_1-1)(k_2-1)+\omega V[(k_2-1)\bar{D}_{11}+(k_1-1)\bar{D}_{22}]+\omega^2(\bar{D}_{11}\bar{D}_{22}-\bar{D}_{12}\bar{D}_{21})}{C_1^{I\ II}[V(k_1-1)+\omega(\frac{k_1-1}{k_2-1})\bar{D}_{22}-\omega\bar{D}_{21}]+C_2^{I\ II}[V(k_2-1)+\omega(\frac{k_2-1}{k_1-1})\bar{D}_{11}-\omega\bar{D}_{12}]} \right\} \tag{5-15}$$

In a binary system, a necessary condition for approximating the perturbation function $\tilde{C}$ (corresponding to $\tilde{C}_i^m$ in Eq. (5-2)) with a solution of Laplace's equation is, for a linear geometry, that[40,47]

$$\omega >> \frac{V}{\bar{D}} \quad . \tag{5-16}$$

In the second chapter it was seen that solutions to the ternary diffusion equations, (2-10) and (2-11), can be constructed from solutions of a set of equations, (2-13), which are the binary diffusion equation, (2-18), with the binary diffusion coefficient replaced by the eigenvalues u_k, Eq. (2-17). In analogy with this, the inference is that for

the ternary system, necessary conditions for solutions of Eq. (5-3) to be valid are

$$\omega >> \frac{V}{u_k^m} = \frac{V}{\frac{1}{2}\{(D_{11}^m+D_{22}^m) \pm \sqrt{(D_{11}^m-D_{22}^m)^2+ 4D_{12}^m D_{21}^m}\}} \quad (k=1,2;m=I,II) \quad (5\text{-}17)$$

For dilute ternary solutions, one can demonstrate[58] that the ratio D_{ij}/D_{ii} is of the same order of magnitude as N_i, the mole fraction of component i. As a result, the term $4D_{12}^m D_{21}^m$ is second order with respect to the other terms in Eq. (5-17). Thus for dilute ternary systems, the eigenvalues $u_k^m \rightarrow D_{kk}^m$ and the necessary conditions for the $\tilde{C}_i^m$ in Eq. (5-2) to be approximated by solutions of (5-3) are simply

$$\omega >> \frac{V}{D_{kk}^m} . \quad (5\text{-}18)$$

By employing relations (5-14), it can easily be demonstrated that relations (5-18) imply that the final term dominates the initial two terms in the numerator of the second term of Eq. (5-15). Similarly, one can show that in the corresponding denominator the first term in each of the two sets of square brackets is dominated by the second term. Thus, application of conditions (5-18) allows (5-15) to be simplified to

$$\frac{d\delta/dt}{\delta} = \omega \left\{ \begin{array}{l} V - \psi\omega^2 \, (\bar{D}_{11}\bar{D}_{22} - \bar{D}_{12}\bar{D}_{21})/ \\ \{(k_1-1)C_1^{I\ II}[(k_1-1)\bar{D}_{22} - (k_2-1)\bar{D}_{21}] + \\ (k_2-1)C_2^{I\ II}[(k_2-1)\bar{D}_{11} - (k_1-1)\bar{D}_{12}]\} \end{array} \right\}$$

$$= f(\omega). \qquad (5\text{-}19)$$

This result is the focus of attention for the remainder of this chapter. Notice that on integration, Eq. (5-19) has the same form as Eq. (4-7). For a reasonable set of system parameters, a graph of the right side of Eq. (5-19) versus ω would be very similar in form to one of the cases shown in Fig. 4-2.

5.3 DISCUSSION

To analyze Eq. (5-19), it is convenient to first consider the corresponding binary equation. If the concentration of component 2 is zero, $C_2^{I\ II} = 0$ and the second term in the denominator of Eq. (5-19) vanishes. Furthermore, it can be demonstrated that in general as $C_i \to 0$ then $D_{ij} \to 0$ $(i \neq j)$[†](59)

[†]Consider the equation for the unidirectional flux of component 2:

$$J_2 = -D_{21}\frac{\partial C_1}{\partial z} - D_{22}\frac{\partial C_2}{\partial z}$$

Clearly J_2 must vanish as $C_2 \to 0$. Therefore, D_{21} must also vanish as $C_2 \to 0$.

and therefore when component 2 is absent $\bar{D}_{21} = 0$. Hence, in the limit $C_2 \to 0$, Eq. (5-19) reduces to (dropping the subscript 1)

$$f(\omega) = \omega(V - \frac{\psi\omega^2\bar{D}}{C^{I\ II}(k-1)^2}) \tag{5-20}$$

$$= \omega V(1 - \frac{\psi\omega^2}{(k-1)G^{I\ II}}[1 + \frac{C^{II\ I}D_D^{II}}{C^{I\ II}D_D^{I}}]) \tag{5-21}$$

Eq. (5-21) is obtained from (5-20) by noting that for a binary system Eq. (5-4) reduces to $C^{II\ I} = kC^{I\ II}$, Eq. (5-14) becomes $\bar{D} = D^I + kD^{II}$ and Eq. (5-8) yields

$$V = \frac{D^I G^{I\ II}}{C^{I\ II}(k-1)} \tag{5-22}$$

Eq. (5-21) differs slightly from the corresponding result obtained by Shewmon[53] who treated the binary problem in detail. His calculations are applicable to situations in which the matrix is a dilute solution of component 1 and the precipitate is essentially pure component 1, whereas in the present calculations both the precipitate and matrix are assumed to be dilute solutions of component 1. To obtain Shewmon's result, one simply replaces $1/(k-1)$ in Eq. (5-21) with $C^{I\ II}\Omega$ where Ω is the molar volume of the precipitate.

The first term in Eq. (5-21) is always positive and therefore favours instability. It reflects the so-called point effect of diffusion (see Sec. 3.3.2) which for

$(C^{I\ II} - C^{II\ I}) > 0$ arises out of the divergence of diffusional flux away from interfacial perturbations and hence results in the amplification of such disturbances. The second term in Eq. (5-21) is negative and represents the stabilizing influence of capillarity which sets up concentration gradients along the interface in a direction opposing the point effect of diffusion (in an effort to minimize the total surface energy of the system). Situations in which diffusion in the precipitate is unimportant arise if $C^{II\ I}{}_D{}^{II} << C^{I\ II}{}_D{}^{I}$. In these cases the terms in the square brackets of Eq. (5-21) reduce to unity.

Having examined the binary limit, return to the general ternary result, Eq. (5-19). The first term in this expression is always positive and just as in the binary case Eq. (5-21), it reflects the enhancement of instability due to the point effect of diffusion. In the second term, one can see that the numerator is positive since $\bar{D}_{12}\bar{D}_{21}$ is usually second order with respect to $\bar{D}_{11}\bar{D}_{22}$. Indeed, it is easily demonstrated that for dilute ternary systems, the numerator reduces to $\bar{D}_{11}\bar{D}_{22}$ if k_1 and k_2 are of the same order of magnitude and second order terms are discarded. If k_1 and k_2 are not of the same order of magnitude,the numerator can not be simplified in such a manner, although it is undoubtedly positive. Still with the second term of Eq. (5-19), one can see that the

first and third terms in the denominator, $(k_1-1)^2 C_1^{I\ II} \bar{D}_{22}$ and $(k_2-1)^2 C_2^{I\ II} \bar{D}_{11}$ respectively, are positive. The second and fourth terms are usually both positive or both negative since in general $D_{ij}D_{ji} > 0$. However these latter two terms are of a lower order of magnitude than the first and third terms (because D_{ij}/D_{ii} is of the same order as N_i for dilute solutions) and therefore the denominator is generally positive. Accordingly the whole second term of Eq. (5-19) (including the factor $-\psi\omega^2$) is negative which reflects the stabilizing influence of capillarity. Hence one can see that with respect to the influences of capillarity and the point effect of diffusion, Eq. (5-19) has the same general features as (5-21).

It is of interest to consider Eq. (5-19) in certain limiting situations. First assume that $k_j D_{ij}^{II} << D_{ij}^{I}$ $(i = 1,2;$ $j = 1,2)$ and therefore, from Eq. (5-14), $\bar{D}_{ij}$ reduces to D_{ij}^{I}. For this limit, which corresponds to negligible influence due to diffusion in the precipitate, Eq. (5-19) can be written in the form

$$f(\omega) = \omega\left(V - \psi\omega^2\left\{\frac{(k_1-1)\left[C_1^{I\ II}(k_1-1)D_{22}^{I} - C_2^{I\ II}(k_2-1)D_{12}^{I}\right]}{D_{11}^{I}D_{22}^{I} - D_{12}^{I}D_{21}^{I}}\right.\right.$$
$$\left.\left. + \frac{(k_2-1)\left[C_2^{I\ II}(k_2-1)D_{11}^{I} - C_1^{I\ II}(k_1-1)D_{21}^{I}\right]}{D_{11}^{I}D_{22}^{I} - D_{12}^{I}D_{21}^{I}}\right\}^{-1}\right) \quad (5\text{-}23)$$

From Eq. (5-8), one can solve simultaneously these two independent equations and obtain the following expressions for $G_1^{I\ II}$ and $G_2^{I\ II}$:

$$G_1^{I\ II} = \frac{V[D_{22}^I\ C_1^{I\ II}(k_1-1) - D_{12}^I\ C_2^{I\ II}(k_2-1)]}{D_{11}^I\ D_{22}^I - D_{12}^I\ D_{21}^I} \quad (5\text{-}24)$$

$$G_2^{I\ II} = \frac{V[D_{11}^I\ C_2^{I\ II}(k_2-1) - D_{21}^I\ C_1^{I\ II}(k_1-1)]}{D_{11}^I\ D_{22}^I - D_{12}^I\ D_{21}^I} \quad (5\text{-}25)$$

Substitution of these expressions into Eq. (5-23) leads to

$$f(\omega) = \omega V\left(1 - \frac{\psi\omega^2}{(k_1-1)G_1^{I\ II} + (k_2-1)G_2^{I\ II}}\right) \quad (5\text{-}26)$$

Keeping in mind that this result applies to situations in which diffusion in the precipitate is negligible, one can compare it with the corresponding binary result. Thus in the limit $C^{II\ I}D^{II}/C^{I\ II}D^I \ll 1$, Eq. (5-21) differs from (5-26) only in that the denominator of the second term of the former is replaced by a sum of two such terms in the latter equation.

Another limiting case which is of considerable interest is that in which the effects of diffusional interaction are negligible. Indeed, in most ternary systems one can make this assumption (notable exceptions are iron base systems of the form Fe-C-X and Fe-O-X where X is a sub-

stitutional alloying element). The results corresponding to this limit can be obtained by setting $D_{ij}^{m} = 0$ $(i \neq j;\ m=I,II)$ in Eqs. (5-24), (5-25) and (5-19) to give

$$f(\omega)=\omega V\left(1 - \frac{\psi\omega^2}{(k_1-1)G_1^{I\ II}\left(1+\frac{C_1^{II}\ {}_I D_{11}^{II}}{C_1^{I}\ {}_{II}D_{11}^{I}}\right)^{-1} + (k_2-1)G_2^{I\ II}\left(1+\frac{C_2^{II}\ {}_I D_{22}^{II}}{C_2^{I}\ {}_{II}D_{22}^{I}}\right)^{-1}}\right) \quad (5\text{-}27)$$

One can see that the above result differs from the binary limit, Eq. (5-21), in that $(k-1)G^{I\ II}[1 + C^{II}\ {}_I D^{II}/C^{I}\ {}_{II}D^{I}]^{-1}$ is replaced by a sum of two such terms. Naturally for the limit $C_2 \to 0$, $G_2^{I\ II} \to 0$ and Eq. (5-27) reduces to Eq. (5-21) when the subscript 1 is dropped. Notice that in the limit of negligible influence from diffusion in the precipitate $\frac{C_i^{II}\ {}_I D_{ii}^{II}}{C_i^{I}\ {}_{II}D_{ii}^{I}} \ll 1$ $(i=1,2)$ Eq. (5-27) reduces to (5-26).

5.4 CONCLUDING REMARKS

It is interesting to note that if Eqs. (5-26) and (5-27) are rewritten so as to place all terms over a common denominator, in each case, one obtains a stability criterion of the form

$$A_1 G_1^{I\ II} + A_2\ G_2^{I\ II} - \psi\omega^2 > 0 \quad \text{(unstable)}$$

This result suggests that the two solutes act in a cumulative

fashion so as to enhance instability, as was originally suggested by Shewman[53].

The situation with respect to the second term in Eq. (5-19) is not particularly transparent when compared with the corresponding term in Eq. (5-21). Indeed, the limiting cases, Eqs. (5-26) and (5-27), were considered in an attempt to sort out the effects of the presence of a second solute and its interaction with the other solute. It has already been noted that the denominator of the second term in Eq. (5-27) differs from the corresponding term in Eq. (5-21) by virtue of the fact that a single term in the latter is replaced by two such terms in the former. This is not too surprising if it is recalled that Eq. (5-27) corresponds to the limit in which diffusional interaction is negligible and, therefore, except at the interface, the solutes can distribute themselves independently. Moreover, there is an additive aspect to the present capillarity equation (5-5) which could manifest itself in the presence of two terms in the capillarity term of Eq. (5-27).

Unfortunately the literature contains no experimental data on precipitate-matrix interface stability in multicomponent systems. Consequently the theory developed in this chapter can not be tested against experiment. However in the following chapter, 6, perturbation methods are

applied to a ternary stability problem which is examined experimentally in Chapter 7.

CHAPTER 6

INTERFACE STABILITY IN ISOTHERMAL TERNARY SYSTEMS†

6.1 INTRODUCTION

In Sec. 2.4, the concept of the diffusion path was introduced as an aid to the description of unidirectional transport in ternary systems. In that section and in section 3.4.2, it was pointed out that if such calculated diffusion paths dip into a two-phase field and thereby cut tie-lines (eg., segment P'Q' of the path P'S' in Fig. 2-3), then they must be regarded as being "virtual". Such situations are unstable in view of the regions of supersaturation which are developed. The appearance of regions of supersaturation adjacent to phase interfaces in isothermal ternary systems immediately implies the possibility of producing interfacial shape instabilities in such systems. Metallurgical phenomena which relate to this possibility are, for example: a) the high temperature oxidation of binary alloys - under certain circumstances the planar oxide-alloy interface can break down giving rise to a change in oxidation kinetics and b) diffusion bonding of two materials in which a total of three components are involved - the properties of

†For the most part, this chapter is based on two publications by the author and J.S. Kirkaldy[60,61].

the bond between the materials are influenced by the morphology of the interface. A convenient and general means of analyzing these and many thermodynamically analogous problems is to consider the stability of the initially planar interface of a two-phase infinite ternary diffusion couple. That in fact the planar interface of such couples can break down has been demonstrated experimentally for the Cu-Zn-Sn[38], the Fe-Cr-Ni[89] and the Cu-Zn-Ni[75] systems. In the present chapter, this problem is analyzed both in terms of purely constitutional arguments and in terms of perturbation theory.

6.2 CONSTITUTIONAL SUPERSATURATION

Consider the isothermal system shown schematically in Fig. 6-1. The original ternary phase diagram has been replotted onto an orthogonal coordinate system in which the ordinate and abscissa are the concentrations of components 1 and 2, respectively. For a two-phase infinite diffusion couple of terminal compositions designated by the points P and S, one can solve the ternary diffusion equations if a planar I-II interface is assumed. As indicated in Sec. 2.4, one can eliminate $\lambda = z/\sqrt{t}$ between the concentration distributions $C_1(\lambda)$ and $C_2(\lambda)$ to obtain the corresponding calculated diffusion path $C_1(C_2)$. Since the latter is independent of distance and time, it can be plotted on the appropriate

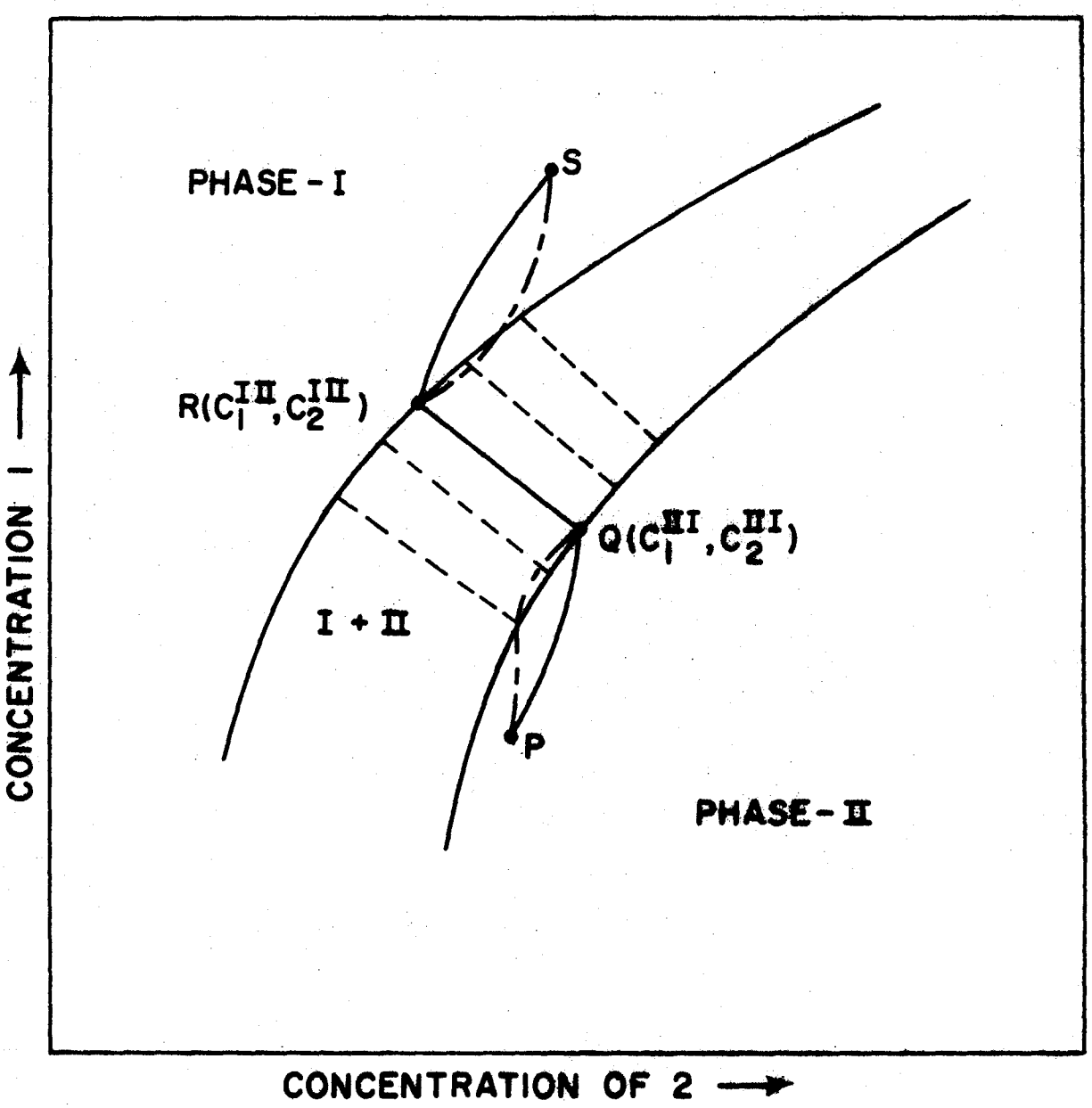

Fig. 6-1 Possible diffusion paths for a two-phase infinite diffusion couple whose terminal compositions are designated by the points P and S.

ternary isotherm. Depending on the values of the diffusion coefficients etc., this calculated diffusion path could enter the two-phase field in either or both phases as is indicated by the dotted lines PQ and RS in Fig. 6-1. Clearly an interface stability criterion based solely on the presence of (constitutional) supersaturation must relate the slope of the diffusion path in each phase to the slope of the corresponding phase boundary line.

Because one is concerned only with the regions adjacent to the planar interface, the concentration distributions in that vicinity can be written as

$$C_i^m = C_i^{mn} + G_i^{mn} z \qquad (i=1,2;\ m \neq n = I, II) \qquad (6\text{-}1)$$

(cf., Eq. (5-2)), where z is the perpendicular distance from the interface (positive in the direction phase II to phase I). Elimination of the distance coordinate yields expressions for the diffusion path in the vicinity of the interface, ie.,

$$C_1^I = \frac{G_1^{I\ II}}{G_2^{I\ II}} C_2^I + \text{constant} \qquad (6\text{-}2)$$

$$C_1^{II} = \frac{G_1^{II\ I}}{G_2^{II\ I}} C_2^{II} + \text{constant} \qquad (6\text{-}3)$$

In view of Eqs. (6-2) and (6-3), the slopes of the diffusion path at the points R and Q in Fig. 6-1 are respectively the

ratios $G_1^{I\ II}/G_2^{I\ II}$ and $G_1^{II\ I}/G_2^{II\ I}$. The slopes (including sign) of the phase boundary lines (I/I+II and I+II/II) at the points R and Q are designated by the symbols m^I and m^{II} respectively. If the transition from planar to nonplanar morphology is to be associated with the coincidence of the diffusion path and phase boundary lines, then the stability criterion for the configuration of Fig. 6-1

$$\frac{G_1^{I\ II}}{G_2^{I\ II}} < m^I \text{ and/or } \frac{G_1^{II\ I}}{G_2^{II\ I}} < m^{II} \text{ (unstable)} \qquad (6\text{-}4)$$

or alternatively

$$m^I G_2^{I\ II} - G_1^{I\ II} > 0 \text{ and/or } m^{II} G_2^{II\ I} - G_1^{II\ I} > 0 \text{ (unstable)} \qquad (6\text{-}5)$$

Notice that the G_i^{mn} all vary as $t^{-\frac{1}{2}}$ and hence relations (6-4) and (6-5) are time independent. It is essential to realize that these inequalities apply specifically to the configuration and nomenclature used in Fig. 6-1. If for example, the names of phases in Fig. 6-1 were exchanged, the inequality signs of (6-5) would be reversed†. To obtain a general criterion of this nature, all possible ternary phase diagrams and sets of

---

†This is clear if one recalls that the positive direction has been taken as always from phase II to phase I. As a result an exchange of phase names results in a change of sign in the G_i^{mn}. Therefore in going from (6-4) to (6-5), one must change the direction of the inequality because $G_2^{II\ I}$ and $G_2^{I\ II}$ are now negative.

terminal compositions (hence diffusion paths) must be considered.

The ensuing derivation is based on rather heuristic reasoning and therefore, at times, may involve steps which are not particularly obvious. In order to determine a stability criterion which functions more or less independently of nomenclature, it is convenient to define two parameters

$$\psi^{I} = m^{I} G_2^{I\ II} - G_1^{I\ II} \qquad (6\text{-}6)$$

$$\psi^{II} = m^{II} G_2^{II\ I} - G_1^{II\ I} \qquad (6\text{-}7)$$

Notice that (6-5) becomes

$$\psi^{I} > 0 \quad \text{and/or} \quad \psi^{II} > 0 \qquad \text{(unstable)} \qquad (6\text{-}8)$$

Given the diffusion path on any ternary isotherm, it transpires that one can characterize the phase diagram according to the signs of $(m^{I}-m)$, $(m^{II}-m)$ and $(C_2^{II\ I} - C_2^{I\ II})$, where m is the slope of the tie-line. For instance, the signs of these parameters for the various configurations shown in Fig. 6-2 are given in Table 6-1.

Table 6-1

Case	$m^{I}-m$	$m^{II}-m$	$C_2^{II\ I}-C_2^{I\ II}$	a^{I}	a^{II}
(a)	+	+	+	+1	+1
(b)	-	-	-	+1	+1
(c)	-	+	-	+1	-1
(d)	+	-	-	-1	+1

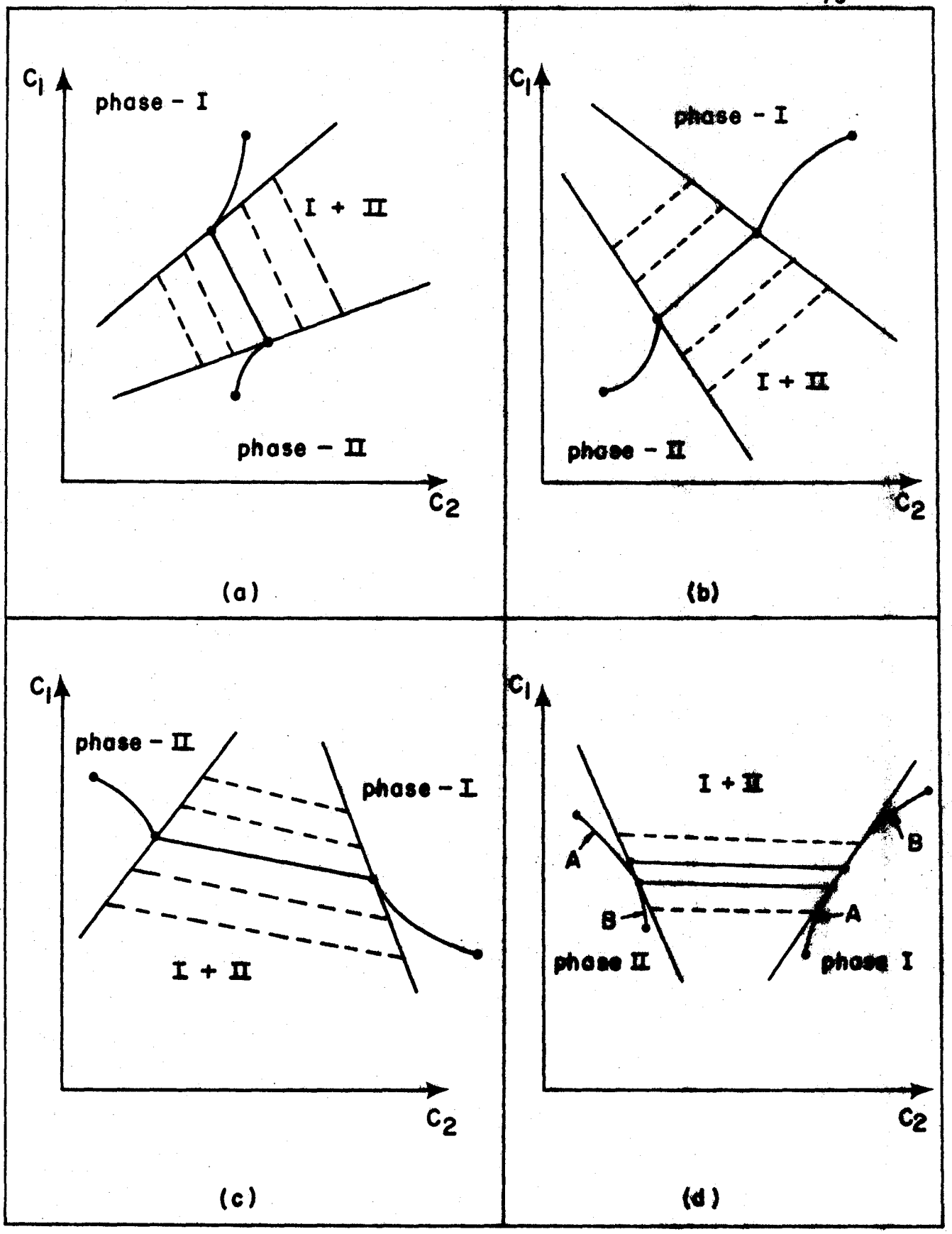

Fig. 6-2 A number of possible ternary isotherms which involve a two-phase field. The corresponding values of m^{I}-m, m^{II}-m, $C_2^{II\ I}$-$C_2^{I\ II}$, a^{I} and a^{II} are shown in Table 6-1. Typical diffusion paths are also shown.

Although there are many other possibilities, the four shown in Fig. 6-2 suffice for illustrative purposes. The problem now is to combine ψ^{I}, ψ^{II}, $(m^{I}-m)$, $(m^{II}-m)$ and $(C_2^{II\ I} - C_2^{I\ II})$ into an inequality which when satisfied signifies that the calculated diffusion path cuts into the two-phase field on the phase diagram, thus producing supersaturation. After some reflection, one can see that what is required is a stability criterion of the form

$$a^{I}\psi^{I} > 0 \quad \text{and/or} \quad a^{II}\psi^{II} > 0 \quad \text{(unstable)} \qquad (6\text{-}9)$$

where a^{I} and a^{II} are equal to +1 or -1 depending on the signs of $(m^{I}-m)$, $(m^{II}-m)$ and $(C_2^{II\ I}-C_2^{I\ II})$. After careful examination of numerous possibilities, the appropriate form for a^{I} and a^{II} is found to be

$$a^{I} = \frac{(m^{I}-m)(C_2^{II\ I}-C_2^{I\ II})}{|(m^{I}-m)(C_2^{II\ I}-C_2^{I\ II})|} \qquad (6\text{-}10)$$

$$a^{II} = \frac{(m^{II}-m)(C_2^{II\ I}-C_2^{I\ II})}{|(m^{II}-m)(C_2^{II\ I}-C_2^{I\ II})|} \qquad (6\text{-}11)$$

In view of (6-9), (6-10) and (6-11), it is obvious that a^{I} and a^{II} actually need not be normalized (by dividing the numerator by the corresponding modulus). To illustrate what is involved in (6-9), (6-10) and (6-11) return to Fig. 6-2 and Table 6-1 where the appropriate values of a^{I} and a^{II} are listed. From (6-9) and Table 6-1 it follows that if $\psi^{I} > 0$ and/or $\psi^{II} > 0$,

$\psi^I > 0$ and/or $\psi^{II} > 0$, $\psi^I > 0$ and/or $\psi^{II} < 0$ and $\psi^I < 0$ and/or $\psi^{II} > 0$, then the corresponding calculated diffusion path cuts into the two-phase field producing a zone of supersaturation in cases (a), (b), (c) and (d) respectively. One can confirm this through reference to Fig. 6-2 and Eqs. (6-6) and (6-7). As an example, consider case (d). Diffusion path (A) will cut into the I+II field from phase I if $G_1^{I\ II}/G_2^{I\ II} < m^I$ and from phase II if $G_1^{II\ I}/G_2^{II\ I} < m^{II}$. Recalling that the positive direction is phase II to phase I, $G_2^{I\ II} < 0$, $G_2^{II\ I} > 0$ and these inequalities become $m^I G_1^{I\ II} - G_2^{I\ II} < 0$ and $m^{II} G_1^{II\ I} - G_2^{II\ I} > 0$ for phases I and II respectively. Using Eqs. (6-6) and (6-7), one therefore has

$$\psi^I < 0 \quad \text{and/or} \quad \psi^{II} > 0 \quad \text{(unstable)}$$

which is in agreement with what was obtained from (6-9) and Table 6-1. One can easily demonstrate for diffusion path (B) that the corresponding inequalities are $G_1^{I\ II}/G_2^{I\ II} > m^I$ and $G_1^{II\ I}/G_2^{II\ I} > m^{II}$, $G_2^{I\ II} > 0$ and $G_2^{II\ I} < 0$, $m^I G_1^{I\ II} - G_2^{I\ II} < 0$ and $m^{II} G_1^{II\ I} - G_2^{II\ I} > 0$ and finally

$$\psi^I < 0 \quad \text{and/or} \quad \psi^{II} > 0 \quad \text{(unstable)}$$

which again is in agreement with what was obtained for case (d) from (6-9) and Table 6-1.

In summary, the stability criterion (6-9) can be applied to any calculated diffusion path on any ternary phase diagram provided only that, after naming components

(1 as ordinate and 2 as abscissa) and phases, one takes the positive direction as phase II to I.

6.3 PERTURBATION ANALYSIS

Having determined a stability criterion based solely on whether or not supersaturation would develop in a zone adjacent to a moving planar interface, a more sophisticated analysis is undertaken with the aid of perturbation theory. On completing the latter investigation, the results of the two approaches can be compared. Throughout the treatment it is assumed that local equilibrium (as defined by the ternary phase diagram) is maintained at phase interfaces, that effects of grain boundary and surface diffusion are negligible and that the on-diagonal diffusion coefficients are not concentration dependent. Two additional important assumptions are made. Firstly it is assumed that the strength of off-diagonal diffusional interaction is negligible. This is in fact the case for most substitutional ternary alloys. Those cases in which this assumption is not valid are sacrificed in order to sustain tractability in the mathematics. To maintain generality with respect to constitution, a matter of paramount importance, it is also necessary to assume that capillarity (ie., surface energy) effects are negligible. It does not appear possible to formulate a tractable Gibbs-Thomson type equation for a ternary system of

arbitrary constitution. This means that the results of this analysis will be precisely applicable only to late time parabolic growth or to systems of low interfacial free energy.

A two-phase (I & II) infinite ternary diffusion couple, in which the interface is planar and moving at the instantaneous velocity V, is considered at time t. At this instant the interface is coincident with the x-axis of a stationary coordinate system having its z-axis directed towards phase I. The position of the interface and the concentration distributions in the two phases can be determined by specializing the analysis given in Sec. 2.3.3 to two-phase systems. This is done in detail in Appendix II. From this point on, the perturbation analysis parallels the treatment given in Sec. 5.2 and therefore reference is made to a number of the equations in that section.

Since the field equations are linear and the boundary conditions can be linearized for perturbations of small amplitude, no loss of generality is suffered by considering the stability of the interface with respect to a sinusoidal perturbation of arbitrary wavelength (see Secs. 4.1 and 4.3). Accordingly such a perturbation is introduced into the shape of the interface and the equation of the latter is given by Eq. (5-1). The concentration distributions of the two independent components for the vicinity of the perturbation are expanded according to Eq. (5-2). In general, the

G_i^{mn} (i=1,2; m≠n=I,II) are nonzero; recall that in Sec. 5.2 $G_1^{II\ I} = G_2^{II\ I} = 0$ because phase II was a precipitate. It is assumed that the average interface advances at a slow enough rate and the perturbation grows or decays slowly enough that the $\tilde{C}_i^m$ are solutions of Laplace's equation, (5-3). The mathematical requirement for use of this approximation is that[40,47]

$$\omega >> \frac{V}{2D_i^m} \qquad (i=1,2;m=I,II) \qquad (6\text{-}12)$$

Throughout the remainder of this chapter, it is convenient to use the symbol D_i^m for D_{ii}^m because the off-diagonal D_{ij}^m are not considered.

The following boundary conditions apply:

1. The $\tilde{C}_i^m$ vanish with distance from the perturbed interface.
2. The C_i^m are subject to local equilibrium at every position on the perturbed interface. That is, for each phase the independent concentrations at a given position along the interface must define a point on the corresponding phase boundary of the ternary phase diagram and the two points thus defined must be joined by a tie-line. Because the amplitude of the perturbation is infinitesimal, these points are infinitesimally removed from the points corresponding to a flat surface (eg., R and Q in Fig. 6-1). It is valid therefore to approximate the phase boundaries in this vicinity of the phase diagram by their tangents at

the points defined by the concentrations at a flat interface. Accordingly, one can write

$$C_{1\phi}^{I} = m^{I} C_{2\phi}^{I} + b^{I} \qquad (6\text{-}13)$$

$$C_{1\phi}^{II} = m^{II} C_{2\phi}^{II} + b^{II} \qquad (6\text{-}14)$$

where $C_{1\phi}^{I}$, $C_{2\phi}^{I}$, $C_{1\phi}^{II}$ and $C_{2\phi}^{II}$ are the equilibrium concentrations at the perturbed interface $z = \phi(x,t)$, m^{I} and m^{II} are the slopes (including sign) of the tangents to the phase boundary lines at the points corresponding to planar interface compositions and b^{I} and b^{II} are the corresponding intercepts. Equations (6-13) and (6-14) ensure that the interface concentrations in each phase define points on the corresponding phase boundaries. However, a further condition is necessary to ensure that these points are joined by a tie-line of the phase diagram. Accordingly, the following condition is imposed,

$$C_{2\phi}^{II} = m^{II\ I} C_{2\phi}^{I} + b^{II\ I} \qquad (6\text{-}15)$$

where $m^{II\ I}$ is defined as the slope of the tangent, at the point defined by the planar interface compositions, to a graph of the equilibrium interface concentration of component 2 in phase II versus component 2 in phase I and $b^{II\ I}$ is the corresponding intercept. Using coordinate geometry, it can be proven that $m^{II\ I}$ is related to the

slope m of the given tie-line by the equation

$$m^{II\ I} = \frac{m^{I} - m}{m^{II} - m} \qquad (6\text{-}16)$$

Equations (6-13), (6-14) and (6-15), taken together, define the local equilibrium boundary condition. The parameters involved in these relationships are obtained directly from the ternary phase diagram in question, after a calculation of the unique diffusion path for a planar interface. The formulation of the local equilibrium boundary condition in this empirical manner allows consideration of all conceivable ternary systems and releases one from any assumptions relating to dilute solution limits and ideal or regular solution behaviour. Furthermore, this formulation yields results which can be related to the elementary approach described in Sec. 6-2.

3. The following mass balance boundary conditions apply to every position along the perturbed interface:

$$v(x) = \frac{1}{(C_{1\phi}^{II} - C_{1\phi}^{I})} \left[D_1^{I} \left(\frac{\partial C_1^{I}}{\partial z}\right)_{\phi} - D_1^{II} \left(\frac{\partial C_1^{II}}{\partial z}\right)_{\phi}\right] \qquad (6\text{-}17)$$

$$= \frac{1}{(C_{2\phi}^{II} - C_{2\phi}^{I})} \left[D_2^{I} \left(\frac{\partial C_2^{I}}{\partial z}\right)_{\phi} - D_2^{II} \left(\frac{\partial C_2^{II}}{\partial z}\right)_{\phi}\right] \qquad (6\text{-}18)$$

For a planar interface $v(x) = V$ and Eqs. (6-17) and (6-18) reduce to

$$V(C_1^{II\ I} - C_1^{I\ II}) = D_1^I G_1^{I\ II} - D_1^{II} G_1^{II\ I} \qquad (6\text{-}19)$$

$$V(C_2^{II\ I} - C_2^{I\ II}) = D_2^I G_2^{I\ II} - D_2^{II}\ G_2^{II\ I} \quad . \qquad (6\text{-}20)$$

Following Mullins and Sekerka[47], the interface concentrations are first written in the form

$$C_{i\phi}^m = C_i^{mn} + a_i^m\ \delta\ \sin\omega x \qquad (6\text{-}21)$$

where the four constants a_i^m are to be determined from the boundary conditions. Solutions of Eq. (5-3), which vanish at distances far removed from the perturbed interface, are introduced into Eq. (5-2) to give complete solutions which, to the first order in δ, reduce to Eq. (6-21) at the interface $z = \delta\ \sin\omega x$. The complete solutions are

$$C_i^I = C_i^{I\ II} + G_i^{I\ II}\ z + \delta(a_i^I - G_i^{I\ II})\sin(\omega x)e^{-\omega z} \qquad (6\text{-}22)$$

$$C_i^{II} = C_i^{II\ I} + G_i^{II\ I}\ z + \delta(a_i^{II} - G_i^{II\ I})\sin(\omega x)e^{\omega z} \qquad (6\text{-}23)$$

Substituting Eq. (6-21) into Eqs. (6-13), (6-14) and (6-15) and equating coefficients of sin ωx in each of the latter equations leads to,

$$a_1^I = m^I\ a_2^I \qquad (6\text{-}24)$$

$$a_2^{II} = m^{II\ I}\, a_2^I \tag{6-25}$$

$$a_1^{II} = m^{II} m^{II\ I} a_2^I \tag{6-26}$$

which leaves a_2^I as the remaining unknown constant. On substituting $z = \delta \sin \omega x$ into the z-derivative of Eqs. (6-22) and (6-23) and expanding to the first order in δ, expressions for the concentration gradients at the perturbed interface are obtained. These, along with Eqs. (6-21), (6-24), (6-25) and (6-26), are introduced into Eqs. (6-17) and (6-18). Coefficients of sin ωx in the latter equations are equated to give an expression for the remaining constant a_2^I. Rearrangement of this expression with Eqs. (6-19) and (6-20) and application of condition (6-12) leads to

$$a_2^I = [(C_1^{II\ I} - C_1^{I\ II})(D_2^I G_2^{I\ II} + D_2^{II} G_2^{II\ I}) - (C_2^{II\ I} - C_2^{I\ II})(D_1^I G_1^{I\ II} + D_1^{II} G_1^{II\ I})]/$$
$$[(C_1^{II\ I} - C_1^{I\ II})(m^{II\ I} D_2^{II} + D_2^I) - (C_2^{II\ I} - C_2^{I\ II})(m^{II} m^{II\ I} D_1^{II} + m^I D_1^I)] \tag{6-27}$$

The right hand side of Eq. (4-12) can be equated to either of Eqs. (6-17) or (6-18); the latter is arbitrarily chosen. Accordingly, the interfacial gradients of Eqs. (6-22) and (6-23) and Eqs. (6-21), (6-25) and (6-27) are introduced into Eq. (6-18). Then the coefficient of sin ωx is equated to $d\delta/dt$ in Eq. (4-12) to give the following result after

application of condition (6-12) and rearrangement with Eqs. (6-19) and (6-20):

$$\frac{d\delta/dt}{\delta} = V\omega \left[(D_1^I G_1^{I\ II} + D_1^{II} G_1^{II\ I})(m^{II\ I} D_2^{II} + D_2^I) - (D_2^I G_2^{I\ II} + D_2^{II} G_2^{II\ I})(m^{II} m^{II\ I} D_1^{II} + m^I D_1^I) \right] / \left[(D_1^I G_1^{I\ II} - D_1^{II} G_1^{II\ I})(m^{II\ I} D_2^{II} + D_2^I) - (D_2^I G_2^{I\ II} - D_2^{II} G_2^{II\ I})(m^{II} m^{II\ I} D_1^{II} + m^I D_1^I) \right] \quad (6\text{-}28)$$

The problem now is to ascertain under what conditions the above expression is positive. To this end, mean diffusivities for each component are defined in the following manner

$$\bar{D}_1 = \frac{1}{2}(m^{II} m^{II\ I} D_1^{II} + m^I D_1^I) \quad (6\text{-}29)$$

$$\bar{D}_2 = \frac{1}{2}(m^{II\ I} D_2^{II} + D_2^I) \quad (6\text{-}30)$$

and weighted interfacial concentration gradients can be defined such that

$$\zeta_i^{mn} = \frac{D_i^m G_i^{mn}}{\bar{D}_i} . \quad (6\text{-}31)$$

Substitution of Eqs. (6-29) and (6-30) into (6-28), division of numerator and denominator by $2\bar{D}_1\bar{D}_2$, introduction of Eq. (6-31) and then slight rearrangement leads to

$$\frac{d\delta/dt}{\delta} = V\omega \left\{ \frac{(\zeta_1^{I\ II} - \zeta_2^{I\ II}) + (\zeta_1^{II\ I} - \zeta_2^{II\ I})}{(\zeta_1^{I\ II} - \zeta_2^{I\ II}) - (\zeta_1^{II\ I} - \zeta_2^{II\ I})} \right\} \quad (6\text{-}32)$$

Noting the similarity between terms in the numerator and denominator, the latter are multiplied by the denominator to

obtain

$$\frac{d\delta/dt}{\delta} = V\omega\left\{\frac{(\zeta_1^{I\ II}-\zeta_2^{I\ II})^2 - (\zeta_1^{II\ I}-\zeta_2^{II\ I})^2}{[(\zeta_1^{I\ II}-\zeta_2^{I\ II}) - (\zeta_1^{II\ I}-\zeta_2^{II\ I})]^2}\right\}. \qquad (6\text{-}33)$$

Only the numerator need be considered to determine the sign of the above expression. Since ω is necessarily positive, the appropriate stability criterion is

$$V\{|\zeta_1^{I\ II}-\zeta_2^{I\ II}| - |\zeta_1^{II\ I}-\zeta_2^{II\ I}|\} > 0 \text{ (unstable)}. \qquad (6\text{-}34)$$

6.4 ANALYSIS OF THE STABILITY CRITERION

Turning for the moment to Eqs. (6-29) and (6-30), one notes that the definition of mean diffusivities $\bar{D}_i$ involves, besides the diffusion coefficients of component i in each phase, the phase diagram parameters m^I, m^{II} and $m^{II\ I}$. Using Eqs. (6-13), (6-14) and (6-15), difference expressions for these parameters can be written in the form

$$m^I = \left(\frac{\Delta C_{1\phi}^I}{\Delta C_{2\phi}^I}\right)_{Flat} \qquad (6\text{-}35)$$

$$m^{II} = \left(\frac{\Delta C_{1\phi}^{II}}{\Delta C_{2\phi}^{II}}\right)_{Flat} \qquad (6\text{-}36)$$

$$m^{II\ I} = \left(\frac{\Delta C_{2\phi}^{II}}{\Delta C_{2\phi}^{I}}\right)_{Flat} \qquad (6\text{-}37)$$

and these give

$$m^{II}\ m^{II\ I} = \left(\frac{\Delta C_{1\phi}^{II}}{\Delta C_{2\phi}^{I}}\right)_{Flat} \qquad (6\text{-}38)$$

Thus m^{I}, $m^{II}m^{II\ I}$ and $m^{II\ I}$ are, respectively, the changes in equilibrium interface concentration for component 1 in phase I, component 1 in phase II and component 2 in phase II accompanying unit change in the interface concentration of component 2 in phase I, about the given planar interface concentrations. Hence Eqs. (6-35) to (6-38) define relative variations in equilibrium interface concentration as produced by some perturbation or fluctuation. On introducing Eqs. (6-35), (6-37) and (6-38) into (6-29) and (6-30), one obtains

$$\bar{D}_1 = \frac{1}{2}\left\{\left(\frac{\Delta C_{1\phi}^{II}}{\Delta C_{2\phi}^{I}}\right)_{Flat} D_1^{II} + \left(\frac{\Delta C_{1\phi}^{I}}{\Delta C_{2\phi}^{I}}\right)_{Flat} D_1^{I}\right\} \qquad (6\text{-}39)$$

$$\bar{D}_2 = \frac{1}{2}\left\{\left(\frac{\Delta C_{2\phi}^{II}}{\Delta C_{2\phi}^{I}}\right)_{Flat} D_2^{II} + D_2^{I}\right\} \qquad (6\text{-}40)$$

Thus $\bar{D}_1$ and $\bar{D}_2$ are means of weighted diffusion coefficients for the given component in each phase; weighted as to the relative size of the corresponding equilibrium interface concentration variations.

The stability criterion as expressed in (6-34) says simply that the absolute value of the difference in diffusivity weighted interfacial gradients for the independent components in the depleting phase (phase I for V positive and

phase II for V negative) must exceed the corresponding difference in the growing phase in order for instability to occur. Although (6-34) represents a very compact expression for determining if a particular system will become unstable, it does not have a form which permits a direct comparison with the constitutional approach described in Sec. 6.2. To establish such a comparison, (6-34) is decomposed using Eqs. (6-29), (6-30) and (6-31) to give, after rearranging

$$V\{|D_1^I D_2^I (m^I G_2^{I\ II} - G_1^{I\ II}) + D_1^{II} D_2^{II} m^{II\ I} (m^{II} \frac{D_2^I}{D_2^{II}} G_2^{I\ II} - \frac{D_1^I}{D_1^{II}} G_1^{I\ II})| -$$

$$|D_1^I D_2^I (m^I \frac{D_2^{II}}{D_2^I} G_2^{II\ I} - \frac{D_1^{II}}{D_1^I} G_1^{II\ I}) + D^{II}{}_1 D_2^{II} m^{II\ I} (m^{II} G_2^{II\ I} - G_1^{II\ I})|\} > 0$$

(unstable) (6-41)

It is important to note that the only time dependent parameters in this expression are the G_i^{mn} and V and these all vary as $t^{-\frac{1}{2}}$. Hence, (6-41) is a time independent inequality since each term has identical time dependence which can be factored out. Similar remarks apply to relations (6-6), (6-7), (6-9), (6-34) and (6-44). In view of Eqs. (6-19) and (6-20), the G_i^{mn} are not independent growth parameters and therefore expressions for these four gradients are obtained by simultaneous solution of Eqs. (6-6), (6-7), (6-19) and (6-20). These expressions are substituted into (6-41) to give

$$V\{\left|m^{II\ I}[m^{II}D_1^{II}-\frac{(C_1^{II\ I}-C_1^{I\ II})}{(C_2^{II\ I}-C_2^{I\ II})}\ D_2^{II}]+\frac{m^{II\ I}D_1^{II}D_2^{II}\psi^{II}+D_1^{I}D_2^{I}\psi^{I}}{V(C_2^{II\ I}-C_2^{I\ II})}\right| -$$

$$\left|[\frac{(C_1^{II\ I}-C_1^{I\ II})}{(C_2^{II\ I}-C_2^{I\ II})}\ D_2^{I}-m^{I}D_1^{I}] + \frac{m^{II\ I}D_1^{II}D_2^{II}\psi^{II}+D_1^{I}D_2^{I}\psi^{I}}{V(C_2^{II\ I}-C_2^{I\ II})}\right|\} > 0$$

(unstable) (6-42)

The tie-line which forms part of the calculated diffusion path has a slope given by (see for example Fig. 6-1)

$$m = \frac{(C_1^{I\ II}-C_1^{II\ I})}{(C_2^{I\ II}-C_2^{II\ I})} = \frac{(C_1^{II\ I}-C_1^{I\ II})}{(C_2^{II\ I}-C_2^{I\ II})} \qquad (6\text{-}43)$$

and the above is substituted directly into the first and third terms of (6-42). Relation (6-42) now contains all four of m^{I}, m^{II}, m and $m^{II\ I}$. Using Eq. (6-16), $m^{II\ I}$ is eliminated because the remaining three can be obtained directly from the phase diagram. Hence, from (6-42), (6-43) and (6-16), one obtains after some rearranging

$$V\{\left|\frac{(m^{II}D_1^{II}-mD_2^{II})}{(m^{II}-m)} + \frac{D_1^{II}D_2^{II}\psi^{II}/(m^{II}-m)+D_1^{I}D_2^{I}\psi^{I}/(m^{I}-m)}{V(C_2^{II\ I}-C_2^{I\ II})}\right| - \left|\frac{(mD_2^{I}-m^{I}D_1^{I})}{(m^{I}-m)}\right.$$

$$\left. + \frac{D_1^{II}D_2^{II}\psi^{II}/(m^{II}-m)+D_1^{I}D_2^{I}\psi^{I}/(m^{I}-m)}{V(C_2^{II\ I}-C_2^{I\ II})}\right|\} > 0 \quad \text{(unstable)} \qquad (6\text{-}44)$$

This stability criterion is the focus of attention for the remainder of the present chapter. It should be noted that (6-44)

carries the requirement that the positive direction be from phase II to phase I. Otherwise, the above result is independent of any prescribed nomenclature.

At this point the perturbation result (6-44) can be compared with the results of the constitutional approach, (6-9). Notice that with respect to (6-44) the multiplication factor V and the V in the denominator of the second and fourth terms are self compensating in that when the absolute value signs are removed, with appropriate sign adjustments, the V's will cancel and leave the signed factors $[(m^{II}-m)(C_2^{II\ I}-C_2^{I\ II})]^{-1}$ and $[(m^{I}-m)(C_2^{II\ I}-C_2^{I\ II})]^{-1}$ in front of $D_1^{II}D_2^{II}\psi^{II}$ and $D_1^{I}D_2^{I}\psi^{I}$, respectively. These factors are reminiscent of the a^{II} and a^{I} defined in Eqs. (6-10) and (6-11) and used in (6-9).

A marginal state with respect to the constitutional approach can be defined by setting $\psi^{I} = \psi^{II} = 0$. Under these conditions, the second and fourth terms of (6-44) are zero and thus (6-44) will yield the same marginal state (ie., attain equality to zero) if, and only if

$$\left|\frac{(m^{II}D_1^{II}-mD_2^{II})}{(m^{II}-m)}\right| = \left|\frac{(mD_2^{I}-m^{I}D_1^{I})}{(m^{I}-m)}\right| \qquad (6\text{-}45)$$

Normally Eq. (6-45) is not satisfied and therefore it appears that the development of supersaturation is neither a necessary nor a sufficient condition for instability to set in. There are two special cases in which Eq. (6-45) does hold and these are:

i) when $m = m^I = m^{II}$, which is trivial since it defines a two-phase field of zero width and, ii) when all four of the diffusion coefficients have the same value.

It is of some interest to consider the second case cited above. On setting $D_1^I = D_1^{II} = D_2^I = D_2^{II} = D$, (6-44) reduces to

$$V\{|1 + \frac{Y'}{V}| - | - 1 + \frac{Y'}{V}|\} > 0 \quad \text{(unstable)} \qquad (6\text{-}46)$$

where

$$Y' = \frac{D[\psi^{II}/(m^{II}-m) + \psi^I/(m^I-m)]}{(C_2^{II\ I}-C_2^{I\ II})} \qquad (6\text{-}47)$$

Regardless of the sign of the velocity V, the above inequality is satisfied if $Y' > 0$ and hence, if

$$\frac{1}{(C_2^{II\ I}-C_2^{I\ II})}\left[\frac{\psi^{II}}{(m^{II}-m)} + \frac{\psi^I}{(m^I-m)}\right] > 0 \quad \text{(unstable)} \qquad (6\text{-}48)$$

Clearly a^I and a^{II} in (6-9), (6-10) and (6-11) have the same signs as the coefficients of ψ^I and ψ^{II}, respectively, in (6-48). Thus the perturbation results predict that for the case of equal diffusivities, although supersaturation in both phases is a sufficient condition for instability, supersaturation in just one phase is only a necessary condition. From (6-48) one can also see that the contributions to instability due to supersaturation in each phase (a negative contribution corresponds to lack of supersaturation) form a weighted sum in which the magnitude of weighting depends on the slopes of the phase boundaries and tie-line.

6.5 APPLICATIONS OF THE PERTURBATION ANALYSIS

In Chapters 7 and 8 of this dissertation the results of the preceding sections will be compared with experiments involving the Cu-Zn-Ni system. In the meantime, it is of interest to consider more general applications of these results.

Thus far the treatment has been specific to two-phase ternary infinite diffusion couples. In Sec. 6.1 it was indicated that this is a convenient formulation for a generalized study of phase interface stability in systems of metallurgical interest. The utility of the present point of view will now be demonstrated by briefly showing how this formalism can describe a number of (seemingly) quite different problems relating to morphological stability. One should keep in mind, however, that in order to maintain generality a simple boundary condition at the interface had to be used (ie., local equilibrium without capillarity).

It is to be emphasized, however, that this limitation is in many cases more apparent than real. For growth problems involving parabolic kinetics (eg., precipitation, oxidation or diffusion bonding), the velocity of the interface eventually slows to a point where the lateral transport necessary to produce long wavelength perturbations is possible. Thus, if the interface is unstable, perturbations of long enough wave-

length that capillarity effects are negligible are sustained in preference to shorter wavelength ones. Accordingly the stability criteria are a first approximation for early times of growth and become (assuming local equilibrium) exact for later times of parabolic growth. One is concerned with the stability of interfaces over the total elapsed time of growth and therefore the later times are more important since earlier time effects tend to be obliterated. Hence, for parabolic growth problems, the results will be adequate. For steady state transformations in which the velocity of the interface is a constant fixed by the boundary conditions (as in steady state solidification experiments), the above argument does not apply. In this case the criteria must be regarded as first approximations whose accuracy increases with decrease in imposed interface velocity and interfacial free energy.

6.5.1 Binary Alloy Solidification

Consider first the steady state binary alloy solidification problem treated initially by Tiller et al[35], using constitutional arguments (see Sec.3.4.1), and later by Mullins and Sekerka[47], using perturbation methods. This alloy solidification problem is much less general than the ternary stability problem discussed in this chapter. In the former case, the analysis is specific to dilute regions of a binary phase diagram and further, the boundary conditions

allow the possibility of supersaturation on only one side of the interface, ie., in the liquid. Consequently, only one expression is required to express the condition for the onset of constitutional supercooling, ie., (3-7).

Referring to Fig. 6-3, it is quite evident that one can apply the perturbation theory for isothermal ternary systems to the steady state solidification problem. Commencing with the equations for the temperature and solute distributions for a planar interface, one can solve for a time and distance independent function of the form $T = T(C)$ and this relation can be plotted on the binary phase diagram. This analogue to a diffusion path is represented by the line ABCD in Fig. 6-3. In view of the steady state condition the points A, B and D must define a line of constant composition. Clearly, the onset of constitutional supercooling corresponds to the line DC dropping into the solid plus liquid phase field.

If one replaces the diffusion fields of component 1 with thermal fields and then designates phases I and II as liquid and solid, respectively, the ternary phase diagram (on an orthogonal coordinate system) is replaced by the binary phase diagram applicable to the given solidification problem. Taking the dilute solution limit of straight solidus and liquidus lines gives $m^{II} = m^{I}/k_o$ and $m^{II\ I} = k_o$ where k_o is the equilibrium distribution coefficient and m^{I} is the

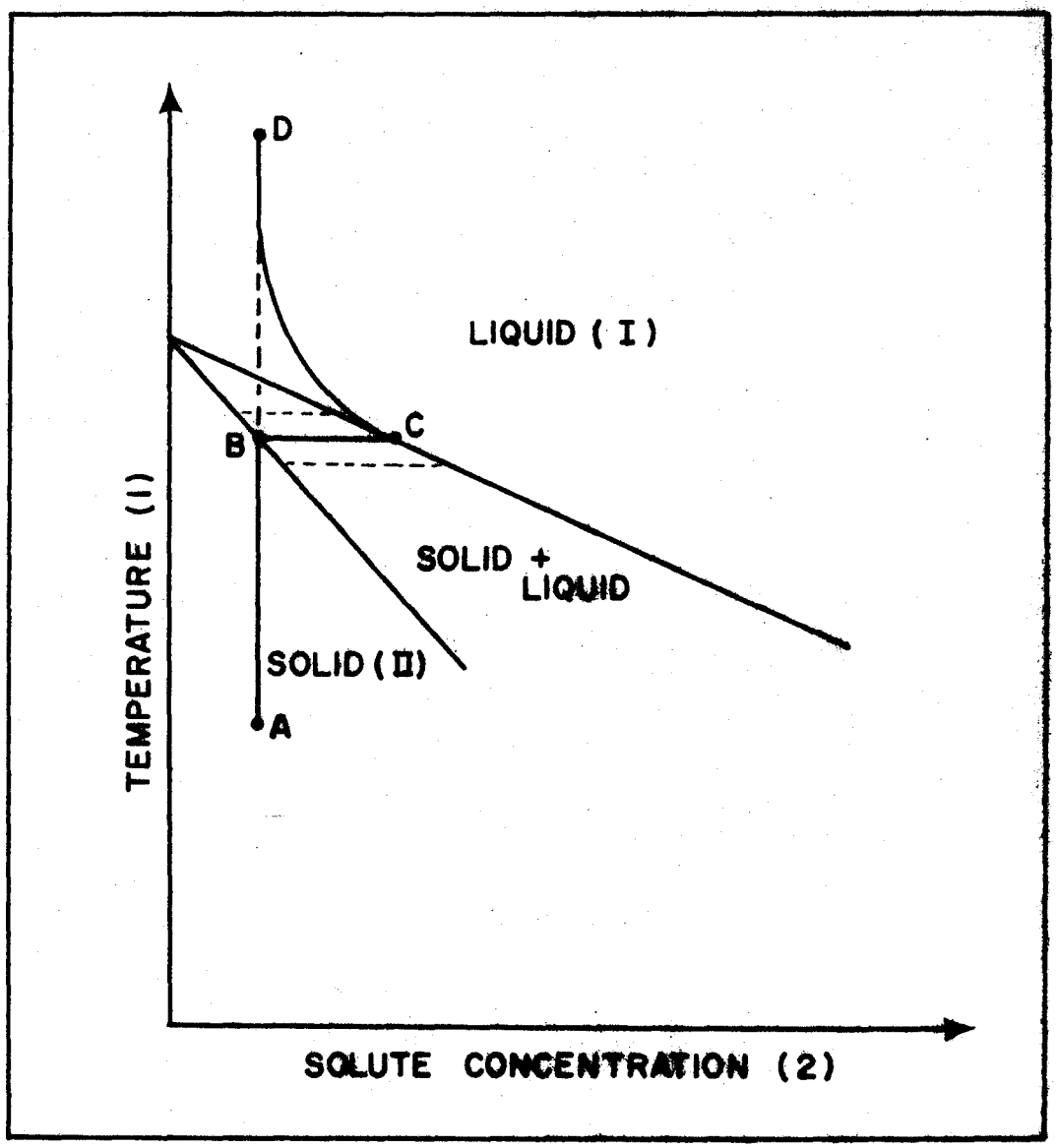

Fig. 6-3 The dilute corner of a binary phase diagram with the relationship between temperature and solute concentration for a steady state solidification experiment superimposed (cf., Fig. 3-6).

slope of the liquidus line. Furthermore, assuming that there is no diffusion in the solid (ie., $D_2^{II} << D_2^I$), (6-41) becomes

$$V\{|D_1^I(m^I G_2^{I\ II} - G_1^{I\ II}) + m^I D_1^{II} G_2^{I\ II}| - |-D_1^{II} G_1^{II\ I}|\} > 0 \quad \text{(unstable)}$$

where D_1^I and D_1^{II} are thermal diffusivities. Noting that $G_1^{II\ I} \geq 0$, this relation reduces to

$$V\{|m^I G_2^{I\ II} - \frac{D_1^I G_1^{I\ II}}{D_1^I + D_1^{II}}| - \frac{D_1^{II} G_1^{II\ I}}{D_1^I + D_1^{II}}\} > 0 \quad \text{(unstable)}$$

Because $m^I G_2^{I\ II} \geq 0$, $G_1^{I\ II} \geq 0$ and $G_1^{II\ I} \geq 0$, one can obtain the following from the above relation (using Eqs. (6-19) and (6-20) and associating $(C_1^{II\ I} - C_1^{I\ II})$ with the latent heat L):

$$m^I G_2^{I\ II} - (D_1^I G_1^{I\ II} + D_1^{II} G_1^{II\ I})/(D_1^I + D_1^{II}) > 0 \quad \text{(unstable)} \quad (6\text{-}49)$$

which is the modified constitutional supercooling stability criterion of Mullins and Sekerka (Eq. (32) of Ref. (47)). One can deduce the above criterion from (6-44) rather than (6-41), although it is necessary to handle the latent heat term differently[60].

6.5.2 Binary Alloy Melting

Woodruff[62] has recently considered the problem of interface stability during the steady state unidirectional melting of binary alloys. This problem is not the precise inverse of the preceding solidification problem. Whereas

in analyzing interface stability during solidification, one can ignore solute diffusion in the solid; in treating the problem for melting, one must allow for diffusion in both phases. Consequently it is not possible to treat the melting problem by the simple expedient of changing the signs of various quantities (eg., velocity) in the expressions of Mullins and Sekerka. However, for those cases in which capillarity can be ignored, the results of the present analysis are applicable. The diffusion field of component 1 is replaced with a thermal field and, in order to have $V > 0$, the liquid is designated as phase II and the solid as phase I. Noting that $m^{I} = m^{II}/k_o$, $m^{II\ I} = 1/k_o$ (where m^{II} is now the slope of the liquidus line) and $G_2^{II\ I} = 0$, (6-41) leads to

$$\left| \frac{m^{II} D_2^I G_2^{I\ II}}{D_2^{II} + k_o D_2^I} - \frac{D_1^I G_1^{I\ II}}{D_1^{II} + D_1^I} \right| + \frac{D_1^{II} G_1^{II\ I}}{D_1^{II} + D_1^I} > 0 \quad \text{(unstable)}$$

For $V>0$, $D_1^{II} G_1^{II\ I} > D_1^I G_1^{I\ II}$ and the above reduces to

$$\frac{D_1^I G_1^{I\ II} + D_1^{II} G_1^{II\ I}}{D_1^I + D_1^{II}} - \frac{m^{II} D_2^I G_2^{I\ II}}{D_2^{II} + k_o D_2^I} > 0 \quad \text{(unstable)} \qquad (6\text{-}50)$$

This criterion, which is applicable when capillarity is negligible, follows directly from relation (28) of Ref. (62) on setting the capillarity constant $\Gamma = 0$.

6.5.3 Isothermal Diffusion Bonding

Consider next the simple isothermal diffusion bonding of two materials in which a total of three components are involved (eg. a binary alloy clad with a pure element). Provided no new phases form during interdiffusion, such a system is represented by a two-phase ternary diffusion couple. Subject to the appropriate boundary conditions (finite or infinite), one solves the diffusion equations for a planar interface in order to obtain the concentration distributions and hence the G_i^{mn} and other growth parameters. Using these parameters, the results of the present analysis can be utilized directly for the study of interfacial stability in diffusion bonded materials. However, it is only when one is dealing with infinite boundary conditions that the solution to the diffusion equations are parametric in $\lambda = zt^{-\frac{1}{2}}$. Thus, for finite, aged systems, Eqs. (6-9), (6-10), (6-11), (6-34) and (6-44) are in general time dependent, which is an unfortunate complication. In the event that an intermediate phase or phases form during interdiffusion, the diffusion equations can still be solved if the terminal phases are infinite in extent. The stability criterion is then applied to each interface in turn.

It is of interest to note that one can also conceive of isothermal diffusion bonding of a solid phase to a liquid phase (provided the two phases can coexist at the given tempera-

ture). For example, one might consider a situation wherein a solid alloy, AB, is immersed in a large bath of C and seek to establish if a "smooth" interface is stable during the dissolution process. In fact, Harrison and Wagner[63] have considered in detail the attack of solid alloys by liquid metals and salt melts. On the basis of qualitative 'kinetic' arguments, they contend that when a solid alloy is brought in contact with a liquid phase which dissolves one component of the alloy preferentially, a planar solid-liquid interface is not stable. They demonstrated this experimentally for Cu-Ni alloys in liquid Ag, Au-Cu alloys in liquid Bi and Ag-Au alloys in molten AgCl.

Consider (6-41) in relation to the problem treated by Harrison and Wagner and designate the solid and liquid phases by I and II respectively†. That one of the components must be dissolved (or rejected) preferentially by the liquid in order to produce instability is obvious since if the solubilities are the same in both phases, the various $G_i^{mn} \to 0$ and (6-41) is indeterminant (in fact the interface is stable because of capillarity). The morphological breakdown discussed by Harrison and Wagner is apparently the result of 'kinetic' rather than constitutional (ie., supersaturation)

---

†Recall that by convention the positive direction is from phase II to I .

effects (cf., Sec. 3.5). Therefore assume that the second and fourth terms of (6-44) can be ignored. Hence, noting that for dissolution V>0, the latter reduces to

$$\left|\frac{(m^{II}D_1^{II}-mD_2^{II})}{(m^{II}-m)}\right| - \left|\frac{(mD_2^{I}-m^{I}D_1^{I}}{(m^{I}-m)}\right| > 0 \qquad \text{(unstable)} \qquad (6\text{-}51)$$

Diffusion in the liquid is many orders of magnitude faster than in the solid (ie., $D_i^{II} >> D_i^{I}$) and thus on the basis of (6-51) one would expect an unstable solid-liquid interface, a prediction which is in agreement with the experiments of Harrison and Wagner. This mathematical result is a reflection of the fact that, physically, breakdown arises because the rate of dissolution is controlled by the rate at which the independent components are transported through the solid to or away from the solid-liquid interface.Transport through the solid to or away from an interfacial perturbation is more efficient than for a planar interface (the point effect of diffusion) and, as a result, the dissolution process is accelerated near the perturbation and it is magnified.

6.5.4 Binary Alloy Oxidation

The stability of a planar oxide-alloy interface can be analyzed using the results of the present paper. The isothermal diffusion controlled formation of an oxide scale, X_mO_n, of uniform thickness on the planar surface of a binary alloy, X-Y, can be considered as a three-phase (vapour, oxide

alloy) ternary diffusion couple. The corresponding diffusion path can be calculated and then plotted on the appropriate ternary isotherm. Two of the possible configurations are shown in Fig. 6-4. In the first case (dotted line PR) no regions of supersaturation are indicated by the calculated diffusion path. A second possibility (solid line PR) indicates a region of supersaturation in contact with the interface. In this case transition to a nonplanar morphology will relieve the supersaturation and one can apply the perturbation results developed in the present chapter. Of course, if the calculated diffusion path associated with this second possibility cuts deep into the two phase field, internal oxidation as well as morphological breakdown may result.

To obtain the appropriate interface stability criterion, adopt a nomenclature in which component 1 is oxygen, component 2 is Y (the more noble alloying element), component 3 is X, phase I is the oxide and phase II is the alloy. Relations (6-41) or (6-44) can now be applied directly to the situation described in Fig. 6-4.

It is also of interest to consider the pseudo-binary limit in which component 2 is insoluble in I and component 1 is insoluble in II. The phase diagram and calculated diffusion path corresponding to this situation is shown in Fig. 6-5 (cf., Fig. 6-4). Noting that $m^{II} = 0$, $G_1^{II\ I} \to 0$ and $G_2^{I\ II} \to 0$, (6-41) reduces to

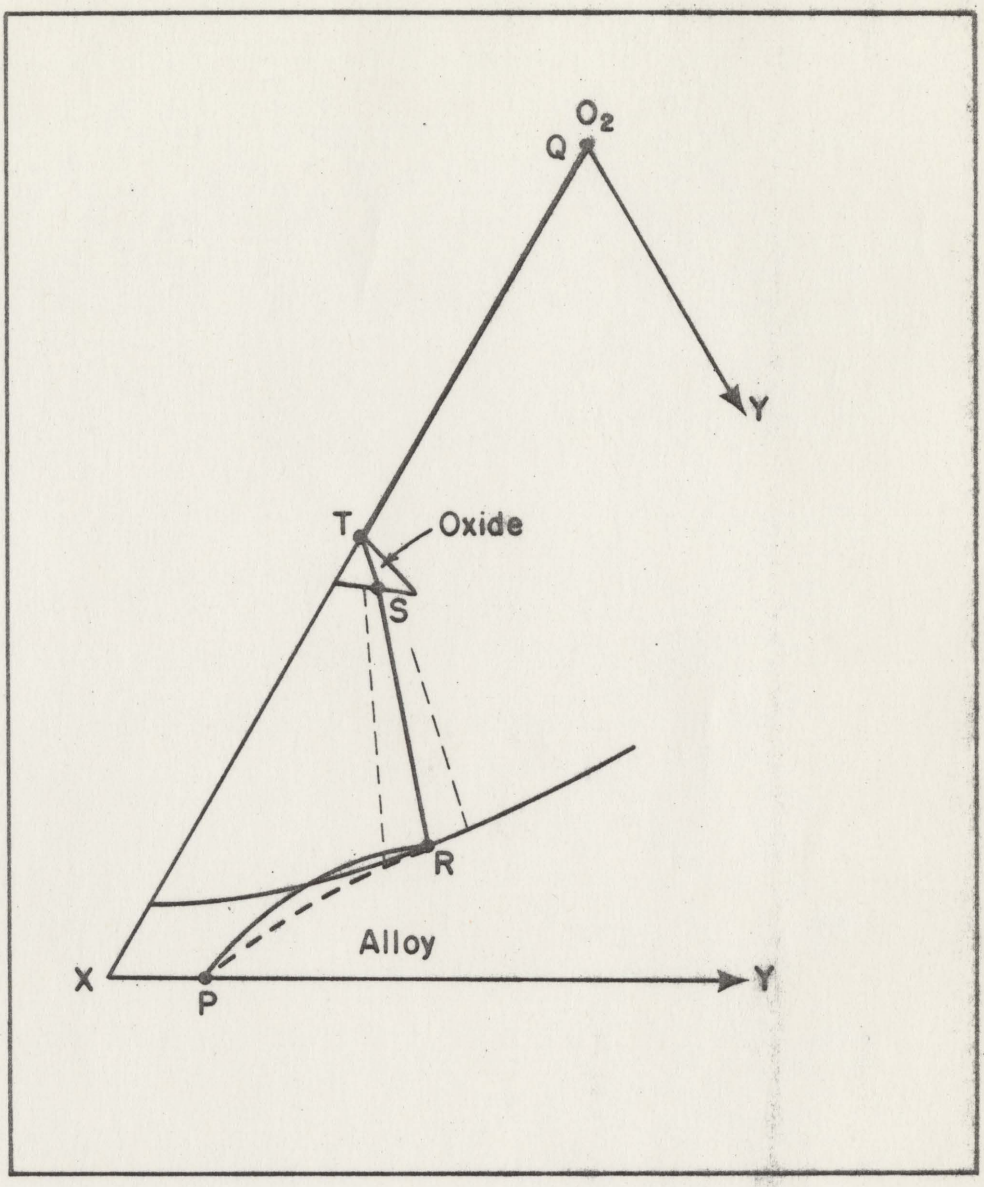

Fig. 6-4 Example of an isothermal phase diagram which is relevant to alloy oxidation. Also shown are two possible diffusion paths corresponding to oxidation of a binary alloy of composition P.

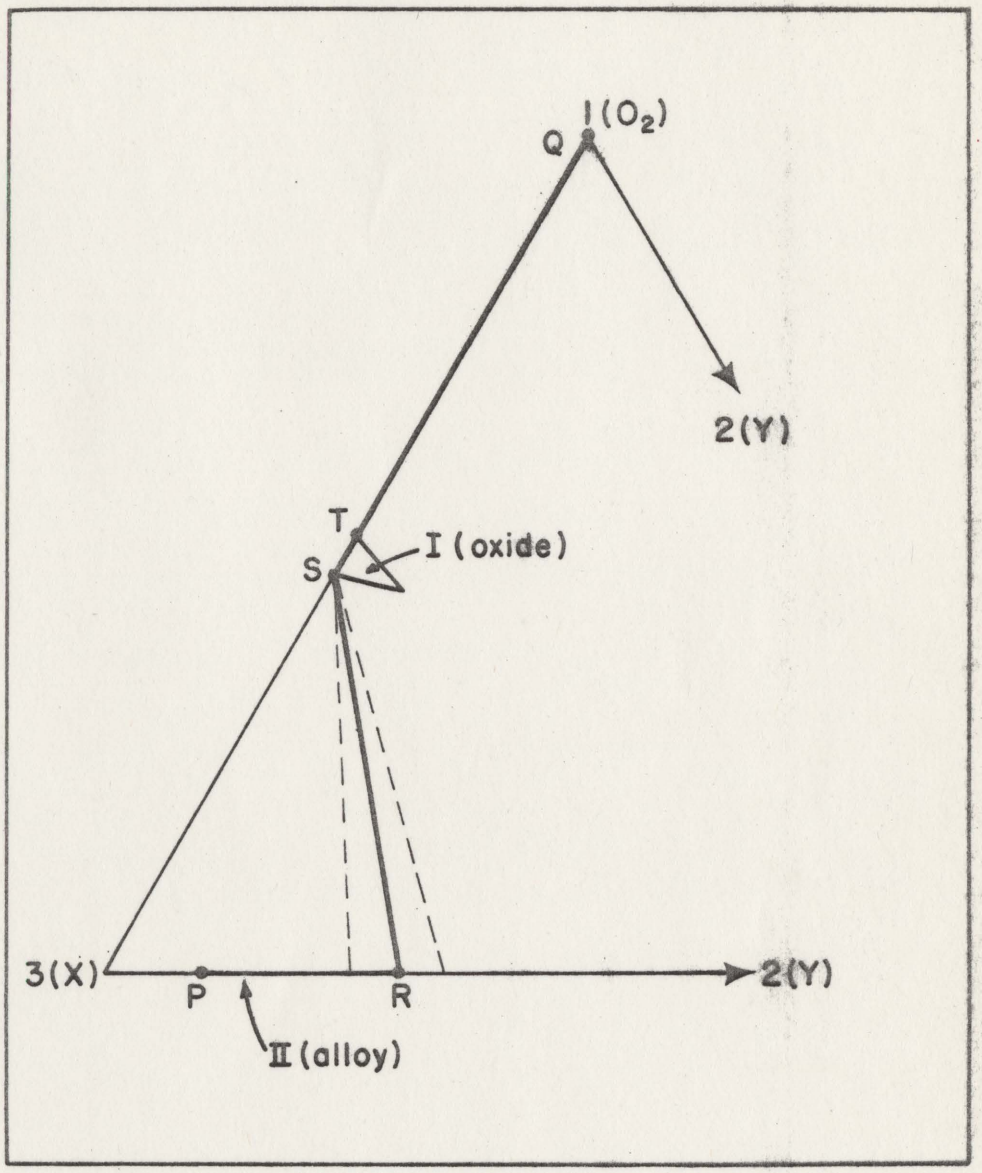

Fig. 6-5 The phase diagram and diffusion path corresponding to Fig. 6-4 in the pseudo-binary limit.

$$V\{|-D_2^I G_1^{I\ II} - m^{II\ I} D_2^{II} G_1^{I\ II}| - |m^I D_2^{II} G_2^{II\ I}|\} > 0 \quad \text{(unstable)}$$

Since the alloy-oxide interface moves toward the alloy (II) $V<0$ and the above yields

$$\left| - \frac{D_2^I G_1^{I\ II}}{m^I D_2^{II} G_2^{II\ I}} - \frac{m^{II\ I} G_1^{I\ II}}{m^I\ G_2^{II\ I}} \right| < 1 \quad \text{(unstable)} \qquad (6\text{-}52)$$

From relations (6-19), (6-20) and (6-43), it follows that if $G_1^{II\ I} = G_2^{I\ II} = 0$, then

$$\frac{G_1^{I\ II}}{G_2^{II\ I}} = - m \frac{D_2^{II}}{D_1^I}$$

and (6-52) becomes

$$\left| \frac{m\ D_2^I}{m^I\ D_1^I} + \frac{(m-m^I)}{m^I} \frac{D_2^{II}}{D_1^I} \right| < 1 \quad \text{(unstable)} \qquad (6\text{-}53)$$

after setting $m^{II} = 0$ in Eq. (6-16) and substituting the latter. It should be kept in mind that relation (6-53) is a very special case of the more general criterion, (6-41) or (6-44).

Wagner[45] has considered the above stability problem in a similar pseudo-binary limit. Unfortunately it has not been possible to establish a unique correspondence between the two treatments because of differing assumptions about the thermodynamics of the system.

Referring to Fig. 6-5, one notes that in the limit as the bulk alloy composition approaches pure component 3, the magnitude of the slope of the tie-line approaches infinity (ie., the tie-line must coincide with the 1-3 binary axis). This situation, of course, corresponds to oxidation of a pure metal. Imposing the condition $|m| \to \infty$ in (6-53), this criterion predicts absolute stability as one would expect for what is in fact a binary diffusion couple.

The first term in (6-53) involves the ratio D_2^I/D_1^I. One might be disturbed by the appearance of the diffusion coefficient of 2 in the oxide because the concentration of this component in the oxide is assumed to be very small. However, although the amount of 2 in the oxide may be small, even infinitesimal, it cannot be ignored because local equilibrium with the alloy (which contains 2) must be maintained. Thus the diffusion of 2 in the oxide plays a role in determining if the alloy-oxide interface is stable with respect to perturbations of infinitesimal amplitude.

CHAPTER 7

EXPERIMENTAL PROCEDURE AND RESULTS

7.1 INTRODUCTION

It is obviously beyond the capabilities of a single dissertation to provide quantitative experimental confirmation for all aspects of the theoretical developments in chapters 5 and 6. Thus it was decided to restrict attention to the problem of phase interface stability in two-phase infinite diffusion couples. The primary goal of the experimental program is to systematically index the transition from a stable to an unstable planar interface in a particular ternary system. Such an investigation has hitherto never been attempted. After reviewing various possibilities it was decided to select a system in which it was judged possible to index the stable-unstable transition by simply varying one of the terminal compositions in a series of infinite diffusion couples. Referring to Fig. 7-1,the idea is to prepare diffusion couples of the form A-B, A-C, A-D etc. and to establish where the transition from stable to unstable occurs (if it does at all). The binary couple A-B necessarily has a stable interface. It was also deemed to be valuable to observe the evolution of morphology in those diffusion couples whose interface is unstable.

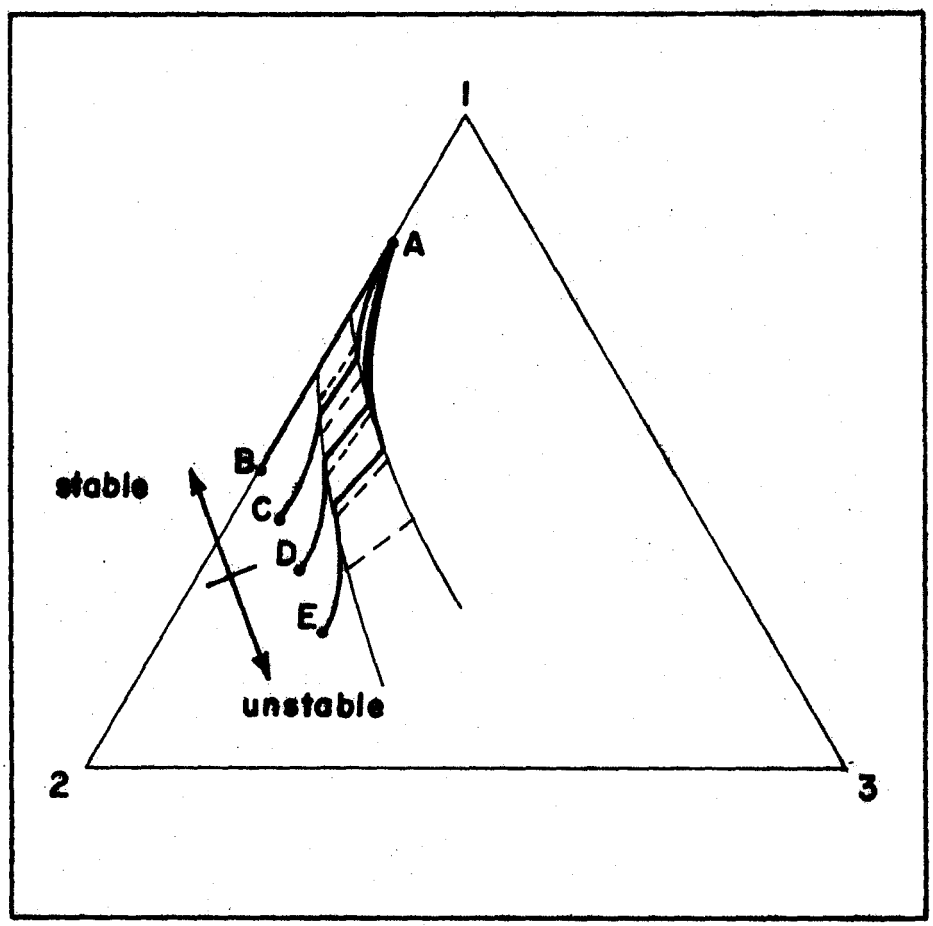

Fig. 7-1 Diffusion paths corresponding to a series of two-phase diffusion couples. Each couple has the same terminal composition for one of the phases

7.2 THE Cu-Zn-Ni SYSTEM

The Cu-Zn-Ni system at 775°C (Fig. 7-2) was selected after examining the properties of numerous other systems via the literature and, in a few cases, via preliminary experiments. Of interest with respect to the present study is the region 35-50 wt.% Zn and 0-10 wt. % Ni.

The early and mid 1950's brought forth precise measurements of tracer[65,66], intrinsic and chemical diffusivity[67,68,69,70] in the binary system Cu-Zn. Most of this work was inspired by a desire to test the validity of Darken's analysis[71] of the Kirkendall effect[72]. As a result the chemical diffusion coefficient in Cu-Zn is known as a function of concentration and temperature for both the α and β phases. DeHoff et al[73] and Oikawa et al[74] have studied the diffusion of tracer, Zn^{65}, in the copper-rich corner of the α phase in Cu-Zn-Ni and found that the diffusivity correlates strongly with the solidus temperature. To date there have been no measurements of chemical diffusivity in the ternary system.

Recently multiphase diffusion in the ternary system Cu-Zn-Ni at 775°C was investigated by Taylor et al[75] with two groups of infinite diffusion couples, (22 wt. % Ni, 46.5 wt. % Zn/100 wt. % Cu) and (22 wt. % Ni, 46.5 wt. % Zn/100 wt. % Ni). That study is essentially a metallographic examination of the development of highly irregular interfaces and of the

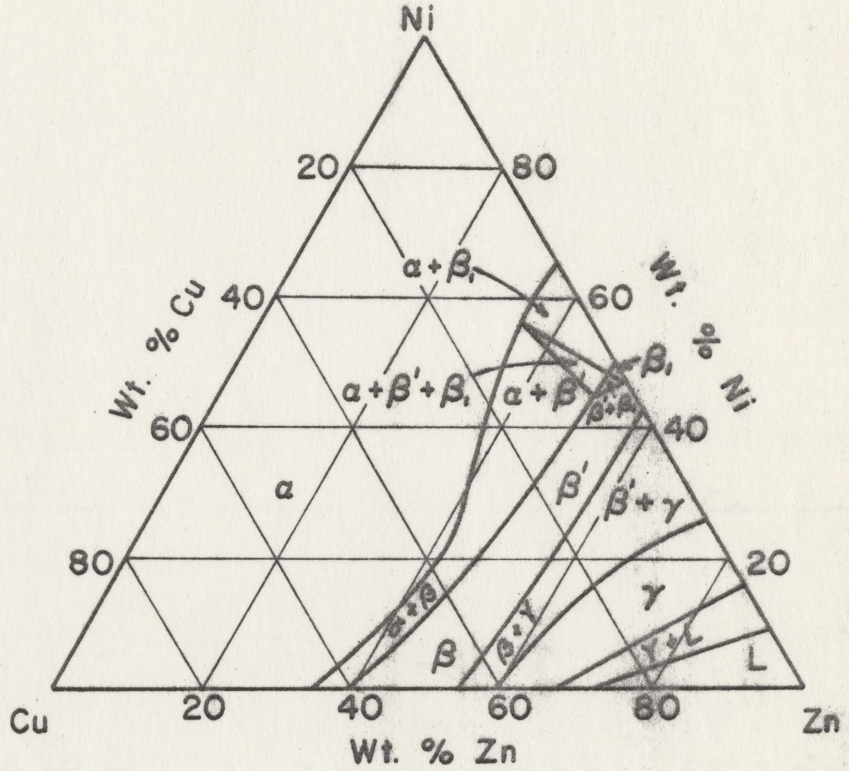

Fig. 7-2 The Cu-Zn-Ni system at 775°C (after Schramm[64])

evolution of very complex diffusion structures. Apart from a few electron microprobe traces across the diffusion zone, no attempt is made to examine the morphological breakdown in quantitative terms. Indeed, the very large concentration variations involved and the lack of diffusion and equilibrium data for those composition ranges excludes the possibility of quantitative interpretation. The experimental program in the present dissertation involves a much smaller (and different) range of compositions and includes evaluation of diffusion and equilibrium data. As a result quantitative measurements and interpretation are possible.

Henceforth Ni and Zn are regarded as the independent components in the ternary system Cu-Zn-Ni and therefore the chemical diffusion coefficients are D^{m}_{ik} (i,k = Ni,Zn; m = α,β). In view of the fact that the melting points of Zn and Ni are 419°C and 1453°C, respectively, it follows that $D_{NiNi} << D_{ZnZn}$ and therefore $\partial C_{Ni}/\partial z >> \partial C_{Zn}/\partial z$. Noting the latter and the fact that in general $D_{ij} < D_{ii}$ [8], one can ignore $D_{NiZn}\ \partial C_{Zn}/\partial z$ in the Ni flux equation

$$J_{Ni} = -D_{NiNi}\ \frac{\partial C_{Ni}}{\partial z} - D_{NiZn}\ \frac{\partial C_{Zn}}{\partial z}\ .$$

Accordingly, if diffusional interaction is significant, it will involve the Ni distribution influencing that of Zn and not the reverse. Therefore, it is necessary that a check be made as to whether $D_{ZnNi}\ \partial C_{Ni}/\partial z$ is significant in the Zn flux equation

$$J_{Zn} = - D_{ZnZn} \frac{\partial C_{Zn}}{\partial z} - D_{ZnNi} \frac{\partial C_{Ni}}{\partial z} .$$

For the analysis of interface stability, the Cu-Zn-Ni system has the following advantages:

i) The fact that Zn diffuses much more rapidly than Ni is of considerable significance in relation to the possibility of producing a (virtual) zone of supersaturation in two-phase infinite diffusion couples. Because Ni diffuses slowly, its interfacial gradients likely will be much steeper than those of Zn, especially when the terminal composition in β has a high Ni content. Thus referring to Eqs. (6-2) and (6-3) and Fig. 7-3, one would expect the diffusion path for regions adjacent to the interface to approach that which is shown. Clearly, as the Ni content of the terminal composition in β is reduced, the above behaviour is less pronounced

ii) In the range 0-10 wt. % Ni, the two phase field α+β (see Fig. 7-2) is narrow with approximately straight and parallel phase boundary lines.

iii) One expects that diffusion in the F.C.C. α phase is much slower than the more open structured B.C.C. β phase. Indeed this is certainly the case for diffusion in binary Cu-Zn[67, 68,69,70]. This feature should permit simplifications in certain calculations.

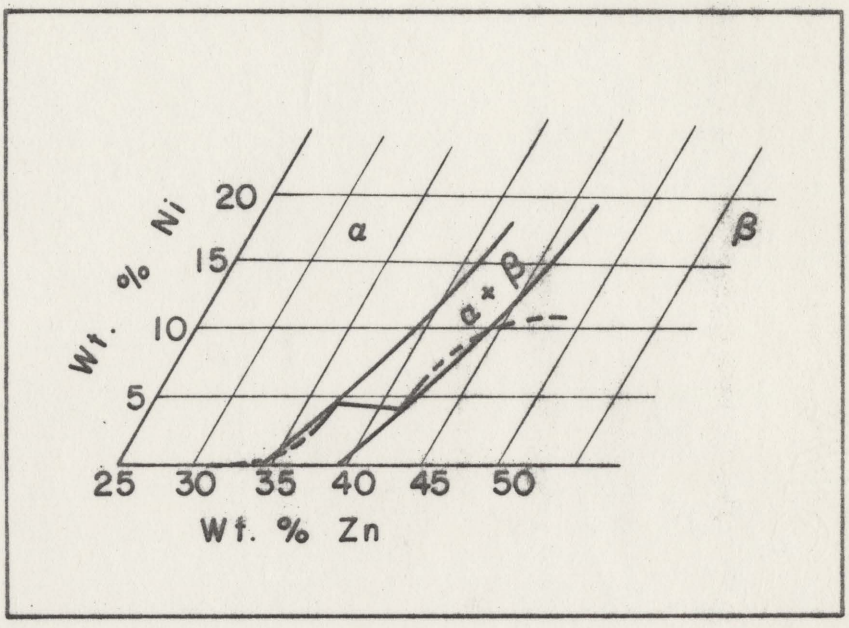

Fig. 7-3 Typical diffusion path for the Cu-Zn-Ni system at 775°C. The path is very steep near the phase boundaries because of low Ni diffusivity.

The only important disadvantage to the Cu-Zn-Ni system is the high vapour pressure of Zn at 775°C. Special care is necessary to avoid Zn losses during annealing treatments.

7.3 OUTLINE OF EXPERIMENTAL PROGRAM

The experimental program is divided into four parts, as follows:

i) The positions of the $\alpha/\alpha+\beta$ and $\alpha+\beta/\beta$ phase boundaries at 775°C have been determined by Schramm[64] (Fig. 7-2). However, nothing is known regarding the position of the tie-lines in the two-phase $\alpha+\beta$ field. Such information is a prerequisite to specification of interfacial concentrations under conditions of local equilibrium. Experiments aimed at determining the positions of these tie-lines were therefore undertaken.

ii) Because the present study is concerned with low concentrations of Ni in Cu-Zn alloys, D^m_{ZnZn} for the α and β phases are approximately the corresponding chemical diffusion coefficients in binary Cu-Zn. This data is readily available in the literature[67,68,69,70]. However, because of the complete lack of information on the diffusivity of Ni in the α and β phases of Cu-Zn, it was necessary to determine D^m_{NiNi} ($m = \alpha,\beta$) experimentally. It was also necessary to check whether a steep Ni gradient influences the distribution of Zn for the regions of

composition of present interest.

iii) The next part of the experimental program involved indexing the transition from a stable to unstable planar α-β phase interface. Numerous two-phase (α-β) infinite diffusion couples were prepared with each couple having the same terminal composition for the α phase. However, the terminal compositions for the β phase corresponded to increasing amounts of Ni (ie., increasing in a direction approximately parallel to the $\alpha+\beta/\beta$ phase boundary). This tactic is schematically summarized in Fig. 7-4. In progressing from couple A-B to A-F, one hopes there is a transition in the α-β interface morphology from planar to non-planar.

iv) The final aspect of the experimental program was to examine metallographically the time evolution of non-planar α-β interfaces in the diffusion couples just described.

7.4 EXPERIMENTAL PROCEDURE

7.4.1 Alloy Preparation

In Table 7-1 a list of the compositions of the alloys used in the present study is given, along with a system of nomenclature to specify a particular alloy. The various alloys were prepared from elemental Cu, Zn and Ni

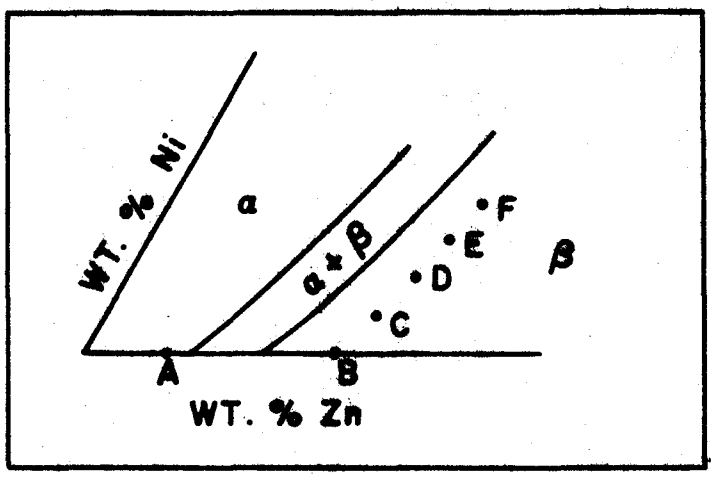

Fig. 7-4 Schematic drawing of the diffusion couple terminal compositions to be used in the stability studies.

Table 7-1

Symbol	Ni (wt.%)	Zn (wt.%)
α1	0	34.1
α2	2.5	35.2
α3	5.0	35.0
β1	0	43.9
β2	2.5	44.1
β3	5.0	44.0
β4	7.5	45.9
β5	5.0	43.0
β6	6.5	43.9
β7	7.5	44.4
β8	10.0	46.0
β9	15.0	48.0
αβ1	2.5	39.3
αβ2	5.0	40.6
αβ3	7.5	41.6
αβ4	10.0	41.9

of better than 99.99% purity. The alloy constituents, in the appropriate proportions, were sealed in Argon filled quartz capsules. These were then placed in a pot furnace for two hours at approximately 1000°C (just above the liquidus surface). Four or five times during the two hour period, the quartz capsules were quickly removed from the furnace, were tipped

back and forth to cause convective mixing of the melt and then were quickly returned to the furnace. At the end of the two hours, the capsules were removed from the furnace and quenched in water. The resultant cylindrical ingots weighed from 50 to 100 grams. In the above manner, alloys in relatively small amounts could be rapidly prepared with close composition control.

Using a lathe, a few grams of turnings were removed from each ingot. The ingots were then hot rolled to a thickness of about 1/8 inch. After the surfaces were cleaned, the alloys and corresponding turnings were then sealed in argon filled Vycor capsules. The turnings were used to minimize the specimen Zn losses which arise out of the high Zn vapour pressure at the annealing temperatures. Alloys $\beta 1$ to $\beta 9$ were annealed for three days at 850°C. Alloys $\alpha 1$, $\alpha 2$ and $\alpha 3$ were annealed for one week at 775°C. Alloys $\alpha\beta 1$, $\alpha\beta 2$, $\alpha\beta 3$ and $\alpha\beta 4$ were annealed for two weeks at 775°C ± 1°C. On completion of the anneal, all samples were quenched in water. The homogeneity of the annealed specimens was checked with the electron microprobe and the alloy compositions as listed in Table 7-1 were checked by wet chemical analyses.

7.4.2 Tie-Line Study

The four two-phase specimens which had been equilibrated for two weeks were sectioned, mounted in bakelite,

polished, etched† and examined metallographically. Hardness indentations were then used to indicate an α-β phase interface in each specimen and the direction perpendicular to it. The specimens were then repolished with due care taken not to remove the hardness indentations. By point-to-point counting with an Acton (Cameca MS-64) electron microprobe, the composition variation from the α phase, across the α-β interface, to the β phase was determined. Analyses were made for Ni and Zn by measuring the intensities of the NiK_α and ZnK_α X-ray lines. The microprobe was operated with an electron energy of 20 kv and a beam current of 150 nanoamps as measured on a Faraday cage.

7.4.3 Diffusion Couple Preparation

Table 7-2 gives the terminal compositions of the diffusion couples which were prepared and their corresponding position on the Cu-Zn-Ni isotherm is shown in Fig. 7-5. The couples were prepared in the following manner. Pieces $\frac{1}{4} \times \frac{1}{4} \times \frac{1}{8}$ inch were cut from the annealed alloys. One face of each piece was polished to No. 600 grit. The

---

†The etchant used for all of the metallography in this dissertation was a solution comprised of 20 g. Cr_2O_3, 3.25 g. NH_4Cl, 25 mℓ. HNO_3, 25 mℓ. H_2SO_4 and H_2O to 0.5 ℓ.

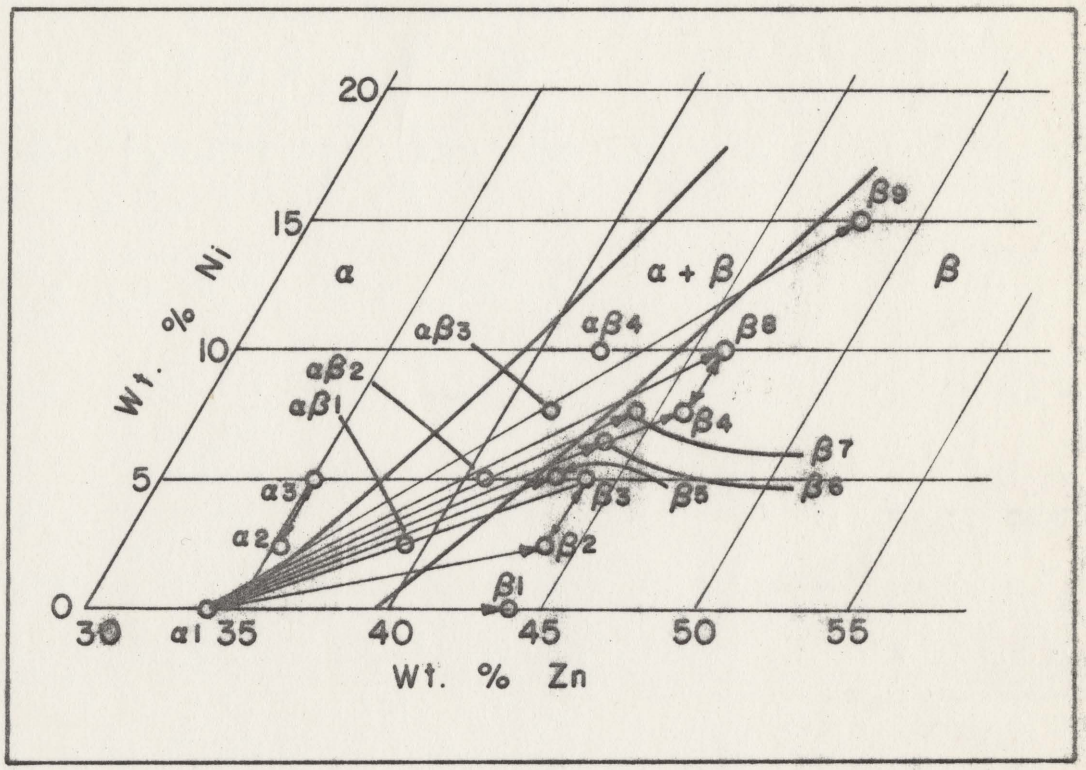

Fig. 7-5 Location of alloy compositions (Table 7-1) on the 775°C Cu-Zn-Ni isotherm. The terminal compositions of the various diffusion couples (Table 7-2) are joined by arrows

Table 7-2

Couple	Purpose	Time-Diffusion Anneal (hr)
α2-α3	diffusion coefficient	5-2/3
β2-β3	diffusion coefficient	1
β4-β8	diffusion coefficient	1
α1-β1	stability study	16
α1-β2	stability study	16
α1-β3	stability study	1, 4
α1-β4	stability study	1, 4
α1-β5	stability study	$\frac{1}{4}$, 1, 4, 9
α1-β6	stability study	$\frac{1}{4}$, 1, 4, 9
α1-β7	stability study	$\frac{1}{4}$, 1, 4, 9
α1-β8	stability study	$\frac{1}{4}$, 1, 4, 9
α1-β9	stability study	1, 4, 9

polished faces of the two halves of each of the diffusion couples were placed in contact and were then pressure welded at 550°C for 1 hr in a furnace through which a continuous flow of hydrogen was maintained. The purpose of the hydrogen was to reduce any oxide which formed on the polished faces before the weld was effected. The diffusion couples were then annealed for the appropriate length of time ($\frac{1}{4}$ to 16 hours) at 775°C±1°C. Each diffusion anneal was terminated with a rapid water quench.

The diffusion couples were then sectioned in a plane parallel to the diffusion direction, mounted in bakelite, polished, etched and examined metallographically. The morphology of the α-β phase interface was of particular interest in those diffusion couples used for stability studies (ie., couples α1-β1 to α1-β9 of Table 7-2).

Hardness indentations were used to indicate the direction normal to the original weld (ie., the diffusion direction) on the three diffusion couples (α2-α3, β2-β3, and β4-β8) to be employed for the determination of D^{α}_{NiNi}, D^{β}_{NiNi} and the extent of diffusional interaction. The diffusion couples were then repolished. Operating under the same conditions as described in Sec. 7.4.2, the Acton electron microprobe was used to measure the intensity variations of the NiK_{α} and ZnK_{α} X-ray lines in the direction of diffusion. The two bulk alloys of a given diffusion couple (ie., the regions on either side of the diffusion zone) were used as standards because their compositions were known (see Table 7-1). Compositions within the diffusion zone were determined by assuming a linear composition-intensity relationship between the two terminal compositions. To ensure that this assumption was valid, the difference in the bulk alloy Ni contents, for each of the three diffusion couples examined with the electron microprobe, was purposely chosen to be small, ie., 2.5 wt. %.

7.5 EXPERIMENTAL RESULTS

7.5.1 Tie-Line Determination

The compositions of the four alloys which were used to determine the tie-lines were selected to lie approximately at the center of the α+β phase field at 775°C (see Fig. 7-5). The corresponding microstructures are shown in Fig. 7-6 and these indicate that the two phases are, in fact, present in about equal amounts. A typical electron microprobe trace across an α-β phase interface is shown in Fig. 7-7. The fact that no concentration gradients exist in either phase indicates that the alloy is completely equilibrated. As a result the compositions of the two phases should lie on the corresponding phase boundaries and also define a tie-line on the ternary phase diagram. Let the average measured X-ray intensity minus background for each component in each phase be depicted by the symbols I^{α}_{Ni}, I^{α}_{Zn}, I^{β}_{Ni}, and I^{β}_{Zn}. Because the bulk alloy compositions were selected to lie near the center of the two-phase field, one can construct an internal standard by assuming that the following mean intensities, $\frac{1}{2}(I^{\alpha}_{Ni} + I^{\beta}_{Ni})$ and $\frac{1}{2}(I^{\alpha}_{Zn} + I^{\beta}_{Zn})$, correspond to the bulk alloy compositions, $\bar{C}_{Ni}$ and $\bar{C}_{Zn}$ respectively, as given in Table 7-1. The difference in equilibrium concentration of a given component in each phase is simply

$$C^{\alpha\beta}_i - C^{\beta\alpha}_i = \frac{I^{\alpha}_i - I^{\beta}_i}{\frac{1}{2}(I^{\alpha}_i + I^{\beta}_i)} \times \bar{C}_i \qquad (7\text{-}1)$$

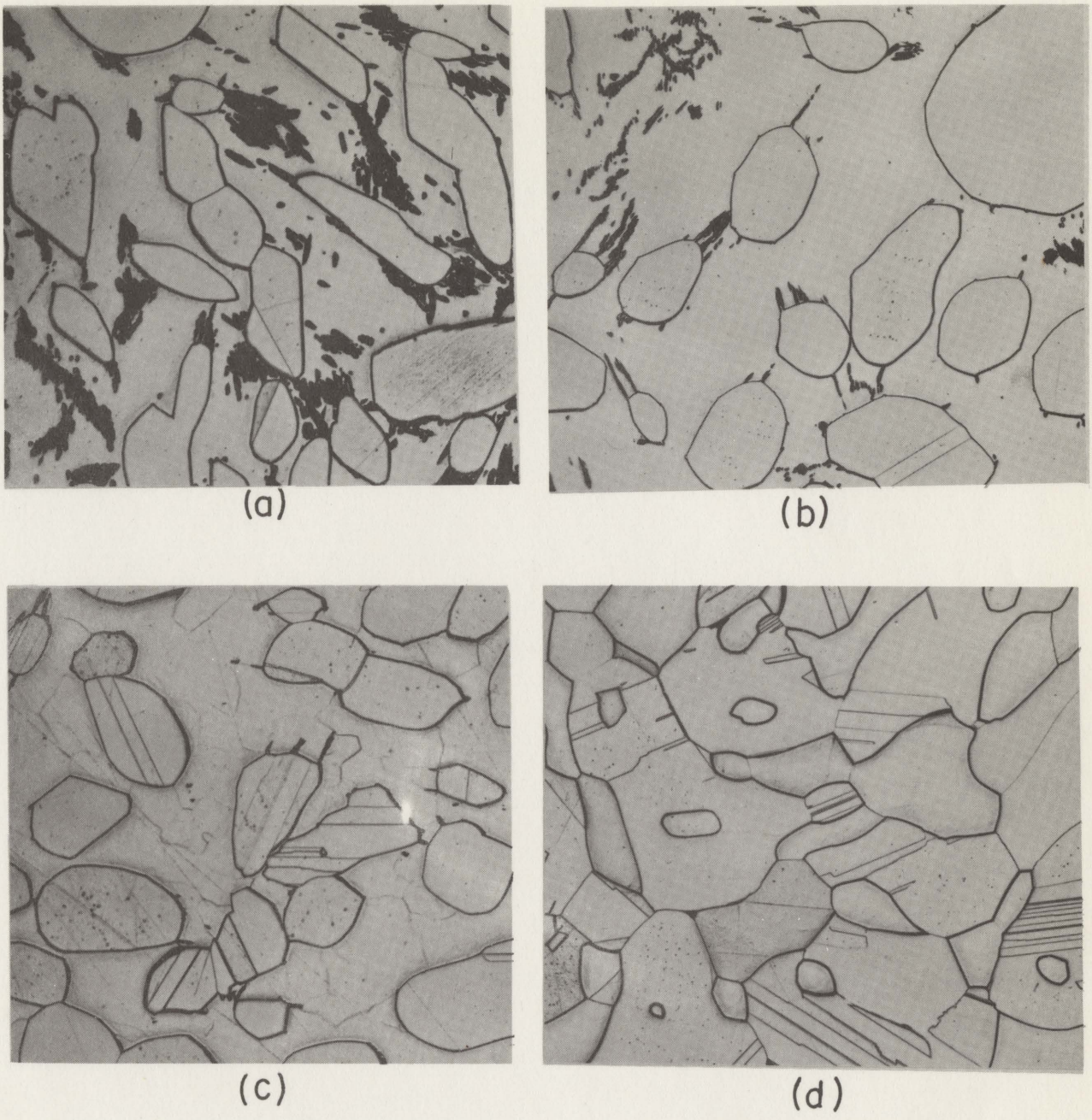

Fig. 7-6 Micrographs of two-phase alloys (Table 7-1) annealed for two weeks at 775°C. The β phase is the matrix. The α phase contains annealing twins. The black precipitate in β is Widmanstätten α which forms during the quench from the annealing temperature. (a) αβ1 - 80X, (b) αβ2 - 80X, (c) αβ3 - 80X and (d) αβ4 - 64X.

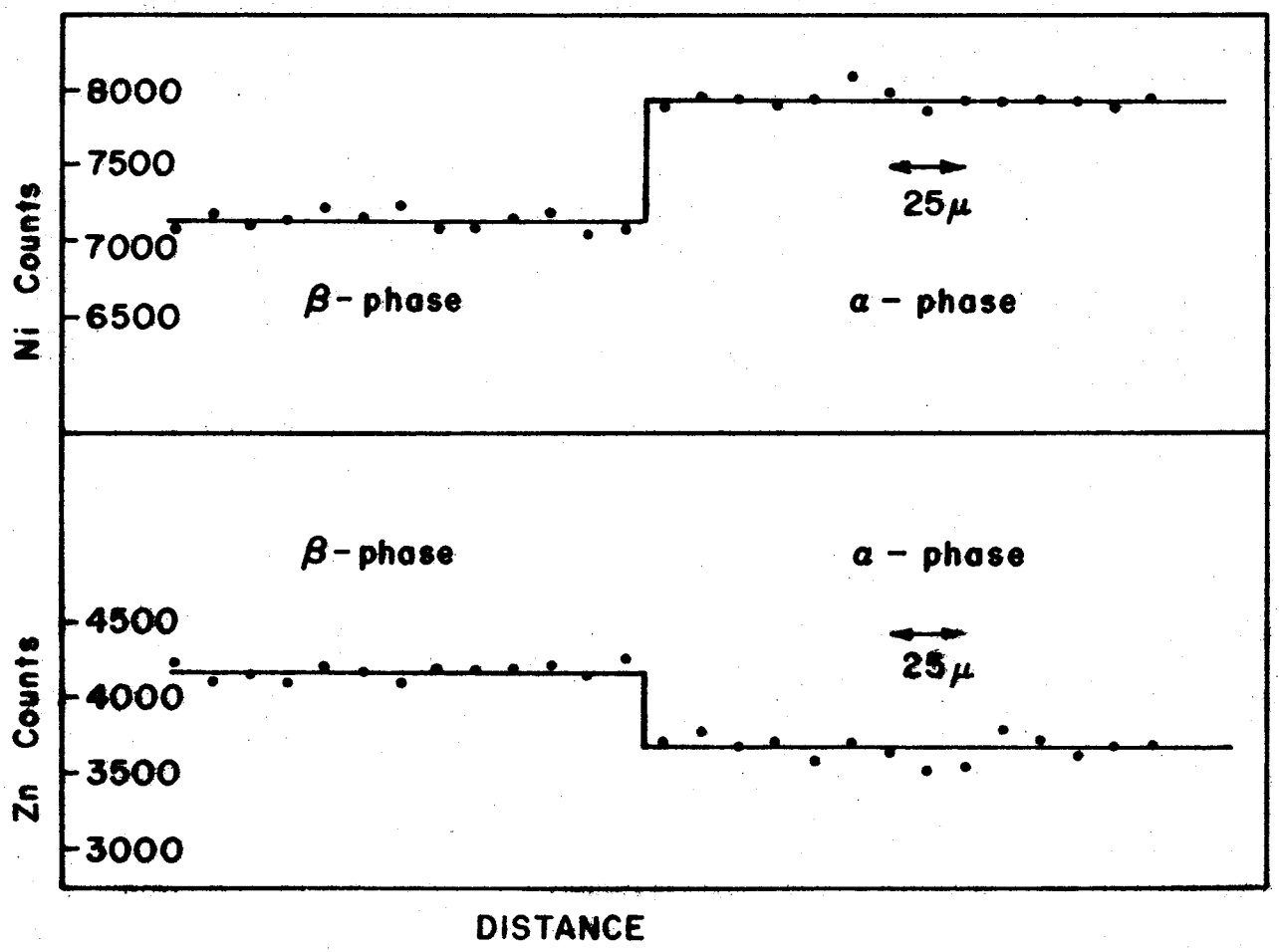

Fig. 7-7 Electron microprobe trace across a phase interface in sample αβ3

where a linear intensity-composition relationship is assumed.

The above means of introducing an internal standard is very accurate because one is concerned only with relatively small changes in concentration (or intensity). The following calculation perhaps clarifies this point. If the true intensities corresponding to $\bar{C}_{Ni}$ and $\bar{C}_{Zn}$ are $\bar{I}_{Ni}$ and $\bar{I}_{Zn}$ respectively, one can write

$$\bar{I}_i = \tfrac{1}{2}(I_i^\alpha + I_i^\beta) + \varepsilon_i \qquad (7\text{-}2)$$

where it is necessarily true that $|\varepsilon_i| < |\tfrac{1}{2}(I_i^\alpha - I_i^\beta)|$ for $\bar{C}_{Ni}$ and $\bar{C}_{Zn}$ to define a point in the two phase field. Because $\bar{C}_{Ni}$ and $\bar{C}_{Zn}$ were purposely chosen to define a point near the center of the $\alpha+\beta$ field,

$$|\varepsilon_i| \ll |\tfrac{1}{2}(I_i^\alpha - I_i^\beta)| \ . \qquad (7\text{-}3)$$

The intensity ratio which should appear in Eq. (7-1) is

$$\frac{I_i^\alpha - I_i^\beta}{\bar{I}_i} = \frac{I_i^\alpha - I_i^\beta}{\tfrac{1}{2}(I_i^\alpha + I_i^\beta) + \varepsilon_i} \ .$$

Expanding the denominator to the first order gives

$$\frac{I_i^\alpha - I_i^\beta}{\bar{I}_i} \cong \frac{I_i^\alpha - I_i^\beta}{\tfrac{1}{2}(I_i^\alpha + I_i^\beta)} \left(1 - \frac{\varepsilon_i}{\tfrac{1}{2}(I_i^\alpha + I_i^\beta)}\right) \qquad (7\text{-}4)$$

Clearly the error involved in using Eq. (7-1) is $|\varepsilon_i| / \tfrac{1}{2}(I_i^\alpha + I_i^\beta)$. Of the four specimens which were examined, the highest value of the ratio $(I_i^\alpha - I_i^\beta)/\tfrac{1}{2}(I_i^\alpha + I_i^\beta)$ was 0.14. Using this value and noting the fact that $|\varepsilon_i| < \left|\tfrac{1}{2}(I_i^\alpha - I_i^\beta)\right|$, it follows that

$$\frac{|\varepsilon_i|}{\frac{1}{2}(I_i^{\alpha} + I_i^{\beta})} < \frac{1}{2} \times \frac{I_i^{\alpha} - I_i^{\beta}}{\frac{1}{2}(I_i^{\alpha} + I_i^{\beta})} = 0.07 \quad .$$

In view of (7-3), the actual value for the error in $C_i^{\alpha\beta}$-$C_i^{\beta\alpha}$ is much lower, probably in the range 1-2%. Clearly it is meaningless to attempt to use the above procedure to calculate $C_i^{\alpha\beta}$ and $C_i^{\beta\alpha}$ individually, rather than the difference between them.

The values of $C_{Ni}^{\alpha\beta} - C_{Ni}^{\beta\alpha}$, $C_{Zn}^{\alpha\beta} - C_{Zn}^{\beta\alpha}$ and $m = (C_{Ni}^{\alpha\beta} - C_{Ni}^{\beta\alpha})/(C_{Zn}^{\alpha\beta} - C_{Zn}^{\beta\alpha})$ corresponding to the specimens $\alpha\beta 1$ to $\alpha\beta 4$ were determined through application of Eq. (7-1) to the electron microprobe measurements. Noting that in the limit $C_{Ni} \to 0$, $(C_{Ni}^{\alpha\beta} - C_{Ni}^{\beta\alpha}) \to 0$, a graph of $C_{Ni}^{\alpha\beta} - C_{Ni}^{\beta\alpha}$ versus $C_{Ni}^{\beta\alpha}$ is shown in Fig. 7-8. To a good approximation, a linear relationship exists. In Fig. 7-9 a graph of -m versus $C_{Ni}^{\beta\alpha}$ is given.

The sign of the slope m of the tie-lines is of considerable significance, particularly in relation to interface stability. For the composition range of present interest in the Cu-Zn-Ni system, it has just been determined that m is negative. Because m^{α} and m^{β} are both positive in this region, this result is not at all surprising.

It is convenient to write

$$(C_{Ni}^{\alpha\beta} - C_{Ni}^{\beta\alpha}) = (k_{Ni} - 1)\, C_{Ni}^{\beta\alpha}$$

where $k_{Ni} = C_{Ni}^{\alpha\beta}/C_{Ni}^{\beta\alpha}$ is the Ni partition coefficient. In view of this relation, the fact that the difference, $C_{Ni}^{\alpha\beta} - C_{Ni}^{\beta\alpha}$,

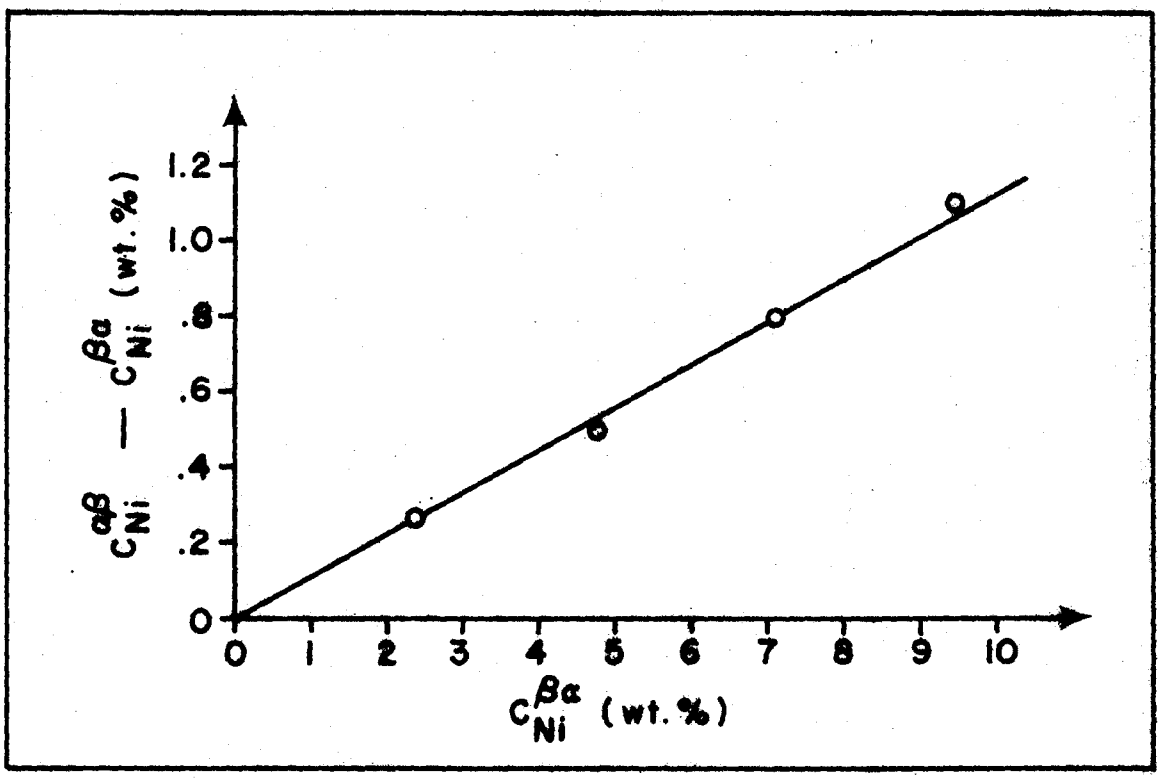

Fig. 7-8 $(C_{Ni}^{\alpha\beta} - C_{Ni}^{\beta\alpha})$ versus $C_{Ni}^{\beta\alpha}$ as obtained from specimens αβ1 to αβ4.

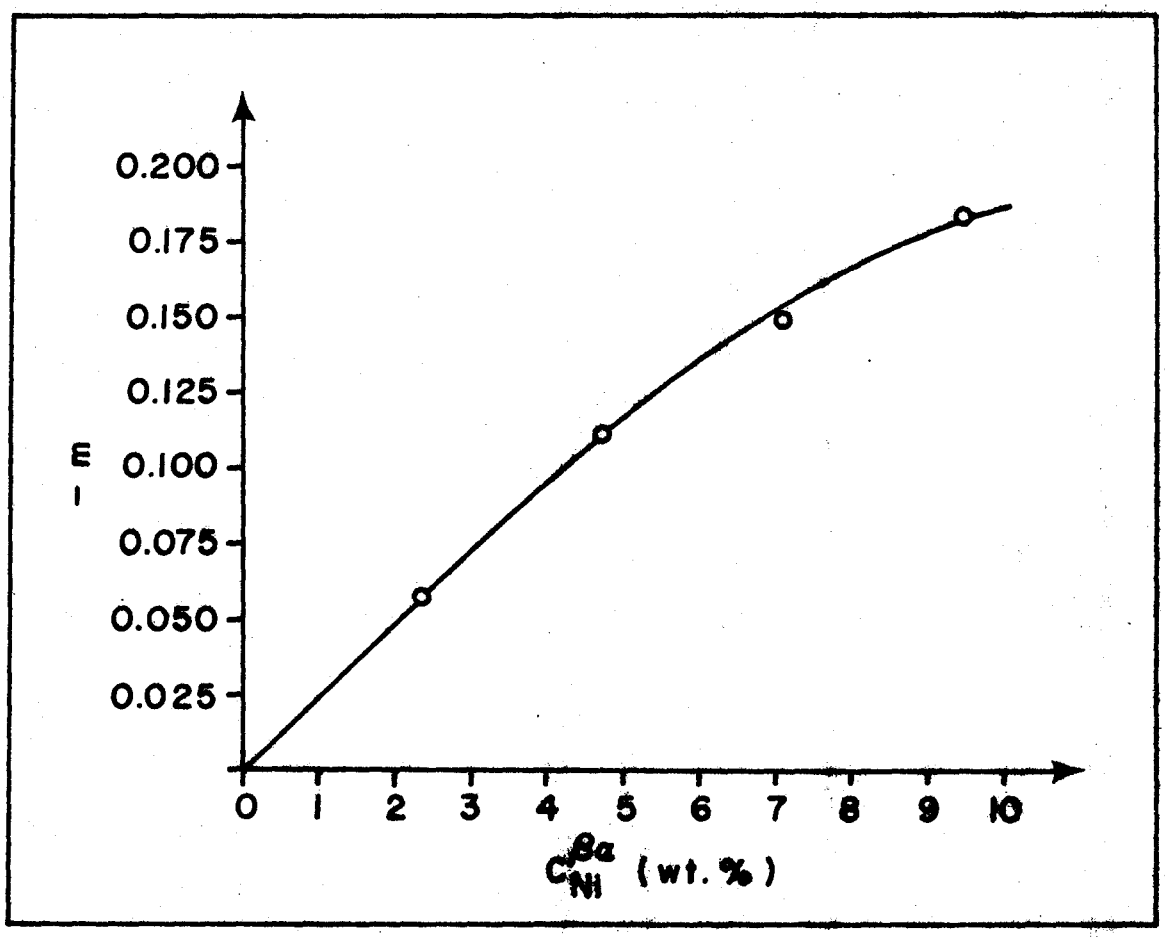

Fig. 7-9 -m versus $C_{Ni}^{\beta\alpha}$ as obtained from specimens αβ1 to αβ4.

increases linearly with $C_{Ni}^{\beta\alpha}$ indicates that the Ni partition coefficient is a constant. This result is consistent with a recent analysis of phase equilibria in ternary systems[57] wherein it was found that dilute partition coefficients tend to be constant.

The graph of -m versus $C_{Ni}^{\beta\alpha}$, Fig. 7-9, is to a good approximation linear for values of $C_{Ni}^{\beta\alpha}$ less than 5 wt. %. Beyond that value the curve becomes a less sensitive function of $C_{Ni}^{\beta\alpha}$.

7.5.2 Diffusion Coefficients

The three diffusion couples α2-α3, β2-β3 and β4-β8 were prepared to measure D_{NiNi}^{α} and D_{NiNi}^{β} and, at the same time, to determine if a steep Ni gradient influences the Zn distribution. Two measurements were made in the β phase because of the higher diffusivities in that phase. This fact results in the presence of larger concentration variations in the β phase of the two-phase α-β diffusion couples used for the stability studies. It was thus felt that it would be of interest to check on the concentration dependence of D_{NiNi}^{β}. The diffusion couples were of the so-called "Darken" type[76] wherein one commences with a uniform distribution of the faster diffusing component and a step in the distribution of the other (see Fig. 7-10). This type of diffusion couple provides the maximum sensitivity to diffusional interaction.

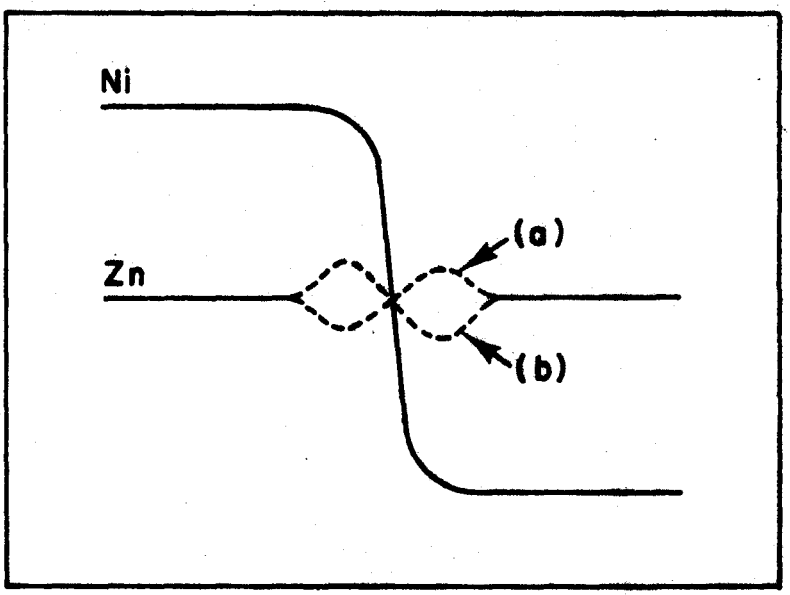

Fig. 7-10 Possible influence of Ni on the Zn distribution: (a) $D_{ZnNi} < 0$ and (b) $D_{ZnNi} > 0$.

If such interaction is significant, then the Zn distribution readjusts to case (a) or case (b), depending on whether D_{ZnNi} is negative or positive respectively. Analysis of the Ni distribution after the diffusion anneal yields D_{NiNi} directly.

In all three diffusion couples, it was observed that after the diffusion anneal, the Zn distribution remained uniform. Thus for the composition range of interest in the present study, ternary diffusional interaction can be ignored completely. Henceforth therefore, it is convenient to adjust the nomenclature so that D^{α}_{NiNi}, D^{β}_{NiNi}, D^{α}_{ZnZn} and D^{β}_{ZnZn} are depicted by D^{α}_{Ni}, D^{β}_{Ni}, D^{α}_{Zn} and D^{β}_{Zn}, respectively.

In each of the three diffusion couples the initial Ni step was 2.5 wt. %. By introducing such a relatively small concentration difference, one can avoid complications such as arise out of the Kirkendall effect and diffusion coefficient concentration dependence. In addition, one can employ a linear X-ray intensity - concentration relationship between the terminal compositions. If in fact the diffusion coefficients are independent of concentration, the present boundary conditions imply a concentration distribution as given by Eq. (2-20), ie.,

$$\frac{C - C_0}{C_1 - C_0} = \frac{1}{2}\left[1 - \operatorname{erf}\left(\frac{z}{2\sqrt{Dt}}\right)\right]$$

Assumption of a linear X-ray intensity-concentration relationship allows one to write

$$\frac{C - C_0}{C_1 - C_0} = \frac{I - I_0}{I_1 - I_0}$$

and therefore the above becomes

$$I_R \equiv \frac{I - I_0}{I_1 - I_0} = \frac{1}{2}[1 - \text{erf}(\frac{z}{2\sqrt{Dt}})] \qquad (7\text{-}5)$$

where I_R is the normalized X-ray intensity. It is convenient to plot normalized X-ray intensity versus distance on probability graph paper.† Data which satisfies Eq. (7-5) yields a straight line whose slope depends only on the product Dt. Probability paper thus furnishes not only a rapid method for determining the value of D but also an accurate test of the constancy of D with composition, for if D varies with composition a straight line will not result.

Figures 7-11, 7-12 and 7-13 are plots, on probability paper, of I_R versus distance for the diffusion couples α2-α3, β2-β3 and β4-β8, respectively. In using probability paper one should be aware of the fact that the scale in the ranges 0 to .1 and .9 to 1.0 are greatly expanded and therefore measurements of I_R in these ranges exhibit a correspondingly amplified scatter. Thus it is common practice not to include the measured concentration (or intensity) ratios at the tail ends of distributions[77,78]. The three graphs are essentially linear and therefore for a 2.5 wt. % Ni variation, the dif-

---

†The use of such graph paper for the analysis of diffusion data is discussed by Johnson[77] and Wells[78].

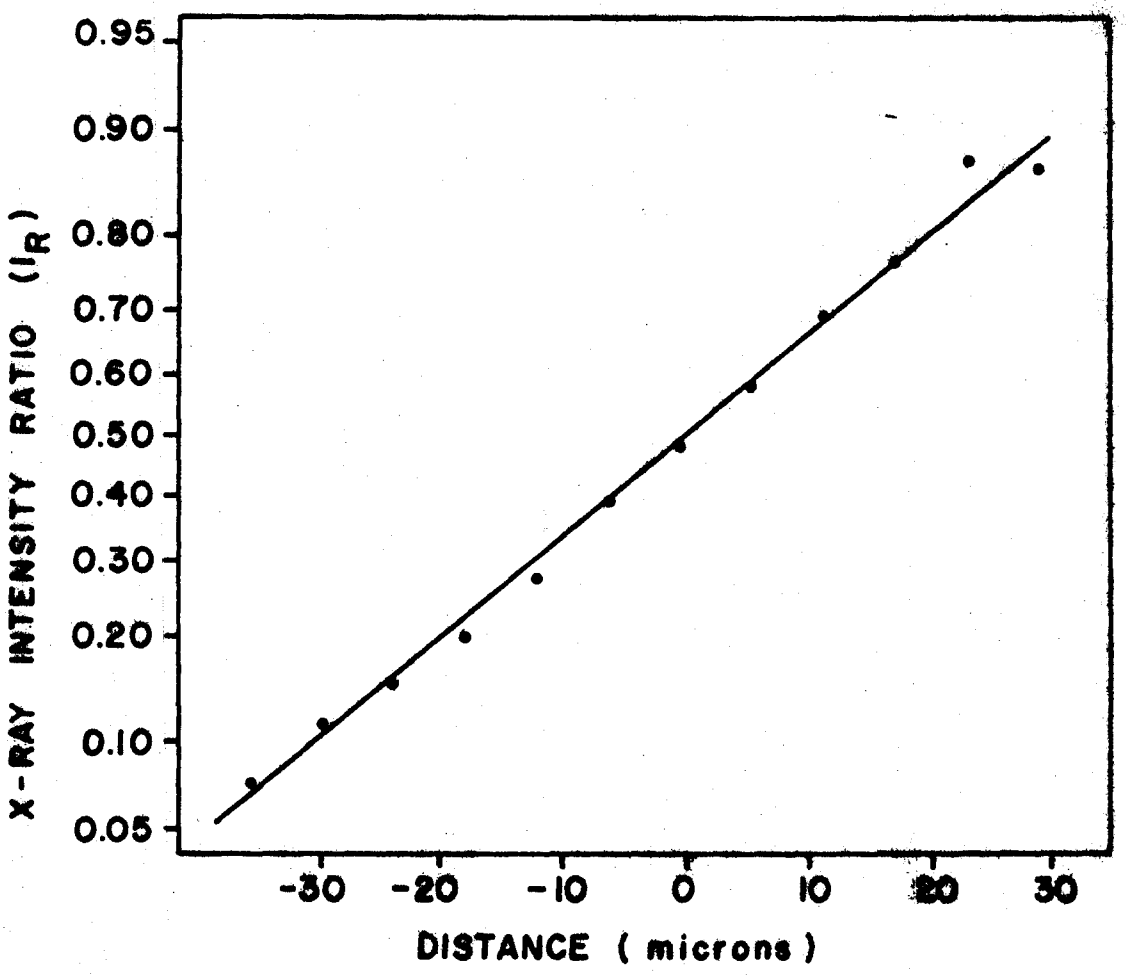

Fig. 7-11 Diffusion couple α2 -α3: X-ray intensity ratio versus distance plotted on probability paper.

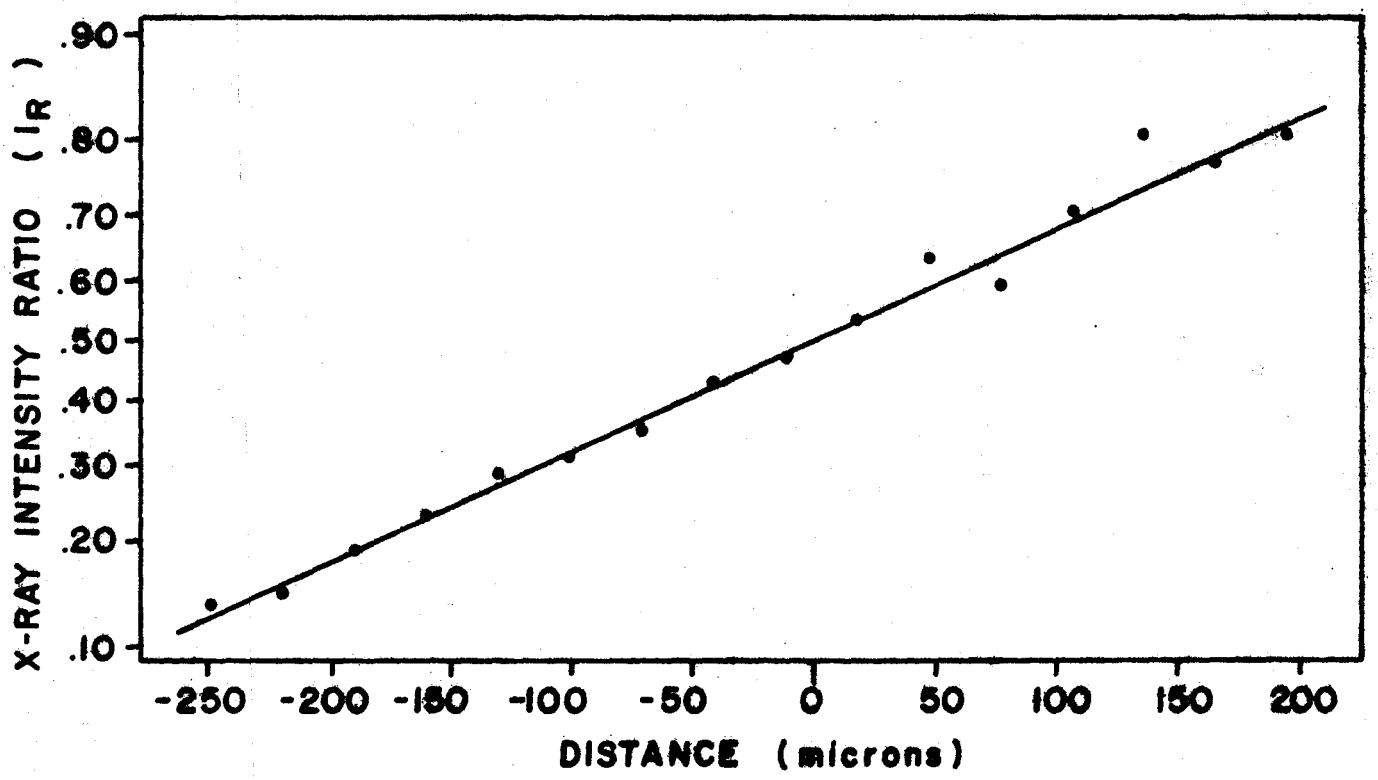

Fig. 7-12 Diffusion couple β2-β3: X-ray intensity ratio versus distance plotted on probability paper.

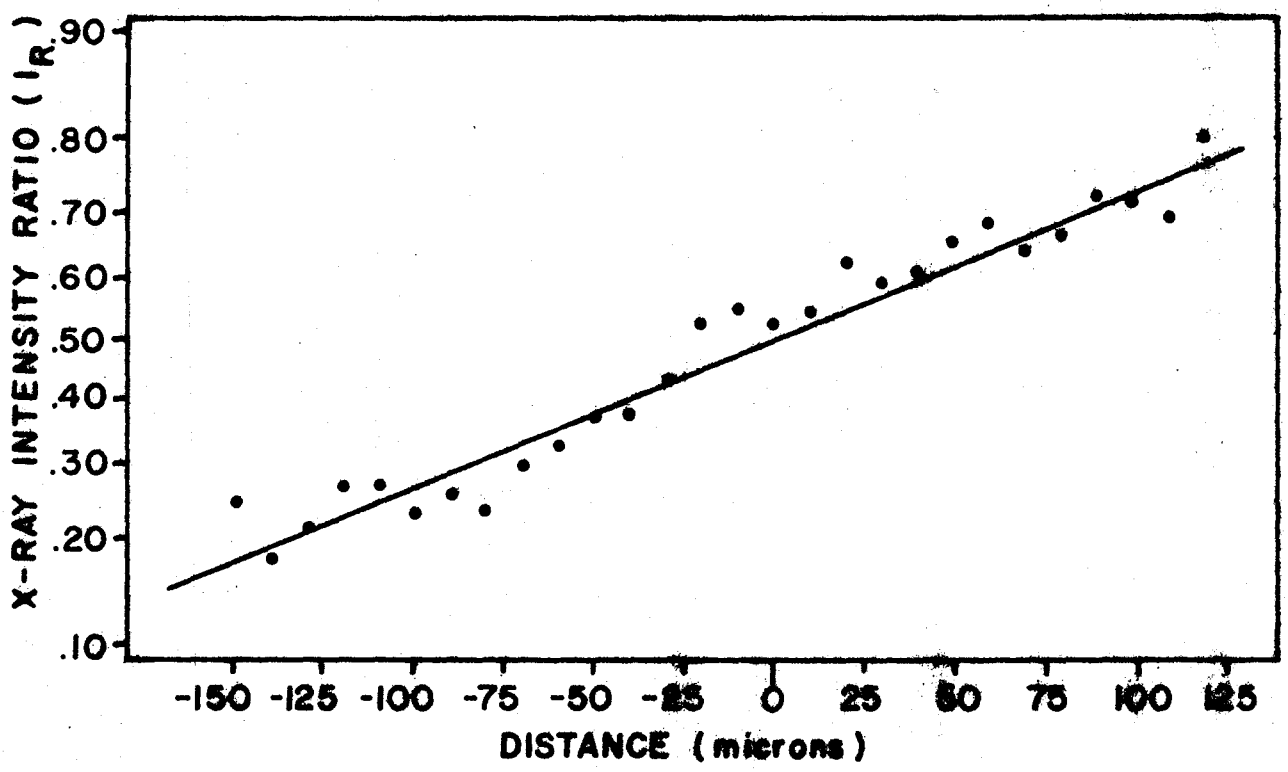

Fig. 7-13 Diffusion couple β4-β8: X-ray intensity ratio versus distance plotted on probability paper.

fusion coefficients are not sensitive functions of concentration. Linear regression analysis was used to determine the slopes of the graphs and the corresponding 95% confidence limits. The correlation coefficients for these analyses were 0.9963, 0.9931 and 0.9770 respectively. The calculated slopes were used to determine the corresponding diffusion coefficients in the following manner. Manipulation of Eq. (7-5) yields

$$\frac{z}{2\sqrt{Dt}} = \text{erf}^{-1}\ (1 - 2I_R) \qquad (7\text{-}6)$$

where erf^{-1} is taken as meaning the inverse of the error function (ie., -1 is not an exponent). The ordinate on probability paper is determined by the function on the right side of Eq. (7-6). If (I_R', z') and (I_R'', z'') are the coordinates of two points on the best straight line fit to the data, as plotted on probability paper, then from Eq. (7-6) it follows that

$$D = \frac{1}{4t}\left[\frac{z' - z''}{\text{erf}^{-1}(1-2I_R') - \text{erf}^{-1}(1-2I_R'')}\right]^2 . \qquad (7\text{-}7)$$

Calculations based on this equation lead to the diffusion coefficients listed in Table 7-3. The error limits on the diffusion coefficients correspond to the 95% confidence limits on the regression analyses.

Table 7-3

couple	D(cm^2/sec)
α2-α3	$1.35\pm.15\times10^{-10}$
β2-β3	$6.4\pm.9\times10^{-8}$
β4-β8	$3.5\pm.7\times10^{-8}$

The fact that there is no indication of diffusional interaction for the composition range of interest in the present study is a very fortunate simplification. If one were dealing with alloys which contained greater amounts of Ni, matters might have been more complicated.

As was expected, the Ni diffusivity in the open structured B.C.C. β phase was much greater than in the F.C.C. α phase (Table 7-3). The results for the β phase indicate a tendency to decreased Ni diffusivity with increased Ni content. Reference to the liquidus surface for the Cu-Zn-Ni system[64] indicates that this direction corresponds to increasing liquidus temperature. Thus the decrease in Ni diffusivity is consistent with the previously observed correlation between diffusivity and liquidus temperature for this sytem[73,74].

Nominally the diffusion coefficients obtained from the β2-β3 and β4-β8 diffusion couples correspond to (3.75 wt. % Ni, 44 wt. % Zn) and (8.75 wt. % Ni, 46 wt. % Zn), respectively. It transpires that for each of the diffusion couples used in the stability studies, the β phase directly adjacent

to the α-β interface has a composition much closer to the former nominal composition. Thus in all calculations to be undertaken, the value of D_{Ni}^{β} is taken as 6.4×10^{-8} cm^2/sec.

7.5.3 Stability Studies

The diffusion couples α1-β1 to α1-β9 (see Table 7-2 and Fig. 7-5) were used for the study of α-β interface stability. Couples α1-β1, α1-β2, α1-β3 and α1-β4 were observed to maintain stable planar interfaces. Typical micrographs, Figs. 7-14 and 7-15, show the diffusion zones of the α1-β3 and α1-β4 couples respectively, after one and four hour diffusion anneals in both cases. In general, it was observed that the lower the Ni content of the β phase, the more difficult it was to suppress the α → β (Widmanstätten) transformation during the quench terminating the diffusion anneal. Because it is such a good site for heterogeneous nucleation, the original α-β interface usually is covered with Widmanstätten α plates which formed during the quench. The particular etchant used for all the metallography (see footnote on page 121) had the very useful property of etching up the original α-β interface even in the absence of Widmanstätten α plates (eg., Figs. 7-20 and 7-21). Notice that the interface moves towards the α phase and hence α is being transformed to β. Graphs of interface migration distance versus the square root of diffusion time for couples α1-β3 and α1-β4 are shown in Fig. 7-16. Noting that such graphs

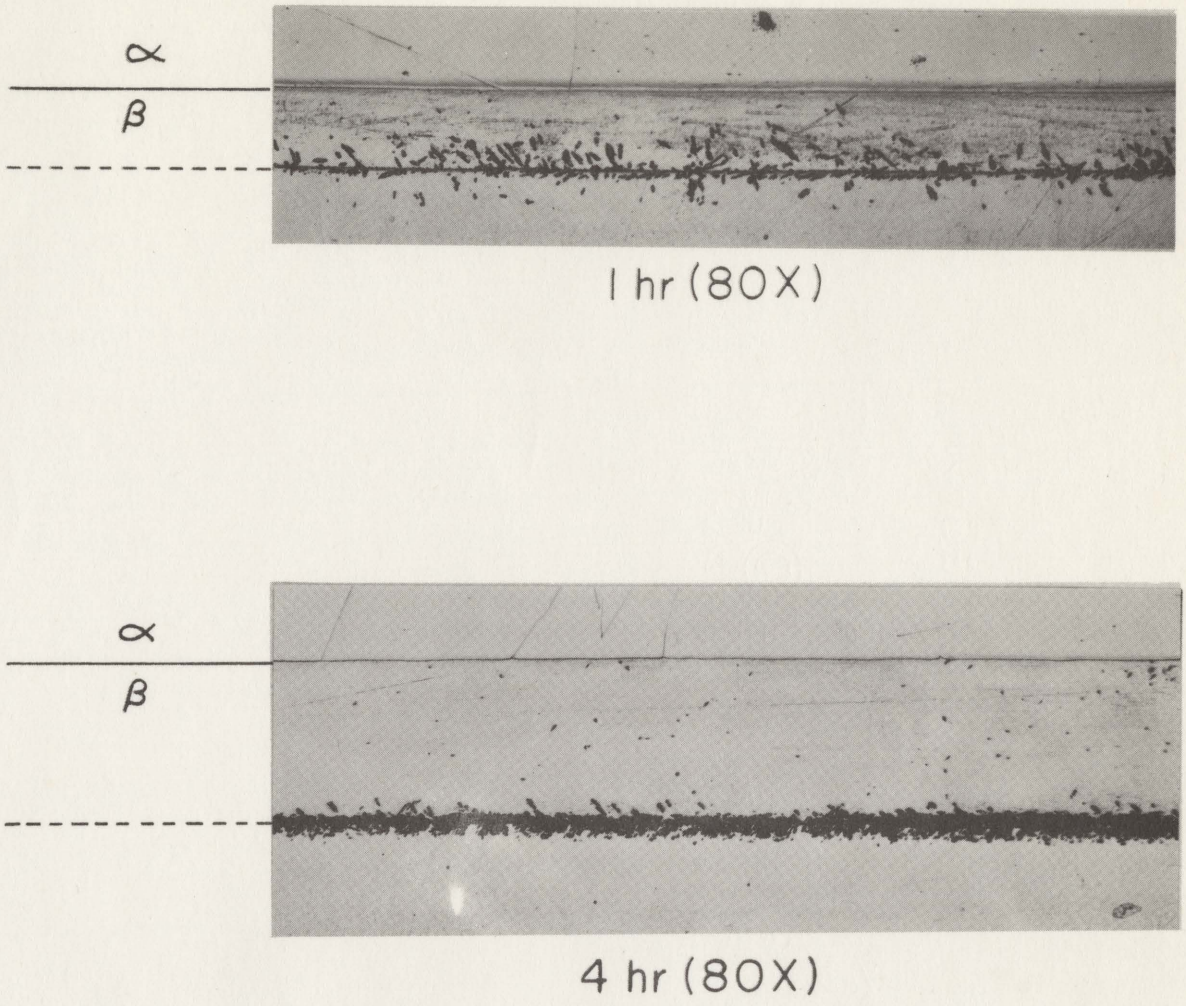

Fig. 7-14 Position of the α-β interface in diffusion couple α1-β3 after annealing 1 and 4 hrs. During the quench from the annealing temperature, Widmanstätten α has nucleated on the original interface.

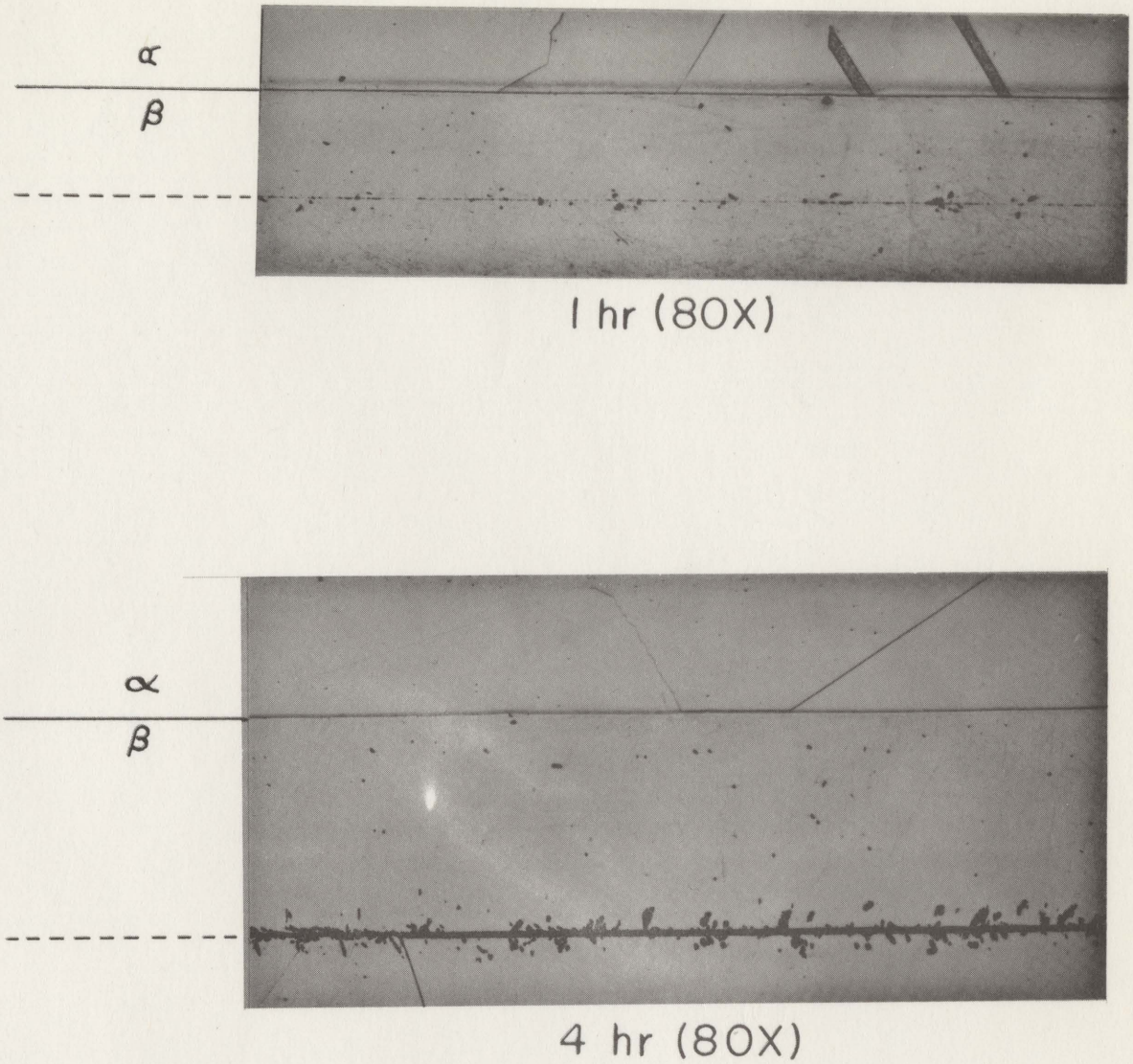

Fig. 7-15 Position of the α-β interface in diffusion couple α1-β4 after annealing 1 and 4 hrs. During the final quench, Widmanstätten α has nucleated on the original interface.

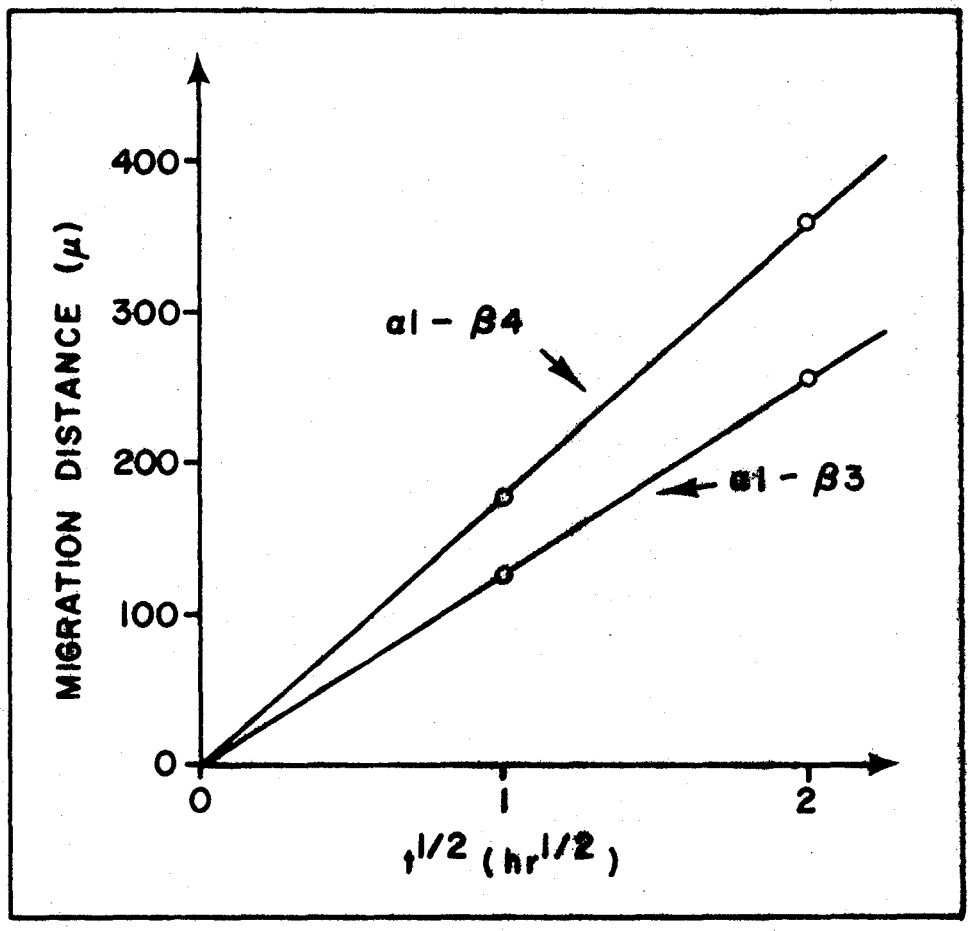

Fig. 7-16 Interface migration distance versus the square root of diffusion time for diffusion couples α1-β3 and α1-β4.

must pass through the origin, one can see that a parabolic relationship exists between migration distance and time. Accordingly there is little doubt that the migration rate of the α-β interface is controlled by transport through the bulk alloys (rather than, for example, by the transport rate of atoms across the actual interface).

The diffusion couples α1-β5, α1-β6, α1-β7, α1-β8 and α1-β9 (see Table 7-2 and Fig. 7-5) involved nonplanar α-β interfaces. Micrographs of the corresponding diffusion zones are shown, as a function of time, in Figs. 7-17, 7-18, 7-19, 7-20 and 7-21. Notice that in all cases the interface moves toward the α phase. Graphs of average interface migration distance versus the square root of diffusion time were made on the basis of Figs. 7-17 to 7-21 and the results are shown in Fig. 7-22. One can see that all the graphs are essentially linear. Although the interfaces are nonplanar and therefore the compositions vary along the interface, the average interface compositions are likely to be approximately constant with time and consequently the average interfaces migrate in the observed parabolic manner. However, the migration rates for nonplanar interfaces are undoubtedly slower than the corresponding rates for planar interfaces because the lateral diffusional flux components required to produce perturbations make the net transport less efficient in the direction perpendicular to the average interface.

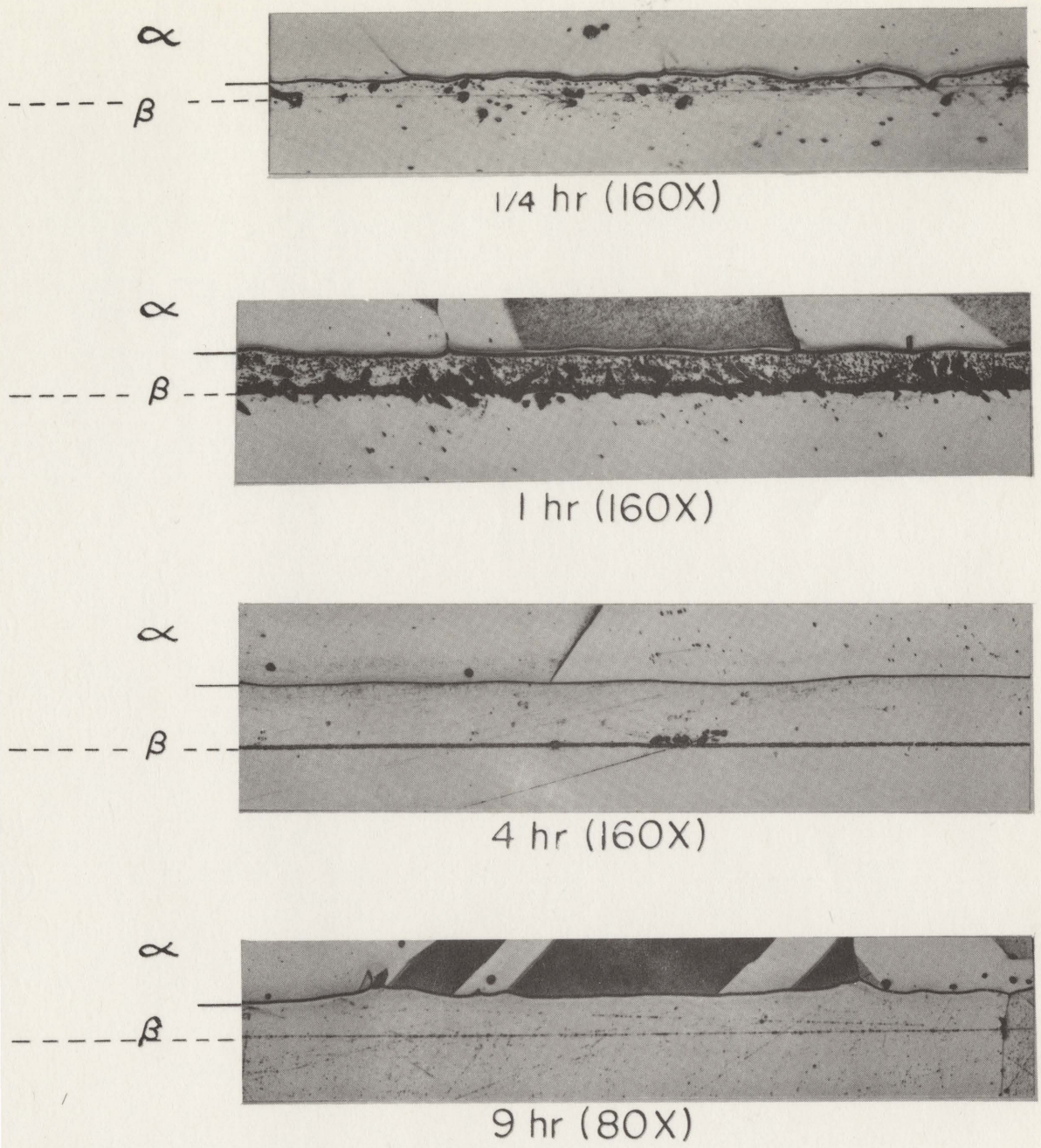

Fig. 7-17 Position of the α-β interface in diffusion couple α1-β5 after annealing 1/4, 1, 4 and 9 hrs. In some cases Widmanstätten α has nucleated on the original interface during the final quench.

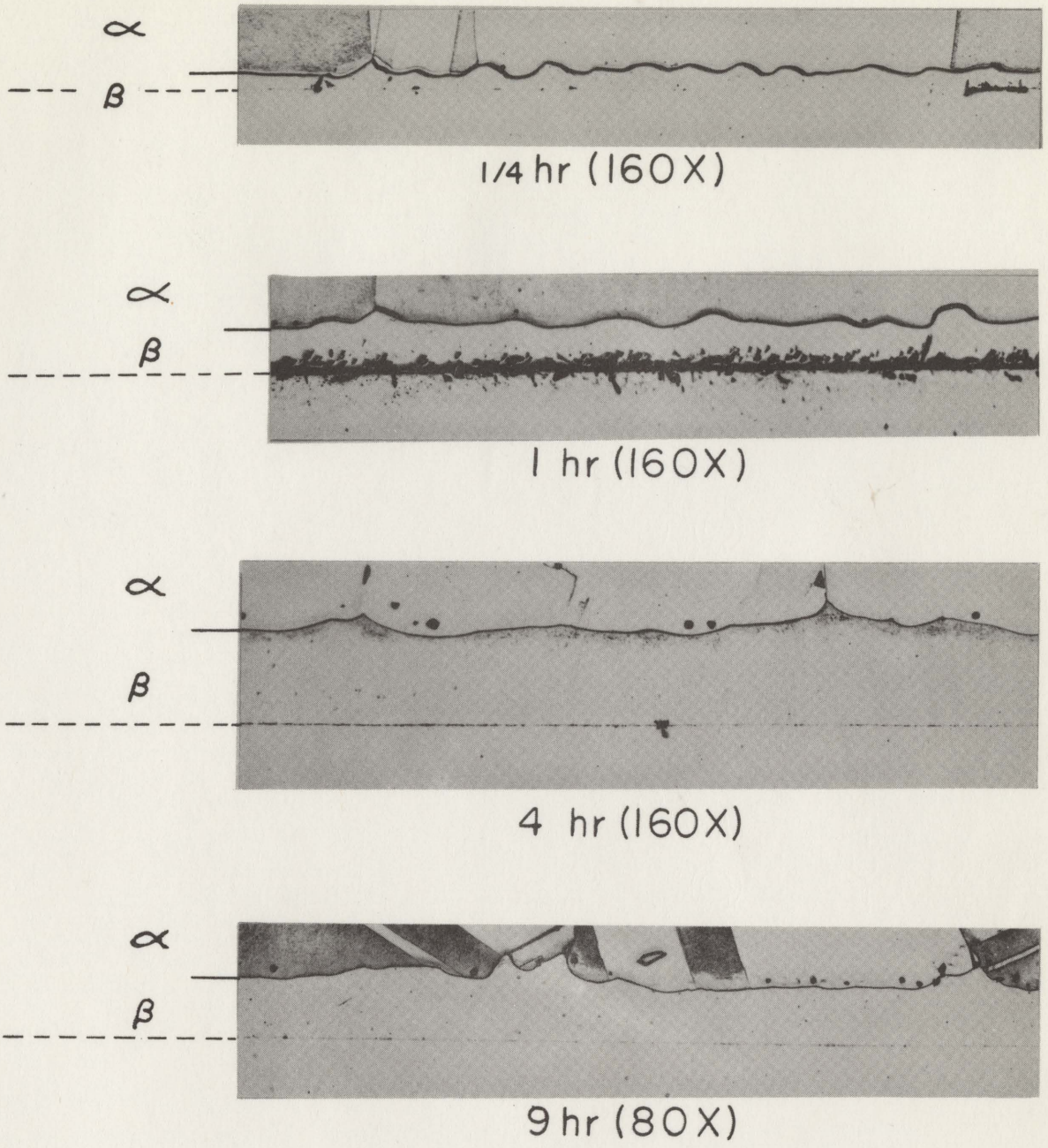

Fig. 7-18 Position of the α-β interface in diffusion couple α1-β6 after annealing 1/4, 1, 4 and 9 hrs. In some cases Widmanstätten α has nucleated on the original interface during the final quench.

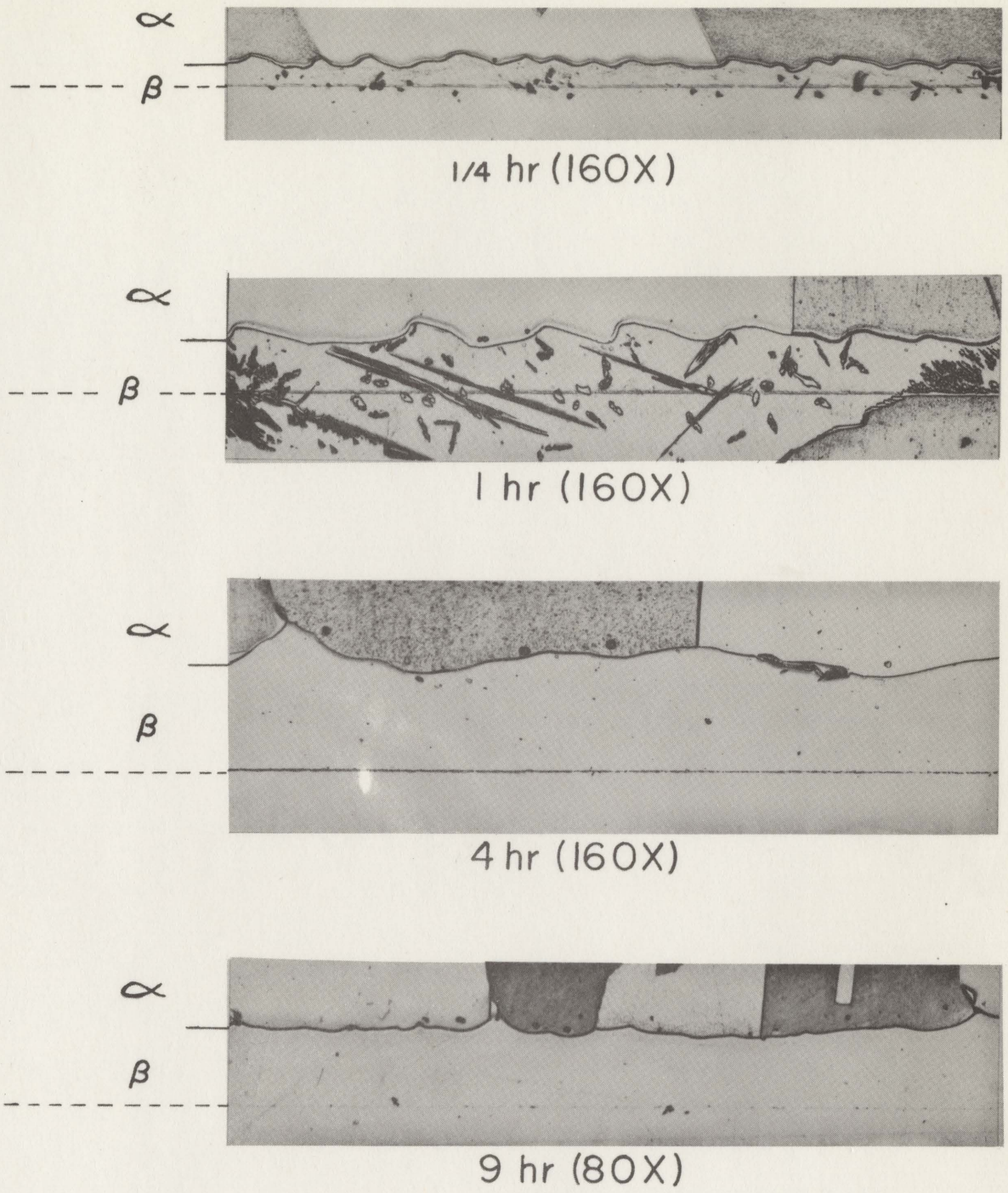

Fig. 7-19 Position of the α-β interface in diffusion couple α1-β7 after annealing 1/4, 1, 4 and 9 hrs. In some cases Widmanstätten α has nucleated on the original interface during the final quench.

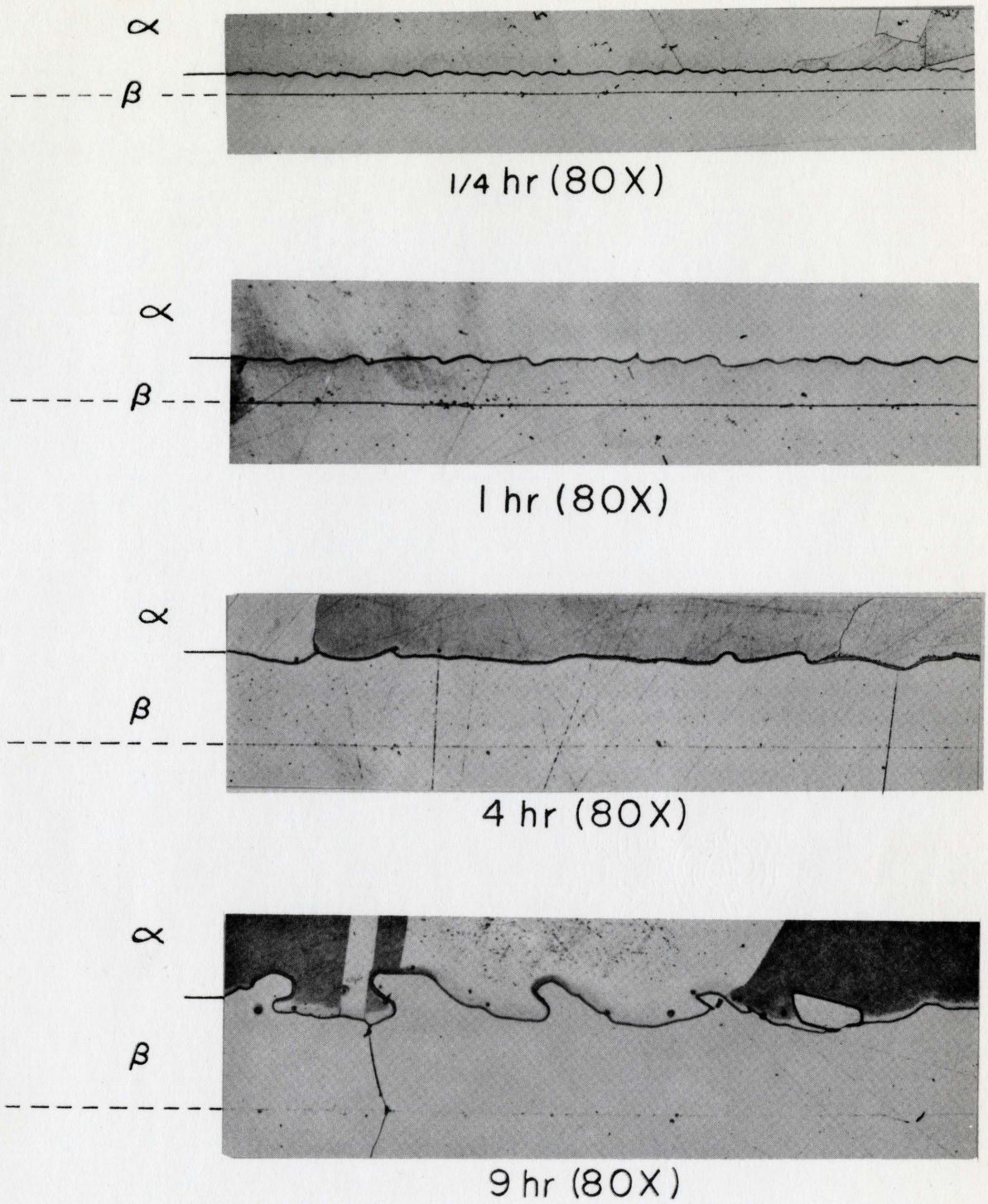

Fig. 7-20 Position of the α-β interface in diffusion couple α1-β8 after annealing 1/4, 1, 4 and 9 hrs.

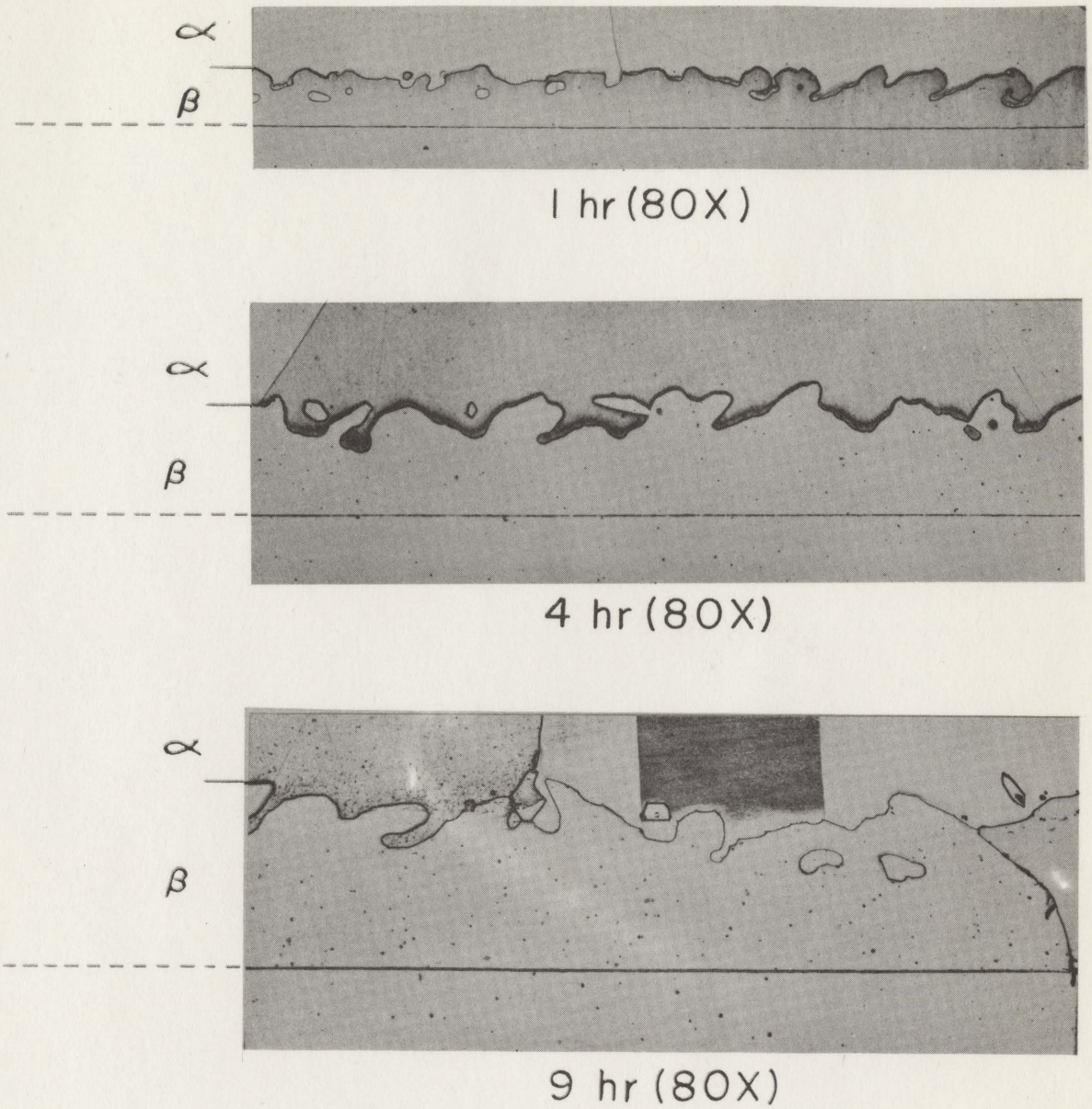

Fig. 7-21 Position of the α-β interface in diffusion couple α1-β9 after annealing 1, 4 and 9 hrs.

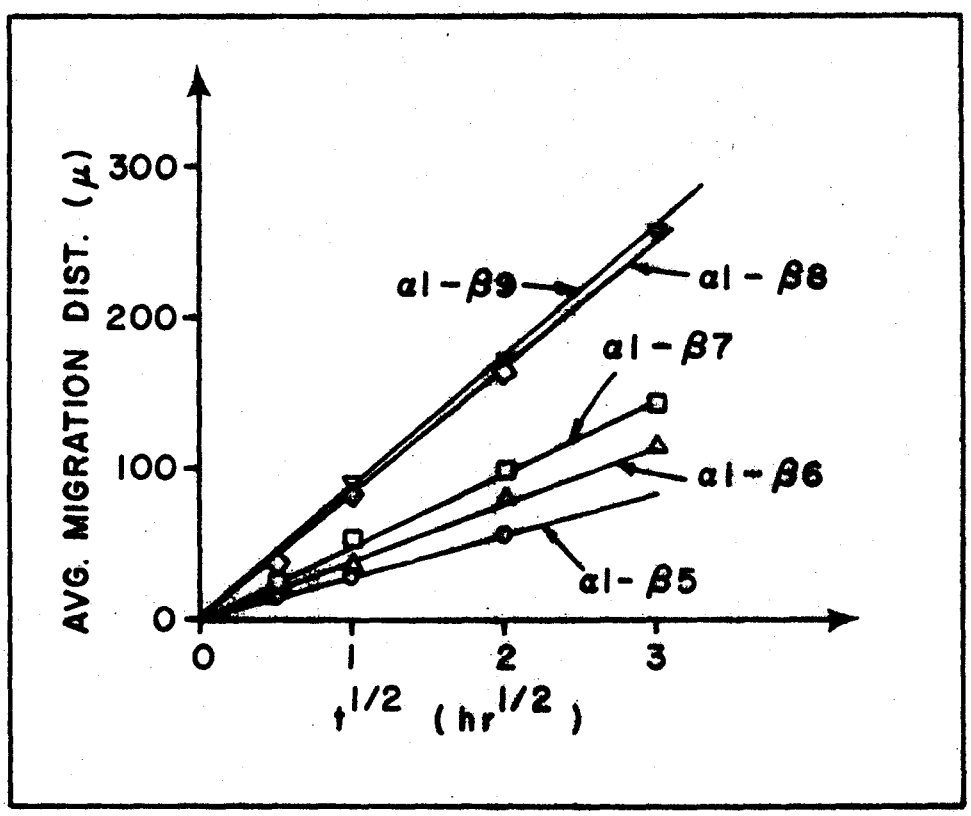

Fig. 7-22 Average interface migration distance versus the square root of diffusion time for diffusion couples α1-β5 to α1-β9.

Consider first the unstable couples α1-β5, α1-β6 and α1-β7 (Figs. 7-17, 7-18 and 7-19). In each case the evolution of interface morphology involves essentially the same sequence. At 1/4 hour the α-β interface has a roughly sinusoidal periodicity. With a wave length increase, this morphology is sustained up to 1 hour. After 4 hours, the interface loses the approximately sinusoidal periodicity and becomes very irregular in shape. For the α1-β6 and α1-β7 couples, it was possible to calculate an average wavelength of periodicity at 1/4 and 1 hours. Graphs of this average wavelength versus the square root of diffusion time are shown in Fig. 7-23 and are found to be approximately linear. It is significant that the average wavelength is of the same magnitude as the average migration distance of the interface.

Turning now to the diffusion couples involving higher Ni content in the β phase, consider the results for the α1-β8 couples, Fig. 7-20. At earlier times, 1/4 and 1 hour, the α-β interface has an approximately sinusoidal periodicity which increases in wave length and amplitude with time. At the later time of 9 hours the morphological breakdown is quite severe. A graph of average wavelength versus the square root of diffusion time is shown in Fig. 7-23. The couples α1-β9, Fig. 7-21, have the most Ni in the bulk β phase. It is quite clear that the morphological breakdown is much more severe in this case than in the other four

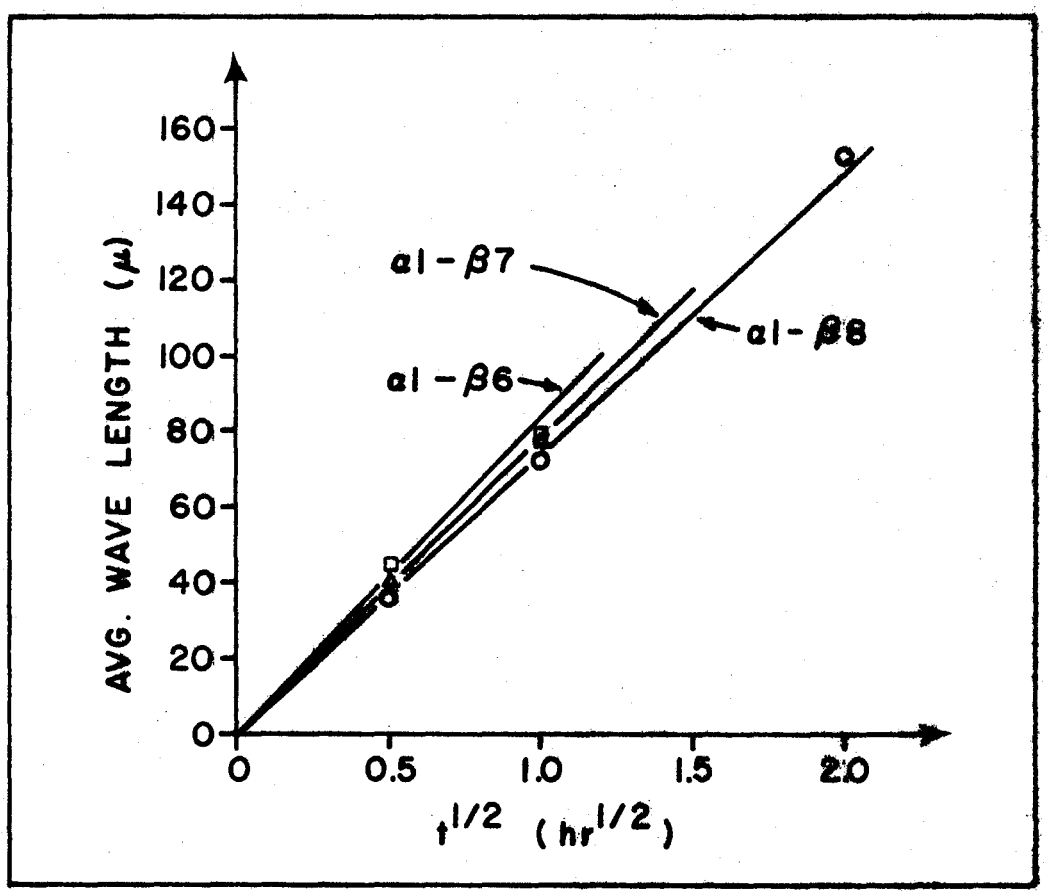

Fig. 7-23 Average wavelength of perturbation versus the square root of diffusion time for diffusion couples α1-β6, α1-β7 and α1-β8.

unstable couples[†]. After only 1 hour the interface is very rugged in appearance with what appears to be two-phase zone formation. Although there is no regular periodicity, the scale of the structure increases with time.

On the basis of the results for the diffusion couples $\alpha 1$-$\beta 1$ to $\alpha 1$-$\beta 9$, it is possible to make a few summary observations regarding the stability of the α-β interface, keeping in mind that the terminal composition in the α phase is never varied. It is observed that for a given Zn terminal concentration in the β phase, there is a tendency for the interface to become unstable as the Ni terminal concentration is increased. On the other hand, it is observed that for a given Ni terminal concentration in the β phase, there is a tendency for the interface to become stable as the Zn terminal concentration is increased.

7.6 SUMMARY REMARKS

At this juncture it is convenient to take stock of the information on the Cu-Zn-Ni system which will be required for the stability calculations to be made in the next chapter. The calculation sequence is as follows. One first specifies a set of terminal compositions ($C_{Ni\alpha}$,$C_{Zn\alpha}$) and ($C_{Ni\beta}$, $C_{Zn\beta}$) for a two-phase diffusion couple. Given

---

[†]It should be kept in mind that the micrographs are not all at the same magnification.

the appropriate diffusion coefficients and ternary phase diagram, this set determines the corresponding diffusion path. The parameters required to utilize the stability criterion (6-44) are established by this diffusion path calculation (see Appendix II). Thus what is essential is to have values for the four diffusion coefficients and to be able to describe the phase diagram analytically.

From Fig. 7-5, one can see that over the composition ranges of interest in the present study, the $\alpha/\alpha+\beta$ and $\alpha+\beta/\beta$ phase boundary lines can be approximated by straight and parallel lines (cf., Eqs. (6-13) and (6-14)). The best straight line fits to the phase boundary lines yield

$$C_{Ni}^{\alpha\beta} = 2.3 \quad C_{Zn}^{\alpha\beta} - 79.35 \qquad (7-8)$$

$$C_{Ni}^{\beta\alpha} = 2.3 \quad C_{Zn}^{\beta\alpha} - 90.85 \qquad (7-9)$$

, ie., $m^{\alpha} = m^{\beta} = 2.3$, $b^{\alpha} = -79.35$ and $b^{\beta} = -90.85$[†]. In addition to these relations, an equation which is analogous to Eq. (6-15) is required, ie., of the form $C_{Zn}^{\beta\alpha}=m^{\beta\alpha}C_{Zn}^{\alpha\beta}+b^{\beta\alpha}$. The slope of the tie-line m is determined from Fig. 7-9 and it determines the values of $m^{\beta\alpha}$ and $b^{\beta\alpha}$. In view of Eq. (6-16)

[†]For numerical calculations, it is convenient to use wt.% as the unit for concentration. On the basis of the Cu-Zn binary phase diagram[(79)], the values of $C_{Zn}^{\alpha\beta}$ and $C_{Zn}^{\beta\alpha}$ corresponding to $C_{Ni}^{\alpha\beta}=C_{Ni}^{\beta\alpha}=0$ are approximately 34.5 and 39.5 wt.% respectively. These values were used in order to determine the values of the intercepts b^{α} and b^{β}.

and the fact $m^{\alpha} = m^{\beta}$, it follows that $m^{\beta\alpha} = 1$. However, the value of $b^{\beta\alpha}$ is not a constant and must be determined graphically from Eqs. (7-8) and (7-9) and Fig. 7-9. In calculating diffusion paths, the following iterative procedure is employed (see Appendix II). A value for $C_{Zn}^{\alpha\beta}$ is guessed and then, via Eqs. (7-8) and (7-9) and Fig. 7-9, a value of $b^{\beta\alpha}$ is determined graphically. The ternary phase diagram now has an analytic description. Next the diffusion path calculation is made as outlined in Appendix II and this yields a second estimate of $C_{Zn}^{\alpha\beta}$, hence a better estimate of $b^{\beta\alpha}$. This iterative cycle is continued until the value of $C_{Zn}^{\alpha\beta}$ does not change. It transpires that the calculations are not very sensitive to the value of $b^{\beta\alpha}$ and only one or two iterations are required.

The next set of parameters which are required are the four diffusion coefficients. In Sec. 7.5.2 the values of D_{Ni}^{α} and D_{Ni}^{β} were determined. It was indicated that 6.4×10^{-8} cm^2/sec would be used as the value of D_{Ni}^{β}. It remains to specify values of D_{Zn}^{α} and D_{Zn}^{β}. The value of the interdiffusion coefficient for the Cu-Zn system at 34 wt.% Zn should be adequate for D_{Zn}^{α}. Thus from the data of Horne and Mehl[69] and Resnick and Balluffi[70] one obtains $D_{Zn}^{\alpha} \cong 4\times10^{-8}$ cm^2/sec at 775°C. Because Zn in beta brass moves extremely rapidly, calculations of α-β interface mobility and stability are sensitive to the value of D_{Zn}^{β}.

The data of Landergren et al[68] indicate that the interdiffusion coefficient in beta Cu-Zn is sensitive to composition. The presence of, on the average, about 5 wt. % Ni in the β phase makes it questionable as to whether or not the value of D^{β}_{Zn} can be reliably determined from binary Cu-Zn data.

To circumvent the difficulties just mentioned, it was decided to fit a value of D^{β}_{Zn} to the data for the interface migration rate of the α1-β4 diffusion couple (Figs. 7-15 and 7-16). The observed rate constant is 3.0×10^{-4} $cm/sec^{\frac{1}{2}}$[†]. Using a spectrum of values for D^{β}_{Zn}, diffusion path calculations were made for the α1-β4 couple and the value $D^{\beta}_{Zn} = 2.55\times10^{-7}$ cm^2/sec gave the observed rate constant. As a check on consistency, a diffusion path calculation for the couple α1-β3 was made using this value of D^{β}_{Zn}. The calculation gave $b = 2.0\times10^{-4}$ $cm/sec^{\frac{1}{2}}$ which is in good agreement with the observed value (Fig. 7-16) of 2.1×10^{-4} $cm/sec^{\frac{1}{2}}$.

Table 7-4 is a summary of the information at hand. It is to be emphasized that the values given for some of the parameters are very approximate.

[†]Recall that the rate constant is simply the position of the interface in λ-space, ie., $b = \xi/t^{\frac{1}{2}}$. This symbol for rate constant is not to be confused with the intercepts b^{α}, b^{β} and $b^{\beta\alpha}$.

Table 7-4

$m^{\alpha} = 2.3$	$b^{\alpha} = -79.35$ wt.%
$m^{\beta} = 2.3$	$b^{\beta} = -90.85$ wt.%
$m<0$ (Fig. 7-9)	
$m^{\beta\alpha} = 1$	$b^{\beta\alpha}$ from Eqs.(7-8) and (7-9) and Fig. 7-9
$D^{\alpha}_{Ni} = 1.35\times10^{-10}$ cm^2/sec	$D^{\alpha}_{Zn} = 4\times10^{-8}$ cm^2/sec
$D^{\beta}_{Ni} = 6.4\times10^{-8}$ cm^2/sec	$D^{\beta}_{Zn} = 2.55\times10^{-7}$ cm^2/sec .

CHAPTER 8

DISCUSSION

8.1 INTRODUCTION

Because the stability criterion (6-44) appears to be an unwieldy conglomerate, one is at first apprehensive about attempting a union of theory and experiment. However, as will be demonstrated shortly, the stability criterion reveals its intricacies in a very satisfying and transparent manner when applied to the Cu-Zn-Ni system.

8.2 APPLICATION OF THE STABILITY CRITERION TO THE Cu-Zn-Ni SYSTEM - MATHEMATICAL MANIPULATION

Although reasonably straightforward, the analysis contained in this section is tedious. To minimize confusion, the nomenclature of chapter 6 is specialized to that corresponding to the Cu-Zn-Ni system. Accordingly, component 1 → Ni, component 2 → Zn, phase I → α, phase II → β and the stability criterion (6-44) becomes[†]

$$V\left\{\left|\frac{(m^{\beta}D^{\beta}_{Ni}-mD^{\beta}_{Zn})}{(m^{\beta}-m)}+\frac{D^{\beta}_{Ni}D^{\beta}_{Zn}\psi^{\beta}/(m^{\beta}-m)+D^{\alpha}_{Ni}D^{\alpha}_{Zn}\psi^{\alpha}/(m^{\alpha}-m)}{V(C^{\beta\alpha}_{Zn}-C^{\alpha\beta}_{Zn})}\right|-\left|\frac{(mD^{\alpha}_{Zn}-m^{\alpha}D^{\alpha}_{Ni})}{(m^{\alpha}-m)}+\frac{D^{\beta}_{Ni}D^{\beta}_{Zn}\psi^{\beta}/(m^{\beta}-m)+D^{\alpha}_{Ni}D^{\alpha}_{Zn}\psi^{\alpha}/(m^{\alpha}-m)}{V(C^{\beta\alpha}_{Zn}-C^{\alpha\beta}_{Zn})}\right|\right\} > 0 \quad \text{(unstable)} \qquad (8\text{-}1)$$

[†]Recalling that by convention the positive direction is II → I, the positive direction is now $\beta \rightarrow \alpha$.

It has already been noted that $m^{\alpha} \cong m^{\beta}$ (Table 7-4) and accordingly the terms $(m^{\alpha}-m)$ and $(m^{\beta}-m)$, both of which are positive, can be factored out of (8-1). From Figs. 7-14, 7-15 and 7-17 to 7-21, it is noted that the β phase grows at the expense of α. Hence $V > 0$ and the stability criterion (8-1) reduces to

$$\left| (m^{\beta} D^{\beta}_{Ni} - m\, D^{\beta}_{Zn}) + \frac{D^{\alpha}_{Ni}\, D^{\alpha}_{Zn}\, \psi^{\alpha} + D^{\beta}_{Ni}\, D^{\beta}_{Zn}\, \psi^{\beta}}{V(C^{\beta\alpha}_{Zn} - C^{\alpha\beta}_{Zn})} \right| - \left| (m\, D^{\alpha}_{Zn} - m^{\alpha} D^{\alpha}_{Ni}) + \frac{D^{\alpha}_{Ni}\, D^{\alpha}_{Zn}\, \psi^{\alpha} + D^{\beta}_{Ni}\, D^{\beta}_{Zn}\, \psi^{\beta}}{V(C^{\beta\alpha}_{Zn} - C^{\alpha\beta}_{Zn})} \right| > 0 \quad \text{(unstable)} \qquad (8\text{-}2)$$

The identical second and fourth terms reflect constitutional effects, weighted according to the diffusivities in the corresponding phases. On the other hand, the first and third terms represent 'kinetic' effects corresponding to the phases β and α respectively.

The stability criterion (8-2) becomes

$$|\phi^{\beta} + \theta^{\alpha} + \theta^{\beta}| - |\phi^{\alpha} + \theta^{\alpha} + \theta^{\beta}| > 0 \quad \text{(unstable)} \qquad (8\text{-}3)$$

when the following parameters are introduced

$$\phi^{\alpha} = m\, D^{\alpha}_{Zn} - m^{\alpha}\, D^{\alpha}_{Ni} \qquad (8\text{-}4)$$

$$\phi^{\beta} = m^{\beta}\, D^{\beta}_{Ni} - m\, D^{\beta}_{Zn} \qquad (8\text{-}5)$$

$$\theta^{\alpha} = D^{\alpha}_{Ni}\, D^{\alpha}_{Zn}\, \psi^{\alpha}/V(C^{\beta\alpha}_{Zn} - C^{\alpha\beta}_{Zn}) \qquad (8\text{-}6)$$

$$\theta^{\beta} = D^{\beta}_{Ni}\, D^{\beta}_{Zn}\, \psi^{\beta}/V(C^{\beta\alpha}_{Zn} - C^{\alpha\beta}_{Zn}) \; . \qquad (8\text{-}7)$$

To be able to deal with (8-3) effectively, one must first establish the possible signs and magnitudes of the four para-

meters contained therein.

Consider ϕ^{α} and ϕ^{β} in Eqs. (8-4) and (8-5). The physical significance of these terms will become apparent as the analysis progresses. Because $m^{\alpha} \cong m^{\beta} > 0$ and $m < 0$, one has that $\phi^{\alpha} < 0$ and $\phi^{\beta} > 0$. Using Table 7-4 the values of m^{α}, m^{β}, D^{α}_{Zn}, D^{β}_{Zn}, D^{α}_{Ni}, D^{β}_{Ni} and a typical value of $m(-.05)$ are substituted into Eqs. (8-4) and (8-5) to give $\phi^{\alpha} \cong -2.3\times10^{-9}$ and $\phi^{\beta} \cong 1.6\times10^{-7}$. Clearly then, when dealing with (8-3), one can impose the following conditions on ϕ^{α} and ϕ^{β}:

$$\left.\begin{aligned} \phi^{\alpha} &< 0 \\ \phi^{\beta} &> 0 \\ |\phi^{\beta}| &>> |\phi^{\alpha}| \end{aligned}\right\} \qquad (8\text{-}8)$$

Noting that $V > 0$ and $(C^{\beta\alpha}_{Zn} - C^{\alpha\beta}_{Zn}) > 0$ (see Fig. 7-2), it follows that the factor $V(C^{\beta\alpha}_{Zn} - C^{\alpha\beta}_{Zn})$ is positive in Eqs. (8-6) and (8-7). Therefore the signs of θ^{α} and $\theta\beta$ depend on the signs of ψ^{α} and ψ^{β} respectively, which in turn depend on whether or not supersaturation develops in the corresponding phase. From Eqs. (6-10) and (6-11), $a^{\alpha} = a^{\beta} = 1$ and hence from (6-9) it follows that $\psi^{\alpha} > 0$ and $\psi^{\beta} > 0$ if supersaturation develops in the α and β phases, respectively. Accordingly, $\theta^{\alpha} > 0$ and $\theta^{\beta} > 0$ if supersaturation develops in the corresponding phase. In view of the preceding discussion, one recognizes the following possi-

bilities for θ^{α} and θ^{β} [†]:

$$\left.\begin{aligned} \theta^{\alpha} &\gtrless 0 \\ \theta^{\beta} &\gtrless 0 \\ |\theta^{\alpha}| - |\theta^{\beta}| &\gtrless 0 \end{aligned}\right\} \qquad (8\text{-}9)$$

Having established some appreciation for the parameters involved in (8-3), it now is possible to study the latter in greater detail. On the basis of the stability criterion alone, there are four possibilities which must be considered to ultimately be able to remove the absolute value signs:

$$\phi^{\beta} + \theta^{\alpha} + \theta^{\beta} > 0 \text{ and } \phi^{\alpha} + \theta^{\alpha} + \theta^{\beta} > 0 \qquad (8\text{-}10)$$

$$\phi^{\beta} + \theta^{\alpha} + \theta^{\beta} > 0 \text{ and } \phi^{\alpha} + \theta^{\alpha} + \theta^{\beta} < 0 \qquad (8\text{-}11)$$

$$\phi^{\beta} + \theta^{\alpha} + \theta^{\beta} < 0 \text{ and } \phi^{\alpha} + \theta^{\alpha} + \theta^{\beta} > 0 \qquad (8\text{-}12)$$

$$\phi^{\beta} + \theta^{\alpha} + \theta^{\beta} < 0 \text{ and } \phi^{\alpha} + \theta^{\alpha} + \theta^{\beta} < 0 \qquad (8\text{-}13)$$

As a result of conditions (8-8), the third case, (8-12), is an impossibility. Since $\phi^{\beta} > 0$, to have $\phi^{\beta} + \theta^{\alpha} + \theta^{\beta} < 0$ one must have $\theta^{\alpha} + \theta^{\beta} < 0$. The latter is in contradiction to the fact that since $\phi^{\alpha} < 0$, to have $\phi^{\alpha} + \theta^{\alpha} + \theta^{\beta} > 0$ one must have $\theta^{\alpha} + \theta^{\beta} > 0$. The other three possibilities are consis-

---

[†]The symbol $\gtrless$ should be interpreted as meaning greater than, less than or equal to.

tent with conditions (8-8) and are now considered in some detail.

Case 1 - (8-10)

First of all notice that in view of conditions (8-8), $\phi^{\alpha} + \theta^{\alpha} + \theta^{\beta} > 0$ is a sufficient, but not necessary, condition for $\phi^{\beta} + \theta^{\alpha} + \theta^{\beta} > 0$ and therefore case I is in fact characterized simply by

$$\phi^{\alpha} + \theta^{\alpha} + \theta^{\beta} > 0 \ . \qquad (8\text{-}14)$$

Combining (8-14) (or equivalently (8-10)) with the stability criterion (8-3), one obtains

$$\phi^{\beta} + \theta^{\alpha} + \theta^{\beta} - (\phi^{\alpha} + \theta^{\alpha} + \theta^{\beta}) > 0 \quad \text{(unstable)}$$

and hence

$$\phi^{\beta} - \phi^{\alpha} > 0 \quad \text{(unstable)} \qquad (8\text{-}15)$$

which is necessarily true because $\phi^{\beta} > 0$ and $\phi^{\alpha} < 0$. Accordingly case I refers to situations in which the system is in a state of what shall be referred to as <u>absolute instability</u>.

Case 2 - (8-11)

Combination of conditions (8-11) with (8-3) yields the stability criterion

$$\phi^{\alpha} + \phi^{\beta} + 2(\theta^{\alpha} + \theta^{\beta}) > 0 \quad \text{(unstable)}. \qquad (8\text{-}16)$$

In view of (8-8), $\phi^{\alpha} + \phi^{\beta} > 0$ and therefore the above criterion can be written in the alternative form

$$\frac{2(\theta^{\alpha} + \theta^{\beta})}{\phi^{\alpha} + \phi^{\beta}} > -1 \quad \text{(unstable)}. \tag{8-17}$$

Depending on the values of the four parameters, one can have either stability or instability in case 2.

Case 3 - (8-13)

From conditions (8-8), it follows that $\phi^{\beta} + \theta^{\alpha} + \theta^{\beta} < 0$ is a sufficient condition for $\phi^{\alpha} + \theta^{\alpha} + \theta^{\beta} < 0$ and hence case 3 is characterized by

$$\phi^{\beta} + \theta^{\alpha} + \theta^{\beta} < 0. \tag{8-18}$$

Application of (8-18) (or equivalently (8-13))to the stability criterion (8-3) yields

$$\phi^{\alpha} - \phi^{\beta} > 0 \quad \text{(unstable)} \tag{8-19}$$

which is in contradiction to (8-8) and therefore can never be true. Case 3 refers to situations in which the system is in a state of what henceforth shall be referred to as <u>absolute stability</u>. The physical significance of the regimes of absolute stability and instability will be dealt with shortly.

One should be cognizant of the fact that the domains of absolute instability and absolute stability represented by cases 1 and 3,respectively, are in fact covered by case 2. That is to say, if (8-14) is applied to (8-16), absolute instability results. On the other hand, if (8-18) is combined with (8-16), one obtains absolute stability. Accordingly the

stability criterion (8-16) is capable of dealing with all possibilities, subject of course to conditions (8-8). Marginal states (ie., states of incipient instability) are defined by

$$\phi^{\alpha} + \phi^{\beta} + 2(\theta^{\alpha} + \theta^{\beta}) = 0 \ . \qquad (8\text{-}20)$$

Similarly, states of incipient absolute instability and absolute stability are defined respectively by

$$\phi^{\alpha} + \theta^{\alpha} + \theta^{\beta} = 0 \qquad (8\text{-}21)$$

and

$$\phi^{\beta} + \theta^{\alpha} + \theta^{\beta} = 0 \qquad (8\text{-}22)$$

8.3 APPLICATION OF THE STABILITY CRITERION TO THE Cu-Zn-Ni SYSTEM - PHYSICAL INTERPRETATION

At this point it is convenient to investigate the physical significance of the parameters ϕ^{α}, ϕ^{β}, θ^{α} and θ^{β} and their relationship to the three cases just discussed.

In all the important expressions, eg., (8-14), (8-16) and (8-18), the constitutional terms occur as the sum $\theta^{\alpha} + \theta^{\beta}$. Recall that θ^{α} and θ^{β} are positive if supersaturation develops in the respective phases. In view of (8-16), the more positive is the sum $\theta^{\alpha} + \theta^{\beta}$, the greater is the tendency toward instability, a result which is qualitatively consistent with the elementary constitutional approach discussed in Sec. 6.2. Notice also that if $(\theta^{\alpha} + \theta^{\beta}) < 0$, the sum represents a stabilizing influence. The terms ψ^{α} and ψ^{β} in Eqs. (8-6) and (8-7) (cf., Eqs. (6-6) and (6-7)) represent thermodynamic

driving forces for morphological breakdown. The effectiveness of the driving force in the phases is determined by diffusional weighting factors D^{α}_{Ni} D^{α}_{Zn} and D^{β}_{Ni} D^{β}_{Zn}, respectively†.

It was mentioned earlier that the parameters ϕ^{α} and ϕ^{β} reflect kinetic influences. To appreciate their physical significance one must examine what actually transpires during interdiffusion of two-phase infinite diffusion couples of the type used in Sec. 7.5.3. Consider first the distribution of Zn as shown schematically in Fig. 8-1. Because $D^{\beta}_{Zn} >> D^{\alpha}_{Zn}$ (Table 7-4) there is a strong tendency for the α-β interface to move to the right and this is in fact what is experimentally observed. This tendency is perhaps better understood if one examines the Zn interfacial mass balance (cf., Eqs. (6-19) and (6-20)):

$$V(C^{\beta\alpha}_{Zn} - C^{\alpha\beta}_{Zn}) = D^{\alpha}_{Zn}\, G^{\alpha\beta}_{Zn} - D^{\beta}_{Zn}\, G^{\beta\alpha}_{Zn} \qquad (8\text{-}23)$$

Since $(C^{\beta\alpha}_{Zn} - C^{\alpha\beta}_{Zn}) > 0$, $D^{\alpha}_{Zn}\, G^{\alpha\beta}_{Zn} < 0$ and $D^{\beta}_{Zn}\, G^{\beta\alpha}_{Zn} < 0$, it follows that for $V > 0$, $|D^{\beta}_{Zn}\, G^{\beta\alpha}_{Zn}|$ must exceed $|D^{\alpha}_{Zn}\, G^{\alpha\beta}_{Zn}|$. Accordingly, the more rapidly Zn is delivered to the interface from the β phase and the less rapidly it is removed into the α phase, the faster the interface moves toward the α phase.

Whereas the situation with respect to the distribution

---

†In the most general case (8-1), there exists constitutional as well as diffusional weighting factors.

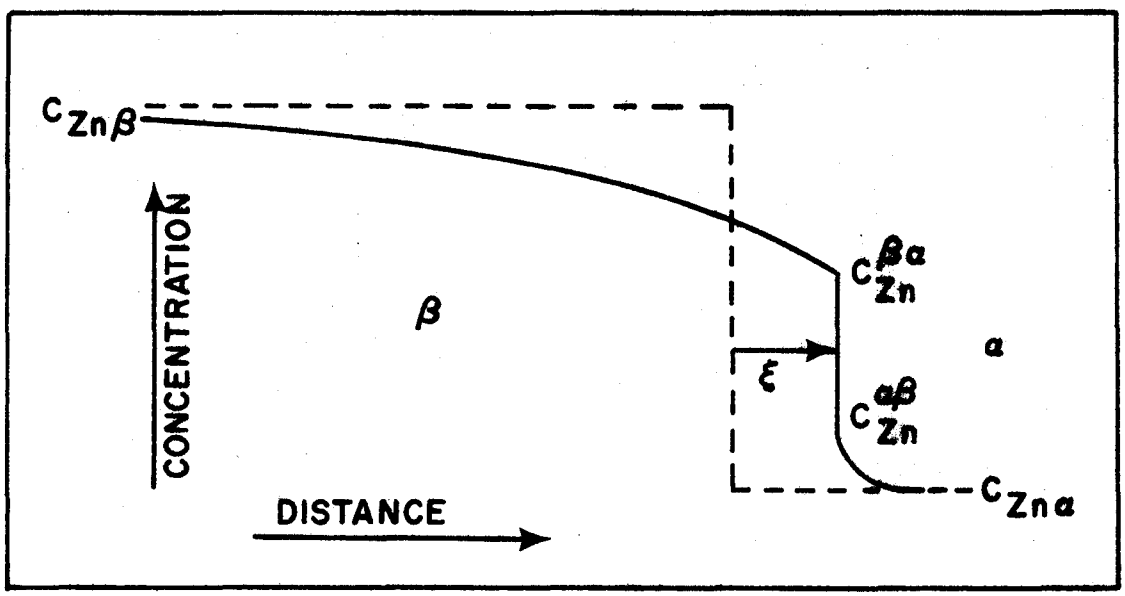

Fig. 8-1 Schematic distribution of Zn for diffusion couples α1-β1 to α1-β9.

of Zn is straightforward, the Ni distribution has interesting peculiarities which influence the stability of the α-β interface. Because $m < 0$, $(C_{Ni}^{\beta\alpha} - C_{Ni}^{\alpha\beta}) < 0$ and the Ni distribution is roughly as shown in Fig. 8-2. Because $D_{Ni}^{\beta} >> D_{Ni}^{\alpha}$ (Table 7-4) it would appear that there exists a strong tendency for the α-β interface to move to the right, just as was the case with Zn. However, the fact that $(C_{Ni}^{\beta\alpha} - C_{Ni}^{\alpha\beta}) < 0$ complicates matters considerably. Consider the interfacial mass balance for Ni (cf., Eqs. (6-19) and (6-20)):

$$V(C_{Ni}^{\beta\alpha} - C_{Ni}^{\alpha\beta}) = D_{Ni}^{\alpha} G_{Ni}^{\alpha\beta} - D_{Ni}^{\beta} G_{Ni}^{\beta\alpha}. \qquad (8\text{-}24)$$

Since $(C_{Ni}^{\beta\alpha} - C_{Ni}^{\alpha\beta}) < 0$, $D_{Ni}^{\alpha} G_{Ni}^{\alpha\beta} < 0$ and $D_{Ni}^{\beta} G_{Ni}^{\beta\alpha} < 0$, it follows that for $V > 0$, $|D_{Ni}^{\alpha} G_{Ni}^{\alpha\beta}|$ must exceed $|D_{Ni}^{\beta} G_{Ni}^{\beta\alpha}|$. Thus the flux of Ni from the interface into the α phase must exceed the flux of Ni to the interface from the β phase. Whereas the rate of α-β interface advance with respect to Zn primarily depends on the rate of delivery of Zn to the interface, with respect to Ni it depends on the rate at which Ni can escape into the α phase from directly ahead of the moving interface. In other words, for the α-β interface to move in the positive direction, a spike of Ni must be pushed ahead of the interface. It is this fact which leads to a potential for purely kinetic morphological breakdown of the α-β interface.

Consider the fate of a small perturbation introduced

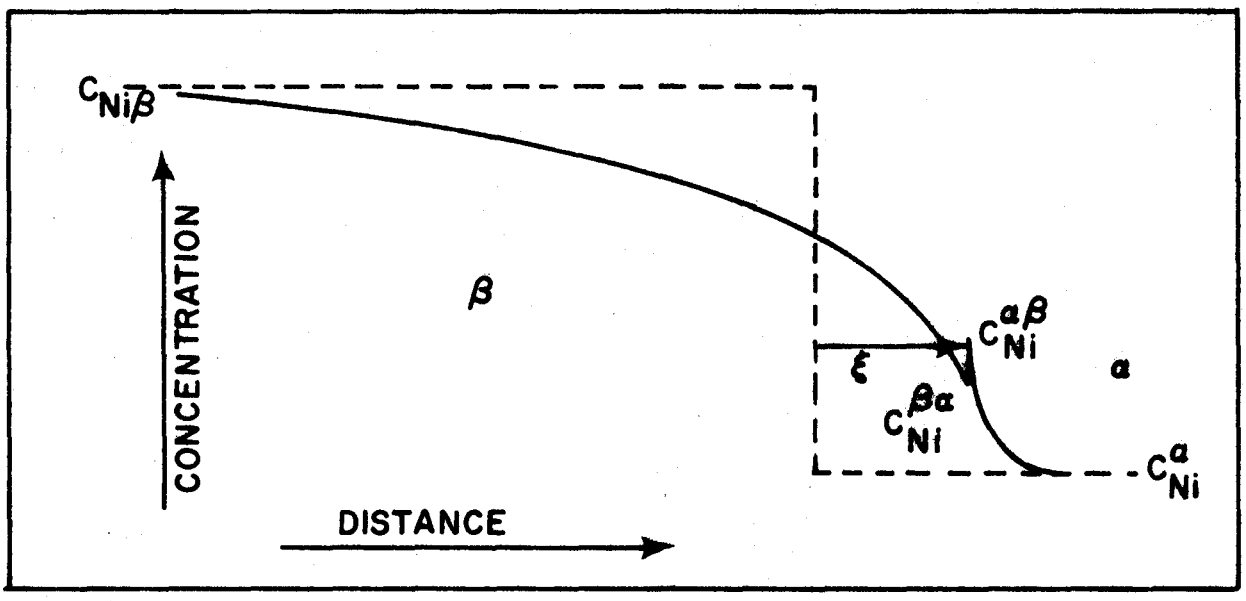

Fig. 8-2 Schematic distribution of Ni for diffusion couples $\alpha 1$-$\beta 1$ to $\alpha 1$-$\beta 9$.

into the shape of an advancing planar α-β interface as shown in Fig. 8-3 (cf., Sec. 3.3.1). It has just been demonstrated that the velocity of the interface is determined by the rate at which Ni can escape into the bulk α phase. In the vicinity of the perturbation the Ni escape rate is enhanced due to the divergence of the corresponding diffusional flux. As a result, the perturbation advances at a faster rate than the remainder (ie., planar part) of the interface. Thus as a result of the well known point effect of diffusion, the α-β interface is morphologically unstable[†]. With reference to the Ni mass balance (8-24), the perturbation effectively increases the magnitude of $G_{Ni}^{\alpha\beta}$ in its vicinity (and hence increases V). On the basis of an elementary geometrical construction one can demonstrate that the relative change in an interfacial gradient is greater, the steeper is the original gradient. Accordingly the perturbation has little influence on $G_{Zn}^{\beta\alpha}$, $G_{Zn}^{\alpha\beta}$ and $G_{Ni}^{\beta\alpha}$ as the latter are relatively flat.

It has been established that the tendency for instability is enhanced by the steepness of the original interfacial Ni gradient (ie., spike) in the α phase. There are three principal effects which influence the sharpness of the Ni spike.

[†]Keep in mind that in the present discussion, the constitutional effects due to θ^{α} and θ^{β} are being ignored.

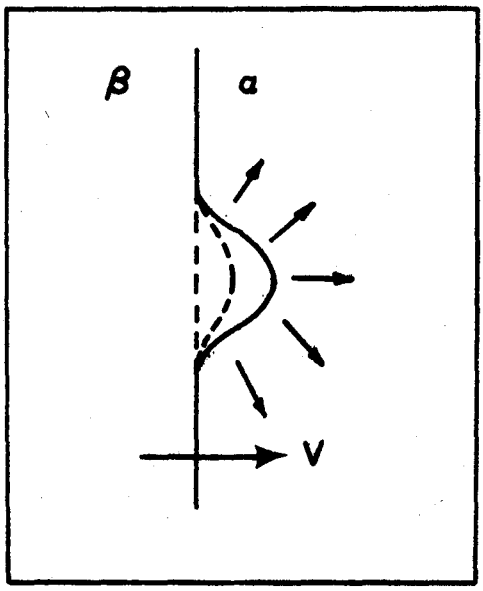

Fig. 8-3 Growth of perturbation in advancing α-β interface.

i) The slower is the diffusivity of Ni in the α phase, the steeper is the Ni spike (ie., the smaller is D^{α}_{Ni}, the greater in magnitude must be $G^{\alpha\beta}_{Ni}$ for $|D^{\alpha}_{Ni}\ G^{\alpha\beta}_{Ni}|$ to exceed $|D^{\beta}_{Ni}\ G^{\beta\alpha}_{Ni}|$ in Eq. (8-24)).

ii) The larger is the value of D^{β}_{Ni}, the greater must be the product $|D^{\alpha}_{Ni}\ G^{\alpha\beta}_{Ni}|$, and hence the value of $G^{\alpha\beta}_{Ni}$, to exceed $|D^{\beta}_{Ni}\ G^{\beta\alpha}_{Ni}|$.

iii) The faster the average interface moves, the sharper is the Ni spike because there is less time available for Ni redistribution into the bulk α phase. On the basis of Eq. (8-23) it has already been pointed out that the greater is the value of D^{β}_{Zn} and the smaller D^{α}_{Zn}, the greater is V.

In summary the tendency for this type of kinetic instability is enhanced by rapid transport in the β phase and slow transport in the α phase (indeed, any transport at all in the α phase must be regarded as contributing to stability). The terms ϕ^{β} and ϕ^{α}, respectively, represent these two influences. From the stability criterion (8-16), the larger is the value of ϕ^{β}, the greater is the tendency for instability. Recalling Eq. (8-5), this result is entirely consistent with the physical arguments just outlined. Because $\phi^{\alpha} < 0$, the smaller in magnitude is ϕ^{α} in (8-16), the greater is the tendency to instability. Recalling Eq. (8-4), this result is also entirely consistent with the

physical arguments just discussed. In the limit $D^{\alpha}_{Zn} \to 0$ and $D^{\alpha}_{Ni} \to 0$, $\phi^{\alpha} \to 0$ and the stabilizing effect of transport in the α phase is negligible.

It is now clear that one has two potential sources of morphological instability. There is the kinetic one just discussed and represented by the terms $\phi^{\alpha} + \phi^{\beta}$ in (8-16) and the constitutional (or thermodynamic) one represented by $2(\theta^{\alpha} + \theta^{\beta})$ in (8-16).

Consider the three cases discussed earlier. Case 1 is characterized by (8-14) and corresponds to absolute instability. From (8-14), this clearly represents situations in which supersaturation dominates the single stabilizing influence, transport in the α-phase (ie., $\phi^{\alpha} < 0$). Case 3 on the other hand is characterized by (8-18) and corresponds to absolute stability. From (8-18) this situation occurs when the constitutional terms exert a sufficiently stabilizing influence (ie., $\theta^{\alpha} + \theta^{\beta}$ sufficiently negative) that they dominate the only term favouring instability (ie., $\phi^{\beta} > 0$). Case 2, (8-16), summarizes all aspects of this stability problem with ϕ^{α} (<0) representing the stabilizing influence of transport in the α-phase, ϕ^{β} (>0) representing the destabilizing influence of transport in the β-phase and θ^{α} and θ^{β} (each $\gtrless 0$) representing the possibility of supersaturation in the corresponding phases.

8.4 COMPARISON OF THEORY AND EXPERIMENT

Mathematical and physical details have now been sufficiently clarified to make possible a detailed correlation between the preceding discussion and the experimental stability studies of Sec. 7.5.3. Recall that the experiments involved examination of the shape of the α-β interface of two-phase infinite diffusion couples which had the same terminal composition in the α phase (0 wt.% Ni, 34.1 wt.% Zn) but different terminal compositions in the β phase ($C_{Ni\beta}$,$C_{Zn\beta}$) (see Sec. 7.3). One now inquires into the influences which variations in the β terminal composition have on the magnitude and signs of the parameters in (8-16).

Given all of the required diffusion and equilibrium data, the diffusion path for a ternary diffusion couple is a function of its terminal compositions. In the present study the terminal composition in the α phase is fixed and therefore one can regard the diffusion path as being a function of $C_{Ni\beta}$ and $C_{Zn\beta}$ only. The values of ϕ^{α}, ϕ^{β}, θ^{α} and θ^{β}, Eqs. (8-4) to (8-7), are all uniquely determined by the diffusion path corresponding to the given diffusion couple and hence they are also functions of $C_{Ni\beta}$ and $C_{Zn\beta}$. It follows therefore that Eq. (8-20), which defines states of incipient instability, can be regarded as a function of the form

$$G(C_{Ni\beta},C_{Zn\beta}) = 0 \ .$$

That is to say, Eq. (8-20) is a relationship between the Ni and Zn contents of the bulk β phase and thus can be plotted on the appropriate ternary phase diagram as a locus of marginally unstable states. Accordingly the phase diagram is divided into stable and unstable domains with respect to the terminal composition of the β phase. Clearly Eqs. (8-21) and (8-22) also define loci on the ternary phase diagram. These loci define domains of absolute instability and absolute stability, respectively, with respect to the terminal composition of the β phase. To round out the present discussion, it is convenient to anticipate the results of the calculations just outlined. They are shown schematically in Fig. 8-4. The three loci are shown as lines having positive slope for the following reason. Because of the nature of the Cu-Zn-Ni phase diagram, the tendency to supersaturate in either phase (cf., the discussion relating to Fig. 7-3) increases with increasing Ni and decreasing Zn in the bulk β-phase. Thus the equation

$$\theta^{\alpha}(C_{Ni\beta}, C_{Zn\beta}) + \theta^{\beta}(C_{Ni\beta}, C_{Zn\beta}) = \text{constant}$$

defines a line of positive slope on the ternary phase diagram. Since ϕ^{α} and ϕ^{β} are not very sensitive functions of β terminal composition, the three equalities (8-20), (8-21) and (8-22) define loci which are lines of positive slope.

Following the procedure developed in Appendix II diffusion path calculations were made for each diffusion

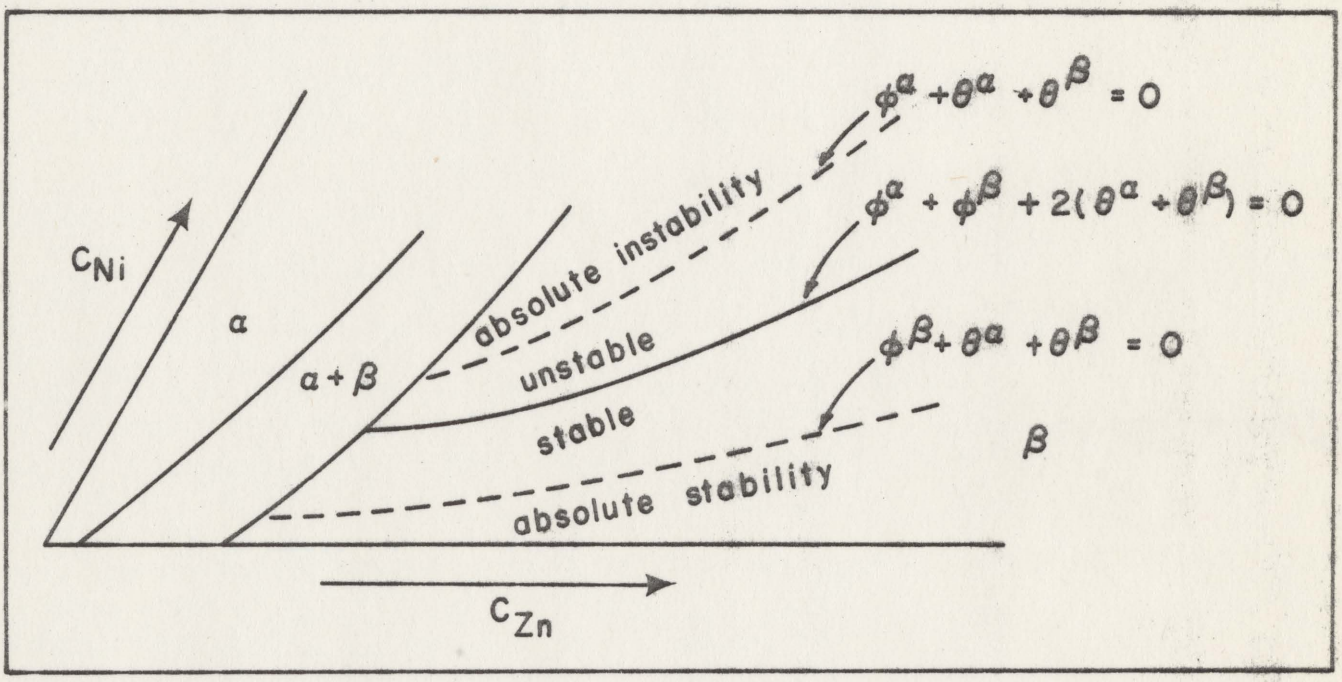

Fig. 8-4 Schematic drawing of the loci of β terminal composition corresponding to Eqs. (8-20), (8-21) and (8-22).

couple, $\alpha 1$-$\beta 1$ to $\alpha 1$-$\beta 9$, used in the stability studies of Sec. 7.5.3. With the exception of couple $\alpha 1$-$\beta 9$, a single real root to the trancendental equation (A2-17) was obtained, indicating a unique diffusion path for the corresponding terminal compositions. The diffusion path calculation corresponding to couple $\alpha 1$-$\beta 9$ yielded two real roots to Eq. (A2-17), which physically means there are two sets of interface composition and velocity which allow the mass balances to be satisfied for a planar interface. In view of the fact the $\alpha 1$-$\beta 9$ couple is observed to be morphologically unstable, it is clear that nature chooses neither of these two possibilities. This problem of multiple roots is further discussed shortly.

A brief outline of the means by which Eqs. (8-22), (8-20) and (8-21) can be used to determine the loci, with respect to β phase terminal composition, of absolute stability, incipient instability (ie., the marginal states) and absolute instability has already been given. These calculations are now considered in greater detail. Since numerous references are made to equations in earlier chapters and in Appendix II, it is appropriate that one recall the system of nomenclature, ie., phase I $\rightarrow \alpha$, phase II $\rightarrow \beta$, component 1 $\rightarrow$ Ni and component 2 $\rightarrow$ Zn. To illustrate the calculations, it is convenient to consider specifically the definition of marginal states, Eq. (8-20).

Substitution of Eqs. (8-4) to (8-7), (6-6) and (6-7) into (8-20) leads to

$$\frac{V}{2}(C_{Zn}^{\beta\alpha} - C_{Zn}^{\alpha\beta})[m(D_{Zn}^{\alpha}-D_{Zn}^{\beta}) + m^{\beta}D_{Ni}^{\beta} - m^{\alpha}D_{Ni}^{\alpha}]$$

$$+ D_{Ni}^{\alpha}\, D_{Zn}^{\alpha}(m^{\alpha}G_{Zn}^{\alpha\beta} - G_{Ni}^{\alpha\beta}) + D_{Ni}^{\beta}\, D_{Zn}^{\beta}(m^{\beta}G_{Zn}^{\beta\alpha} - G_{Ni}^{\beta\alpha}) = 0 \quad (8\text{-}25)$$

One now introduces $V = d\xi/dt = b/2\sqrt{t}$ and Eqs. (A2-6) and (A2-7) to obtain

$$\frac{b}{4}(C_{Zn}^{\beta\alpha}-C_{Zn}^{\alpha\beta})[m(D_{Zn}^{\alpha}-D_{Zn}^{\beta}) + m^{\beta}D_{Ni}^{\beta} - m^{\alpha}D_{Ni}^{\alpha}]$$

$$-m^{\alpha}D_{Ni}^{\alpha}\sqrt{\frac{D_{Zn}^{\alpha}}{\pi}}(C_{Zn}^{\alpha\beta}-C_{Zn\alpha})F^{\alpha}(b/2\sqrt{D_{Zn}^{\alpha}}) + D_{Zn}^{\alpha}\sqrt{\frac{D_{Ni}^{\alpha}}{\pi}}(C_{Ni}^{\alpha\beta}-C_{Ni\alpha})F^{\alpha}(b/2\sqrt{D_{Ni}^{\alpha}})$$

$$-m^{\beta}D_{Ni}^{\beta}\sqrt{\frac{D_{Zn}^{\beta}}{\pi}}(C_{Zn\beta}-C_{Zn}^{\beta\alpha})F^{\beta}(b/2\sqrt{D_{Zn}^{\beta}}) + D_{Zn}^{\beta}\sqrt{\frac{D_{Ni}^{\beta}}{\pi}}(C_{Ni\beta}-C_{Ni}^{\beta\alpha})F^{\beta}(b/2\sqrt{D_{Ni}^{\beta}})$$

$$= 0 \quad (8\text{-}26)$$

On substituting Eqs. (A2-11), (A2-12) and (A2-14), this equation can be rearranged to give the following expression for $C_{Ni\beta}$:

$$C_{Ni\beta} = -\frac{b\sqrt{\pi}\{(m^{\beta\alpha}-1)C_{Zn}^{\alpha\beta} + b^{\beta\alpha}\}}{4D_{Zn}^{\beta}\sqrt{D_{Ni}^{\beta}}\,F^{\beta}(b/2\sqrt{D_{Ni}^{\beta}})}[m(D_{Zn}^{\alpha} - D_{Zn}^{\beta}) + m^{\beta}D_{Ni}^{\beta} - m^{\alpha}D_{Ni}^{\alpha}]$$

$$+\sqrt{\frac{D_{Zn}^{\alpha}}{D_{Ni}^{\beta}}}\frac{m^{\alpha}D_{Ni}^{\alpha}(C_{Zn}^{\alpha\beta}-C_{Zn\alpha})F^{\alpha}(b/2\sqrt{D_{Zn}^{\alpha}})}{D_{Zn}^{\beta}\,F^{\beta}(b/2\sqrt{D_{Ni}^{\beta}})} - \sqrt{\frac{D_{Ni}^{\alpha}}{D_{Ni}^{\beta}}}\frac{D_{Zn}^{\alpha}(m^{\alpha}C_{Zn}^{\alpha\beta}+b^{\alpha}-C_{Ni\alpha})F^{\alpha}(b/2\sqrt{D_{Ni}^{\alpha}})}{D_{Zn}^{\beta}\,F^{\beta}(b/2\sqrt{D_{Ni}^{\beta}})}$$

$$+\sqrt{\frac{D_{Ni}^{\beta}}{D_{Zn}^{\beta}}}\frac{m^{\beta}(C_{Zn\beta}-m^{\beta\alpha}C_{Zn}^{\alpha\beta}-b^{\beta\alpha})F^{\beta}(b/2\sqrt{D_{Zn}^{\beta}})}{F^{\beta}(b/2\sqrt{D_{Ni}^{\beta}})} + m^{\beta}m^{\beta\alpha}C_{Zn}^{\alpha\beta} + m^{\beta}b^{\beta\alpha} + b^{\beta} \quad (8\text{-}27)$$

For a given terminal composition in the α phase, $(C_{Ni\alpha}, C_{Zn\alpha})$, and given bulk Zn content in the β phase, $C_{Zn\beta}$, this function is of the form

$$C_{Ni\beta} = f_4(C_{Zn}^{\alpha\beta}, b) \qquad (8\text{-}28).$$

It specifies the bulk Ni content in the β phase required to define a point on the locus of marginal states (with respect to β terminal composition). There are three unknowns involved and therefore two further equations are needed. The interface mass balance for Zn yields an equation of the form (Eq. (A2-16))

$$C_{Zn}^{\alpha\beta} = f_2(b) \qquad (8\text{-}29)$$

Because $C_{Ni\beta}$ is one of the unknowns, the interface mass balance for Ni, Eq. (A2-15), is regarded as an equation of the form

$$C_{Zn}^{\alpha\beta} = f_1(C_{Ni\beta}, b)$$

which can be inverted to

$$C_{Ni\beta} = f_3(C_{Zn}^{\alpha\beta}, b). \qquad (8\text{-}30)$$

Substitution of Eq. (8-29) into (8-28) and (8-30) gives, respectively

$$C_{Ni\beta} = f_5(b) \qquad (8\text{-}31)$$

and

$$C_{Ni\beta} = f_6(b). \qquad (8\text{-}32)$$

Clearly the value of b, and hence $C_{Zn}^{\alpha\beta}$ and $C_{Ni\beta}$, which satisfies

the two interface mass balances and the condition that the β terminal composition is on the locus of marginal states is obtained by solving the transcendental equation

$$g_2(b) = f_5(b) - f_6(b) = 0. \qquad (8\text{-}33)$$

If $2\phi^{\alpha} = 2(mD^{\alpha}_{Zn} - m^{\alpha}D^{\alpha}_{Ni})$ or $2\phi^{\beta} = 2(m^{\beta}D^{\beta}_{Ni} - mD^{\beta}_{Zn})$ replace the terms in the square brackets of Eqs. (8-27), one obtains transcendental equations analagous to (8-33) but corresponding to Eqs. (8-21) and (8-22),respectively. Accordingly domains of absolute instability and absolute stability are defined.

Having specified $C_{Ni\alpha} = 0$, $C_{Zn\alpha} = 34.1$ wt.% and various values of $C_{Zn\beta}$ in the range 44-50 wt.%, the three transcendental equations defining loci in a 'phase space' of β terminal concentrations were solved in a manner completely analagous to that by which Eq. (A2-17) is solved (ie., the iterative process described in Appendix II). For each equation, two sets of real roots were obtained. The loci corresponding to the set which was accepted are shown in Fig. 8-5 and will be discussed in a moment. They correspond to situations in which the α-β interface moves comparatively fast. The loci corresponding to the other set of roots are three very closely spaced lines situated roughly where the absolute instability locus is in Fig. 8-5. In these cases the interface migration rate is relatively slow. The locus of marginal states corresponding to the second set of roots (low V) is rejected

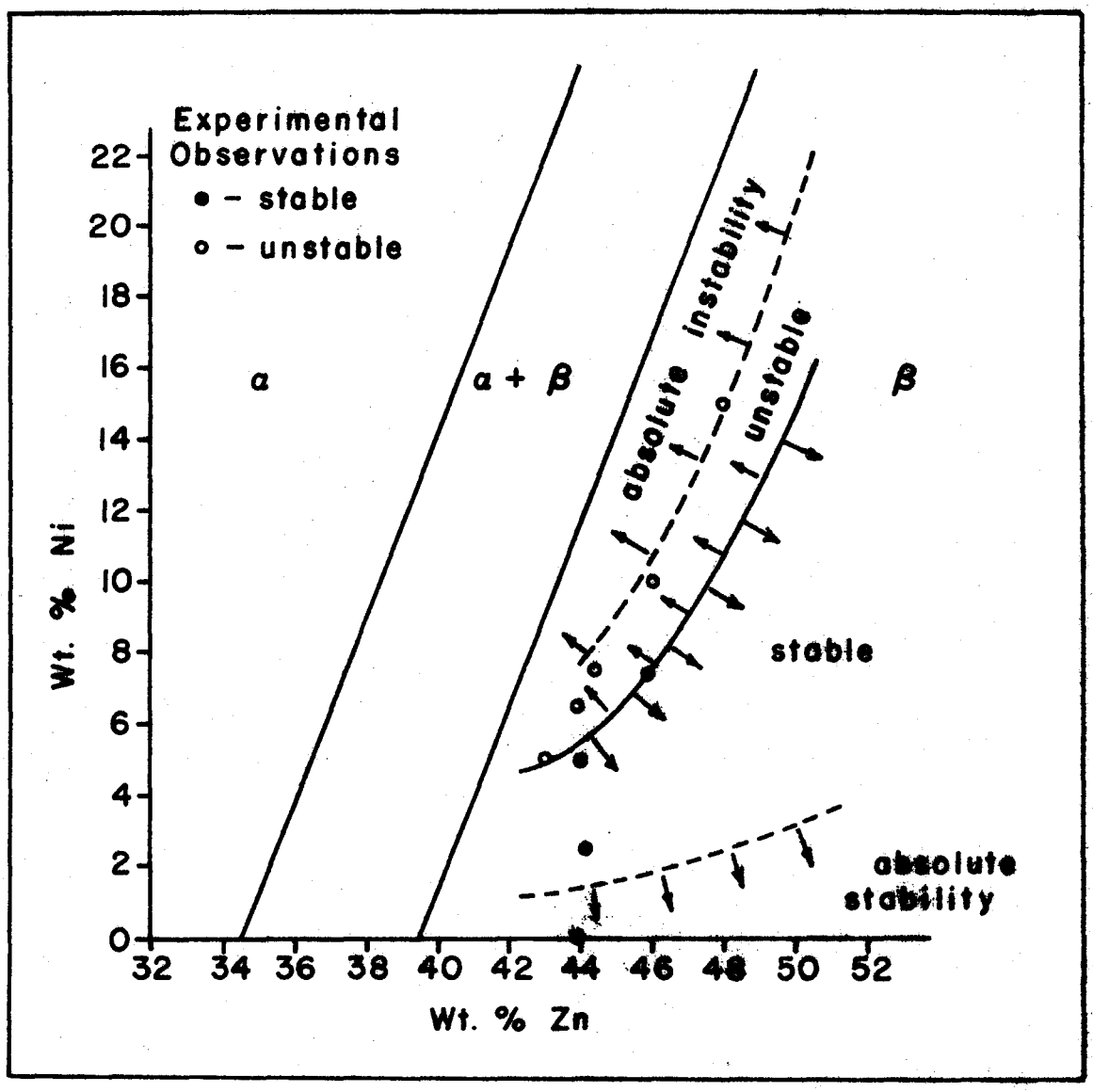

Fig. 8-5 Calculated loci of β terminal composition corresponding to Eqs. (8-20), (8-21) and (8-22). The β terminal compositions of the stable diffusion couples, α1-β1 to α1-β4, and unstable diffusion couples α1-β5 to α1-β9 are superimposed.

because it is situated in a region of the phase diagram which is unstable relative to the other locus of marginal states (high V). Similar arguments apply to the loci which define domains of absolute stability and instability. The fact that the selected set of roots leads to excellent agreement with experiment (Fig. 8-5) reinforces the argument just outlined.

On Fig. 8-5 is plotted the β terminal compositions of the various diffusion couples involved in the experimental stability studies and the loci which evolved out of the perturbation calculations[†]. In view of the fact that some of the parameters used in the calculations are not very precisely known, the agreement between experiment and theory is extremely good. So completely does Fig. 8-5 summarize the experimental program of chapter 7, the theoretical efforts of chapter 6 and the relationship between the two, that the little which remains to be said is best discussed in the following summary chapter.

[†]For β terminal compositions close to the α+β/β phase boundary, diffusion path calculations reveal that the α-β interface moves towards the β phase. This possibility is of no interest with respect to the present set of experiments. Therefore the loci were not calculated right up to the phase boundary.

CHAPTER 9

SUMMARY REMARKS

Using perturbation methods, precipitate-matrix interface stability in ternary systems has been examined in considerable detail (Chapter 5). The appropriate stability criterion was obtained, Eq. (5-19), and then considered in various important limiting situations. This criterion was observed to account for the point effect of diffusion and the stabilizing influence of capillarity in much the same general manner as the corresponding binary relation does, Eq. (5-21).

The stability of a planar interface in a two-phase ternary diffusion couple was treated in chapter 6. The problem was first considered in rather elementary constitutional terms. Then perturbation methods were applied to obtain a more realistic stability criterion, (6-44). This stability problem was formulated in a sufficiently general manner that the results could be applied to other interesting stability problems, eg., solid-liquid interface stability during steady state solidification or melting of binary alloys, interface stability during dissolution of solid alloys in contact with liquid metals and oxide-metal interface stability during alloy oxidation.

An experimental investigation into the stability of α-β phase interfaces in the Cu-Zn-Ni system was undertaken and is described in chapter 7. The first part of the experimental program involved determination of certain significant diffusion and equilibrium parameters. Using two-phase infinite diffusion couples, all with the same α terminal composition but with various β terminal compositions, it was possible to index the transition from a stable to an unstable planar α-β interface. Hitherto this type of experiment has never been attempted. The time evolution of unstable phase interfaces was also examined.

The stability criterion which evolved out of the perturbation analysis was applied to the Cu-Zn-Ni system in chapter 8. It was possible to attach a clear physical significance to each of the mathematical terms which appeared in the resulting criterion. The locus of marginally unstable states was calculated. This locus was plotted on the Cu-Zn-Ni ternary phase diagram thus defining regions of stability and instability with respect to β terminal composition, for the specific α terminal composition used in the experimental stability studies. Superimposed on this diagram were the results of the experimental program. The agreement with the locus calculated on the basis of perturbation theory was excellent. The present study represents one of the first quantitative tests of perturbation theory as applied to

problems of morphological stability in the solid state.

During the course of calculation it was observed that it is mathematically possible to have more than one diffusion path associated with a given set of terminal compositions in a two-phase diffusion couple. This fact lead to the appearance of multiple roots during the calculation of the locus of marginal states. There has long been an awareness of the fact that analyses of certain classes of phase transition, when based solely on solutions of the diffusion equation (or heat equation), lead to indeterminacies[80]. Classic examples are: i) Isothermal eutectoid reaction[81] - a single relation exists between the steady state lamellar spacing and the reaction velocity and therefore these quantities are not uniquely specified and ii) Dendrite needle growth[32,82,83] (or Widmanstätten plate growth[84,85]) - the radius of curvature of the needle (or plate) tip and the steady state tip velocity are not uniquely specified. To remove the degree of freedom, it is invariably assumed that the system will seek a configuration which satisfies some extremum principle. For examples i) and ii) just cited, it is usually assumed that the system seeks a configuration which maximizes the reaction velocity with respect to lamellar spacing and tip radius, respectively. The use of extremum principles are interim procedures in the absence of a detailed kinetic or phenomenological theory of the cooperative pro-

cesses which control the phase transition[80].

It would appear that the possibility of multiple diffusion paths is related to the class of indeterminacies just discussed. However, in the present study it was not necessary to apply an extremum principle to decide which of the two calculated loci of marginally unstable states should be rejected. One locus was situated in the unstable domain defined by the other locus and therefore the former was rejected. It is interesting to note that the accepted locus corresponds to higher interface velocity, in agreement with the maximum velocity principle. It is apparent that there is a need for a detailed re-examination of the existence and uniqueness of virtual ternary diffusion paths associated with phase transition. Such considerations must be clarified for a complete understanding of the problem of interface stability since if no solution exists, the system is unstable, and if more than one solution exists, all but one must be regarded as being unstable (or at best metastable).

APPENDIX I

A CAPILLARITY EQUATION FOR DILUTE TERNARY SYSTEMS

In this appendix, the capillarity equation (5-5) is derived. Recall that the system under consideration, Fig. 5-1, involves two phases which are dilute solutions of components 1 and 2 in component 3. The appropriate Gibbs-Duhem relations are a convenient starting point for the derivation, viz.,

for the precipitate:

$$N_1^{II}d\mu_1 + N_2^{II}d\mu_2 + N_3^{II}d\mu_3 = \Omega dP^{II} \qquad \text{(A1-1)}$$

and for the matrix:

$$N_1^{I}d\mu_1 + N_2^{I}d\mu_2 + N_3^{I}d\mu_3 = \Omega dP^{I} = 0 \qquad \text{(A1-2)}$$

where the N_i^I and N_i^{II} $(i = 1,2,3)$ are mole fractions and Ω is the molar volume (which is assumed to be the same in both the precipitate and matrix). The pressure change in the matrix is equated to zero on assumption that the parent phase is sufficiently plastic that a pressure buildup can not be sustained. Equation (A1-2) is solved for $d\mu_3$ which is then substituted into Eq. (A1-1) to give

$$\left(N_1^{II} - \frac{N_1^I N_3^{II}}{N_3^I}\right) d\mu_1 + \left(N_2^{II} - \frac{N_2^I N_3^{II}}{N_3^I}\right) d\mu_2 = \Omega dP^{II} \qquad \text{(A1-3)}$$

It is assumed that the solid solutions I and II are sufficiently dilute that the ratio N_3^{II}/N_3^I can be approximated by unity and that Henry's law applies, ie., $d\mu_i = RTdN_i/N_i$. Under these

conditions, Eq. (A1-3) simplifies to

$$\frac{(N_1^{II} - N_1^I)}{N_1^I} dN_1^I + \frac{(N_2^{II} - N_2^I)}{N_2^I} dN_2^I = \frac{\Omega dP^{II}}{RT} . \quad (A1-4)$$

From Eq. (5-4), it follows that $k_i = N_i^{II}/N_i^I$ and the above becomes

$$(k_1-1)dN_1^I + (k_2-1)dN_2^I = \frac{\Omega dP^{II}}{RT} . \quad (A1-5)$$

In the present situation, the increments dN_1^I, dN_2^I and dP^{II} are the result of the curvature introduced into the shape of the precipitate-matrix interface by the perturbation $\phi(x,t) = \delta \sin \omega x$. Hence, one can write

$$dN_i^I = N_{i\phi}^I - N_i^{I\ II} \quad (A1-6)$$

The pressure increment is given by[86] $dP^{II} = \sigma K$ where σ is interfacial free energy and K is the mean curvature of the interface (positive when concave toward the precipitate). For a surface $\phi(x,t)$ which only deviates slightly from the planar shape, $K \cong -\nabla^2\phi$ and hence

$$dP^{II} = \sigma\delta\omega^2 \sin\omega x . \quad (A1-7)$$

Equations (A1-5), (A1-6) and (A1-7) yield

$$(N_{1\phi}^I - N_1^{I\ II})(k_1-1) + (N_{2\phi}^I - N_2^{I\ II})(k_2-1) = \frac{\Omega\sigma}{RT} \delta\omega^2 \sin\omega x. \quad (A1-8)$$

To convert the mole fractions N_i to molar concentrations C_i, one divides through by the molar volume Ω. Thus Eq. (5-5) is obtained from Eq. (A1-8) when one introduces $\psi = \sigma/RT$.

APPENDIX II

DIFFUSION PATH CALCULATION

In this appendix, a procedure is outlined for the calculation of diffusion paths for two-phase infinite diffusion couples in ternary systems. The analysis for N-phase systems, Secs. 2.3.3 and 2.4, is specialized to a system of two phases, I and II. As usual the positive direction is from phase II to phase I. In this dissertation, actual diffusion path calculations are made only for the Cu-Zn-Ni system. In Sec. 7.5.2 it was demonstrated that diffusional interaction is not significant for the composition range of interest in this system. For this reason, diffusional interaction is ignored in the present analysis, ie., $D_{ij}^{m} = 0$ $(m = I, II;\ i \neq j)$.

For this problem, the appropriate boundary conditions are (cf., Eqs. (2-30))

$$\left.\begin{aligned} C_i(z<0,0) &= C_i(-\infty,t) = C_{iII} \\ C_i(z>0,0) &= C_i(\infty,t) = C_{iI} \\ C_i(\xi_-,t>0) &= C_i^{II\ I} \\ C_i(\xi_+,t>0) &= C_i^{I\ II} \end{aligned}\right\} (i=1,2) \qquad \text{(A2-1)}$$

where the symbol ξ replaces $\xi^{II\ I}$ since there is only one interface. In view of Eq. (2-33), let

$$\xi = b\sqrt{t} \qquad \text{(A2-2)}$$

where b is a rate constant. Of the four interface concentrations C_i^{mn}, only one can be regarded as being independent; the other three are related to it by the ternary phase diagram. The independent interface concentration and the rate constant b in Eq. (A2-2) are fixed by two mass balances (cf., Eqs. (2-34))

$$\frac{d\xi}{dt}\,(C_i^{II\ I}-C_i^{I\ II}) = \frac{b}{2\sqrt{t}}\,(C_i^{II\ I}-C_i^{I\ II}) = D_i^I G_i^{I\ II}-D_i^{II}G_i^{II\ I}. \quad \text{(A2-3)}$$

The solutions to the diffusion equations are simply

$$C_i^I = C_{iI} + \frac{(C_i^{I\ II}-C_{iI})\ \mathrm{erfc}(z/2\sqrt{D_i^I t})}{\mathrm{erfc}(b/2\sqrt{D_i^I})} \qquad b \le \frac{z}{\sqrt{t}} \le \infty \quad \text{(A2-4)}$$

$$C_i^{II} = C_{iII} - \frac{(C_{iII}-C_i^{II\ I})\ \mathrm{erfc}(-z/2\sqrt{D_i^{II} t})}{\mathrm{erfc}(-b/2\sqrt{D_i^{II}})} \qquad -\infty \le \frac{z}{\sqrt{t}} \le b. \quad \text{(A2-5)}$$

With the help of Eq. (A2-2), one can easily show that Eqs. (A2-4) and (A2-5) satisfy the boundary conditions (A2-1). Noting that

$$\frac{d}{dx}(\mathrm{erfc}\ x) = -\frac{2}{\sqrt{\pi}}\exp(-x^2) = \frac{d}{dx}(\mathrm{erfc}{-}x),$$

one can evaluate the gradients G_i^{mn} from Eqs. (A2-4) and (A2-5) and hence obtain

$$G_i^{I\ II} = \frac{-(C_i^{I\ II}-C_{iI})\exp(-b^2/4D_i^I)}{\sqrt{\pi D_i^I t}\qquad \mathrm{erfc}(b/2\sqrt{D_i^I})} = \frac{-(C_i^{I\ II}-C_{iI})F^I(b/2\sqrt{D_i^I})}{\sqrt{\pi D_i^I t}} \quad \text{(A2-6)}$$

and

$$G_i^{II\ I} = \frac{-(C_{iII}-C_i^{II\ I})\exp(-b^2/4D_i^{II})}{\sqrt{\pi D_i^{II} t}\quad \operatorname{erfc}(-b/2\sqrt{D_i^{II}})}$$

$$= \frac{-(C_{iII}-C_i^{II\ I})\quad F^{II}(b/2\sqrt{D_i^{II}})}{\sqrt{\pi D_i^{II} t}} \qquad \text{(A2-7)}$$

where it is convenient to define the functions[87]

$$F^{I}(x) = \exp(-x^2)/\operatorname{erfc}(x) \qquad \text{(A2-8)}$$

and

$$F^{II}(x) = \exp(-x^2)/\operatorname{erfc}(-x) = F^{I}(-x). \qquad \text{(A2-9)}$$

Eqs. (A2-6) and (A2-7) are now substituted into the mass balances (A2-3) to give

$$\frac{\sqrt{\pi}\ b}{2}\ (C_i^{II\ I}-C_i^{I\ II}) = \sqrt{D_i^{II}}(C_{iII}-C_i^{II\ I})F^{II}(b/2\sqrt{D_i^{II}}) - \sqrt{D_i^{I}}(C_i^{I\ II}-C_{iI}) \times$$

$$F^{I}(b/2\sqrt{D_i^{I}}) \qquad \text{(A2-10)}$$

In effect the phase boundary lines and tie-lines on the ternary phase diagram represent three relations between the four interface concentrations $C_i^{I\ II}$ and $C_i^{II\ I}$. The problem is to express these relations analytically. In the present analysis, they are linearized and an iterative procedure is introduced. For a given system and set of terminal compositions, one can usually guess roughly where the diffusion path will cross the two-phase field on the phase diagram (ie., guess the tie-line involved). The phase boundary lines

in this vicinity are approximated by straight lines having equations of the form (cf. Eqs. (6-13) and (6-14))

$$C_1^{I\ II} = m^I C_2^{I\ II} + b^I \qquad \text{(A2-11)}$$

and

$$C_1^{II\ I} = m^{II} C_2^{II\ I} + b^{II} \ . \qquad \text{(A2-12)}$$

It is also assumed that the system of tie-lines are parallel over a reasonable composition range. Hence one can introduce an equation of the form (cf., Eq. (6-15))

$$C_2^{II\ I} = m^{II\ I} C_2^{I\ II} + b^{II\ I} \qquad \text{(A2-13)}$$

which when combined with Eq. (A2-12) leads to

$$C_1^{II\ I} = m^{II}\, m^{II\ I}\, C_2^{I\ II} + m^{II}\, b^{II\ I} + b^{II}. \qquad \text{(A2-14)}$$

In view of Eqs. (A2-11), (A2-13) and (A2-14), it is clear that $C_2^{I\ II}$ has been selected as the independent interface concentration. The above relations are substituted into Eqs. (A2-10) and the latter are manipulated to give

$$C_2^{I\ II} = \Big[-\frac{\sqrt{\pi}}{2}(m^{II} b^{II\ I} + b^{II} - b^I) b + \sqrt{D_1^{II}}(C_{1II} - m^{II} b^{II\ I} - b^{II}) \times F^{II}(b/2\sqrt{D_1^{II}}) - \sqrt{D_1^I}(b^I - C_{1I}) F^I(b/2\sqrt{D_1^I})\Big] \Big/ \Big[\frac{\sqrt{\pi}}{2}(m^{II} m^{II\ I} - m^I) b + m^{II} m^{II\ I}\sqrt{D_1^{II}}\, F^{II}(b/2\sqrt{D_1^{II}}) + m^I \sqrt{D_1^I}\, F^I(b/2\sqrt{D_1^I})\Big] = f_1(b) \qquad \text{(A2-15)}$$

and

$$C_2^{I\ II} = \Big[-\frac{\sqrt{\pi}}{2} b^{II\ I} b + \sqrt{D_2^{II}}(C_{2II} - b^{II\ I}) F^{II}(b/2\sqrt{D_2^{II}}) + \sqrt{D_2^I}\, C_{2I} \times F^I(b/2\sqrt{D_2^I})\Big] \Big/ \Big[\frac{\sqrt{\pi}}{2}(m^{II\ I} - 1) b + \sqrt{D_2^{II}}\, m^{II\ I}\, F^{II}(b/2\sqrt{D_2^{II}}) + \sqrt{D_2^I} \times F^I(b/2\sqrt{D_2^I})\Big] = f_2(b) \qquad \text{(A2-16)}$$

Clearly, the value of b (and hence $C_2^{I\ II}$) which satisfies the two interface mass balances is obtained by solving the transcendental equation

$$g_1(b) \equiv f_1(b) - f_2(b) = 0. \qquad \text{(A2-17)}$$

The above equation is easily solved with the aid of a computer. The only difficulty which arises in such numerical calculations involves evaluation of the functions $F^I(x)$ and $F^{II}(x)$ defined in Eqs. (A2-8) and (A2-9) respectively. Consider specifically the function $F^I(x)$ and a positive argument x. If $x > 3.5$, the usual methods of evaluating erfc(x) are not reliable[†] and the following finite series approximation is employed[88]

$$\text{erfc}(x) = \frac{\exp(-x^2)}{\sqrt{\pi}\, x}\left[1 - \frac{1}{2x^2} + \frac{1\cdot 3}{(2x^2)^2} - \frac{1\cdot 3\cdot 5}{(2x^2)^2} + \ldots\right]. \qquad \text{(A2-18)}$$

Substitution of the above series into Eq. (A2-8) yields

$$F^I(x) = \sqrt{\pi}\, x/\left[1 - \frac{1}{2x^2} + \frac{1\cdot 3}{(2x^2)^2} - \frac{1\cdot 3\cdot 5}{(2x^2)^3} + \ldots\right]. \qquad \text{(A2-19)}$$

Since the ratio of successive terms in the series is $(2n-3)/2x^2$, it follows that the terms begin to increase in magnitude for $n > (2x^2+3)/2$. Hence during the numerical calculations, the series is terminated if the ratio $(2n-3)/2x^2$ is less than 10^{-8} or greater than unity, whichever comes first.

[†]Clearly one has analogous difficulities with erfc(-x) and hence $F^{II}(x)$, if $x < -3.5$.

To summarize, the calculation procedure is as follows. First the location of the tie-line associated with the diffusion path is estimated, ie., a value of $C_2^{I\ II}$ is guessed. The phase diagram is then linearized in the vicinity of that tie-line to obtain values of the coefficients m^I, m^{II}, $m^{II\ I}$, b^I, b^{II} and $b^{II\ I}$ in Eqs. (A2-11), (A2-12) and (A2-13). Solution of Eq. (A2-17) yields a value of b and hence, via Eq. (A2-15) or (A2-16), a better value of $C_2^{I\ II}$. The iterative cycle is continued until convergence, ie., successive values of $C_2^{I\ II}$ and b do not change.

On the Cu-Zn-Ni ternary phase diagram, the $\alpha/\alpha+\beta$ and $\alpha+\beta/\beta$ phase boundaries are approximated by two straight and parallel lines over the composition range of interest in the present stability studies. Thus in diffusion path calculations, successive iterations influence the values of $m^{II\ I}$ and $b^{II\ I}$, but not the values of m^I, m^{II}, b^I and b^{II}. Starting with an initial guess at $C_2^{I\ II}$ (ie., $C_{Zn}^{\alpha\beta}$), one obtains a value of m from Fig. 7-9 and hence values of $m^{II\ I}$ and $b^{II\ I}$. Solution of Eq. (A2-17) yields a new value of $C_2^{I\ II}$ which in turn leads to new values of $m^{II\ I}$ and $b^{II\ I}$ and so on. It was found that at most three such iterations were required before convergence.

Thus far it has been implicitly assumed that one and only one diffusion path corresponds to a given set of terminal compositions. For a single-phase diffusion couple, there is no doubt about the validity of such an assumption. However, in multi-phase systems, it is questionable. For a two-phase

diffusion couple, one obtains a unique diffusion path if and only if the transcendental equation (A2-17) has a single real root. In view of Eqs. (A2-8), (A2-9), (A2-15) and (A2-16), one can see no mathematical reason that this should be so. It appears possible to have zero, one or more than one real roots. That is to say, it appears possible to have zero, one or more than one tie-line and interface velocity pairs (ie., $C_2^{I\ II}$ and b) which allow the two interface mass balances to be satisfied. If multiple roots do exist it would appear that a thermodynamic principle of some sort must be introduced for unique specification of the diffusion path. On the other hand, if no root exists for the assumed planar interface morphology, then one must seek solutions involving a different morphology or sequence of phases.

REFERENCES

1. L. Onsager, Ann. N.Y. Acad. Sci., 46, 241 (1945).

2. L. Onsager, Phys. Rev., 37, 405 (1931).

3. L. Onsager, Phys. Rev., 38, 2265 (1931).

4. G. J. Hooyman, S. R. DeGroot and P. Mazur, Physica, 21, 360 (1955).

5. J. G. Kirkwood, R. L. Baldwin, P. J. Dunlop, L. J. Gosting and G. Kegeles, J. Chem. Phys., 33, 1505 (1960).

6. D. G. Miller, Chem. Rev., 60, 15 (1960).

7. J. E. Lane and J. S. Kirkaldy, Can. J. Phys.,42, 1643 (1964).

8. J. S. Kirkaldy, D.H. Weichert and Zia-Ul Haq, Can. J. Phys.,41, 2166 (1963).

9. J. S. Kirkaldy, Can. J. Phys.,37, 30 (1959).

10. J. Crank, Mathematics of Diffusion, Oxford University Press, London (1956).

11. W. Jost, Diffusion in Solids, Liquids, Gases, Academic Press Inc., New York (1952).

12. H. S. Carslaw and J. C. Jaeger, Conduction of Heat in Solids, Oxford University Press, London (1959).

13. H. Fujita and L. J. Gosting, J. Am. Chem. Soc., 78, 1099 (1956).

14. J. S. Kirkaldy, Can. J. Phys., 36, 899 (1958).

15. A. Dubé, Phd. Thesis, Carnegie Institute of Technology, Pittsburgh (1948).

16. C. Zener, J. Appl. Phys., 20, 950 (1949).

17. J. S. Kirkaldy, Can. J. Phys., 36, 907 (1958).

18. J. S. Kirkaldy, Can. J. Phys., 36, 917 (1958).

19. J. S. Kirkaldy and L. C. Brown, Can. Met. Quart., 2, 89 (1963).

20. R. F. Sekerka, J. Crystal Growth, 3,4, 71 (1968).

21. P. R. Garabedian, Partial Differential Equations, Wiley and Sons, New York, 531-613 (1964).

22. S. Bergman and M. Schiffer, Kernel Functions and Elliptic Differential Equations in Mathematical Physics, Academic Press, New York, 64-71 (1953).

23. M. N. Özisik, Boundary Value Problems of Heat Conduction, International Textbook Comp., Scranton, 326-374 (1968).

24. I. Stakgold, Boundary Value Problems of Mathematical Physics, Vol. II, MacMillan Comp., New York, 327-328 (1968).

25. F. Neumann, cf. Riemann-Weber, Die partiellen Differentialgleichungen der mathematischen Physik, Vol. II, 121 (1912).

26. J. Stefan, Ann. Phys. u. Chem. (Wiedemann) N.F., 42, 269 (1891).

27. F. C. Frank, Proc. Roy. Soc., A201, 586 (1950).

28. F. S.Ham, J. Phys. Chem. Solids, 6, 335 (1958).

29. F. S. Ham, Quart. Appl. Math., 17, 137 (1959).

30. G. Arfken, Mathematical Methods for Physicists, Academic Press, New York, 92-100 (1968).

31. G. P. Ivanstov, Dokl. Akad. Nauk SSSR, 58, 567 (1947).

32. D. E. Temkin, Dokl. Akad. Nauk SSSR, 132, 1307 (1960).

33. K. A. Jackson, Prog. Solid State Chem., 4, 53 (1967).

34. R. D. Townsend and J. S. Kirkaldy, Trans. ASM., 61, 605 (1968).

35. W. A. Tiller, K. A.Jackson, J. W. Rutter and B. Chalmers, Acta Met., 1, 428 (1953).

36. J. W. Rutter and B. Chalmers, Can. J. Phys., 31, 15 (1953).

37. M. J. Buerger, Z. Krist., 89, 242 (1934).

38. J. S. Kirkaldy and D. G. Fedak, Trans. AIME, 224, 490 (1962).

39. C. Wagner, Zeit. für Electrochemie, 63, 772 (1959).

40. C. Wagner, J. Electrochem. Soc., 103, 571 (1956).

41. S. Chandrasekar, Hydrodynamic and Hydromagnetic Stability, Oxford University Press, London (1959).

42. J. D. Cole, Perturbation Methods in Applied Mathematics, Blaisdell Publishing Comp., Toronto (1968).

43. C. C. Lin, The Theory of Hydrodynamical Stability, Cambridge University Press, London (1955).

44. M. D. Van Dyke, Perturbation Methods in Fluid Mechanics, Academic Press, New York (1964).

45. C. Wagner, J. Electrochem. Soc., 101, 225 (1954).

46. W. W. Mullins and R. F. Sekerka, J. Appl. Phys., 34, 323 (1963).

47. W. W. Mullins and R. F. Sekerka, J. Appl. Phys., 35, 444 (1964).

48. V. V. Voronkov, Soviet Phys.-Solid State, 6, 2378 (1965).

49. R. F. Sekerka, Crystal Growth, Ed. H. S. Peiser, Pergamon, Oxford, 691 (1967).

50. R. F. Sekerka, J. Phys. Chem. Solids,28, 983 (1967).

51. R. T. Delves, Phys. Status Solidi, 16, 621 (1966).

52. R. T. Delves, Phys. Status Solidi, 17, 119 (1966).

53. P. G. Shewmon, Trans. AIME.,233, 736 (1965).

54. J. W. Cahn, Crystal Growth, Ed. H. S. Peiser, Pergamon, Oxford, 681 (1967).

55. S. R. Coriell and R. L. Parker, Crystal Growth, Ed. H. S. Peiser, Pergamon, Oxford, 703 (1967).

56. S. R. Coriell and R. L. Parker, J. Appl. Phys., 37, 1548 (1966).

57. M. Hone, S. V. Subramanian and G. R. Purdy, Can. Met. Quart., 8, 251 (1969).

58. G. Bolze, D. E. Coates and J. S. Kirkaldy, Trans. ASM., 62, 794 (1969).

59. I. J. O'Donnell and L. J. Gosting, Symposium on Electrolytes Wiley and Sons, New York (1957).

60. D. E. Coates and J. S. Kirkaldy, J. Crystal Growth, 3,4, 549 (1968).

61. D. E. Coates and J. S.Kirkaldy, Trans. ASM., 62, 426 (1969).

62. D. P. Woodruff, Phil. Mag., 17, 283 (1968).

63. J. D. Harrison and C. Wagner, Acta Met., 7, 722 (1959).

64. J. Schramm, Kupfer-Nickel-Zinc-Legierungen, Verlag Konrad Triltsch, Würzberg (1935).

65. M. C. Inman, D. Johnston, W. L. Merces and R. Shuttleworth, Proceedings Second Radioisotope Conference, Butterworths, London, C0115 (1954).

66. A. B. Kuper, D. Lazarus, J. R. Manning and C.T. Tomizuka, Phys. Rev., 104, 1536 (1956).

67. L. C. C. da Silva and R. F. Mehl, Trans. AIME., 191, 155 (1951).

68. U. S. Landergren, C. E. Birchenall and R. F. Mehl, Trans. AIME., 206, 73 (1956).

69. G. T. Horne and R. F. Mehl, Trans. AIME.,203, 88 (1955).

70. R. Resnick and R. W. Balluffi, Trans. AIME.,203, 1004 (1955).

71. L. S. Darken, Trans. AIME., 175, 184 (1948).

72. A. D. Smigelskas and E. O. Kirkendall, Trans. AIME., 171, 130 (1947).

73. R. T. DeHoff, A. G. Guy, K. J. Anusavice and T. B. Lindemer, Trans. AIME., 236, 881 (1966).

74. H. Oikawa, K. J. Anusavice, R. T. DeHoff and A. G. Guy, Trans. ASM., 61, 354 (1968).

75. C. W. Taylor, Jr., M. A. Dayananda and R. E. Grace, Met. Trans., 1, 127 (1970).

76. L. S. Darken, Trans. AIME., 180, 430 (1949).

77. W. A. Johnson, Trans. AIME., 147, 331 (1942).

78. C. Wells, Atom Movements, American Society of Metals, Cleveland, 26 (1951).

79. M. Hansen, Constitution of Binary Alloys , McGraw-Hill, New York, 650 (1958).

80. J. S. Kirkaldy, Energetics in Metallurgical Phenomena Vol. IV, Gordon and Breach, New York, 340 (1968).

81. C. Zener, Trans. AIME., 167, 550 (1946).

82. R. Trivedi, Acta Met., 18, 287 (1970).

83. E. G. Holzmann, J. Appl. Phys., 41, 1460 (1970).

84. M. Hillert, Jernkontorets Ann., 141, 757 (1957).

85. R. Trivedi, Met. Trans., 1, 921 (1970).

86. J. W. Gibbs, Scientific Papers Vol. I, Dover, New York, 229 (1962).

87. L. S. Castelman, Nucl. Sci. Eng., 4, 209 (1958).

88. National Bureau of Standards, Table of the Error Function and Its Derivative, Applied Maths. Series No. 41, (1954).

89. R. Pilliar and J. S. Kirkaldy, unpublished research.